THE UNIVERSITY OF CHICAGO

# A *DMC1* MUTANT THAT BYPASSES ACCESSORY FACTOR MEI5-SAE3 PROVIDES INSIGHT INTO THE REGULATION OF FILAMENT LENGTH *IN VIVO*

A DISSERTATION SUBMITTED TO

THE FACULTY OF THE DIVISION OF THE BIOLOGICAL SCIENCES

AND THE PRITZKER SCHOOL OF MEDICINE

IN CANDIDACY FOR THE DEGREE OF

DOCTOR IN PHILOSOPHY

COMMITTEE ON GENETICS, GENOMICS, AND SYSTEMS BIOLOGY

BY

DIEDRE FAYE REITZ

CHICAGO, ILLINOIS

DECEMBER 2019

Table of Contents

List of Figures

List of Tables

Acknowledgments

Many thanks are owed to the people that made it possible for me to complete my PhD dissertation, either through their direct involvement in this work, or through their personal impact on my life during my time as a doctoral candidate. I would like to start by expressing my deep appreciation for my doctoral adviser, Douglas Bishop, for years of helpful advice and constructive feedback on my work. Doug has been instrumental to my success as a scientist, and I could not have completed this dissertation without his patient guidance. I would also like to acknowledge the efforts of my colleagues, Yuen-Ling Chan and Jennifer Grubb, for their training, knowledge, advice, and friendship. I learned most of the techniques that were used in preparation of this work from these two individuals, and they have also both made invaluable contributions to my thesis. The members of my thesis committee, Jonathan Staley, Phoebe Rice, and Benjamin Glick, are likewise gratefully acknowledged. In addition, my day-to-day work in the lab would not have been possible without Lawanda Stewart and Sue Levison, whose assistance allowed me to devote more time to my research. Lastly, I would like to thank my friends and family for their unwavering support. In particular, my husband Nathaniel Jiang has been a constant source of love and encouragement.

Abstract

During meiosis, homologous recombination repairs programmed DNA double-stranded breaks. Meiotic recombination physically links the homologous chromosomes ("homologs"), creating the tension between them that is required for their segregation. The central recombinase in this process is Dmc1. Dmc1's activity is regulated by its accessory factors including the heterodimeric protein Mei5-Sae3 and Rad51. We use a gain-of-function *dmc1* mutant*, dmc1-E157D*, that bypasses Mei5-Sae3 to gain insight into the role of this accessory factor and its relationship to mitotic recombinase Rad51, which also functions as a Dmc1 accessory protein during meiosis. We find that Mei5-Sae3 has a role in filament formation and stability, but not in the bias of recombination partner choice that favors homolog over sister chromatids. Analysis of meiotic recombination intermediates suggests that Mei5-Sae3 and Rad51 function independently in promoting filament stability. In spite of its ability to load onto single-stranded DNA and carry out recombination in the absence of Mei5-Sae3, recombination promoted by the Dmc1 mutant is abnormal in that it forms foci in the absence of DNA breaks, displays unusually high levels of multi-chromatid and intersister joint molecule intermediates, as well as high levels of ectopic recombination products. Using super-resolution microscopy, we show that the mutant protein forms longer foci than those formed by wild-type Dmc1. To determine whether the *in vivo* phenotypes were caused by an increased tendency of the Dmc1 mutant to form multi-invasions, an aberrant recombination intermediate in which a single broken molecule engages two more dsDNA donors, we purified Dmc1-E157D and analyzed its strand exchange activity *in vitro*. Our preliminary results indicate that in comparison to wild-type Dmc1, Dmc1-

E157D is hyper-recombinant and forms more multi-invasions in D-loop assays. Our data support a model in which longer filaments are more prone to engage in aberrant recombination events, suggesting that filament lengths are normally limited by a regulatory mechanism that functions to prevent recombination-mediated genome rearrangements.

# Chapter 1: An overview of homologous recombination in *Saccharomyces cerevisiae*

## 1.1 Introduction

The integrity of a cell's genome is central to its survival and to the prevention of genome instability and tumorigenesis [1]. Damage to a cell's genome can arise through exogenous sources, such as ionizing radiation (IR), ultraviolet (UV) light, and chemotherapeutic agents [2]. DNA damage can also occur through endogenous processes, such as the formation of reactive oxygen species as a result of cellular metabolism, and replication fork stalling or collapse, as when a replication fork encounters transcription machinery, a DNA lesion, or a nick in the template [3,4]. These types of damage can result in DNA double-stranded breaks (DSBs), interstrand cross-links, and single-stranded DNA (ssDNA) gaps. Moreover, during specific cellular processes, including mating type switching in budding yeast, V(D)J recombination in immune cells, and the formation of gametes in nearly all eukaryotes, the cell induces DNA DSBs in its genome to facilitate the formation of new genetic products [5,6]. These scenarios highlight the importance of DNA repair in the survival of the cell, the maturation of immune cells, and the creation of gametes.

There are several primary pathways through which the cell can repair DNA DSBs, including non-homologous end joining (NHEJ), microhomology-mediated end joining (MMEJ), and homologous recombination (HR). Which pathway is employed by the cell to repair the damaged DNA depends on the cell's stage within the cell cycle and the nature of the DNA damage [7]. The simplest form of DNA repair is NHEJ, which involves direct ligation of the two DNA ends to one another. As expected, NHEJ is an

error-prone form of DNA repair that frequently results in small (1-4 nucleotide) insertions/deletions (indels) [8]. Use of NHEJ is precluded if the ends are incompatible with one another or if one of the ends does not have a 3'-hydroxyl or 5'-phosphate group [7]. In budding yeast, NHEJ is preferentially employed during the G1 phase of the cell cycle, when there is no sister chromatid present to act as a template for repair as required during HR [2]. However, in higher eukaryotes, NHEJ and HR compete with one another for the repair of DSBs, even during the S and G2 phases of the cell cycle [5].

If the two ends of the DNA are incompatible with one another, but there is no homologous template for recombination, the cell can utilize MMEJ to heal the DNA break. MMEJ is an inherently erroneous mechanism of DNA repair that always results in deletions flanking the break site, and it can be associated with more complex genome rearrangements including translocations and inversions [8]. MMEJ begins with nucleolytic degradation of the 5' strands of the broken DNA molecules to produce 3' ssDNA tails [7]. It then uses microhomologies of 5-25 nucleotides (nts) to align the broken ends and promote annealing. Following annealing, heterologous flaps are cleaved, DNA synthesis fills in the gaps, and the resulting nicks are ligated [9].

In contrast to NHEJ and MMEJ, HR utilizes an unbroken region of double-stranded DNA (dsDNA) to template the repair of the broken molecule. This method of DNA repair is significantly less error-prone than NHEJ and MMEJ, but it requires that a homologous template be present. HR is therefore the primary DNA repair pathway for DSBs during the S and G2 phases of the cell cycle when the sister chromatid is present in budding yeast, and a major pathway for DSB repair in higher eukaryotes [10]. Moreover, HR can be used in other contexts in which NHEJ and MMEJ are not feasible;

for instance, replication through a DNA substrate containing a nick can produce a one-ended DSB that lacks a readily available partner for end ligation or annealing [11]. Similarly, a recent study by Scully and colleagues revealed that HR, but not NHEJ, functions to promote replication fork restart after collision with a replication fork barrier [12]. Lastly, HR is a necessary and central feature to the meiotic program of nearly all eukaryotes, to physically link the homologous chromosomes (“homologs”) to one another and create the tension that is required for their segregation [13].

HR utilizes specialized enzymes, termed recombinases, which load onto a broken DNA molecule and search for a homologous, unbroken region of dsDNA that can be used to template the repair event. Upon finding a homologous template, the recombinase catalyzes a strand invasion reaction, in which the broken strand pairs with the opposite strand of the unbroken duplex DNA, thus displacing one of the strands of the donor dsDNA and forming what is known as a displacement loop, or D-loop (Figure 1.1). DNA synthesis then uses the unbroken duplex as a template to extend the end to the point at which the second end of the break can be engaged through homologous base pairing in a process referred to as annealing. Two pathways are recognized as being the primary mechanisms through which the second end can be engaged: through synthesis-dependent strand annealing (SDSA), and through the formation of a double-Holliday junction (dHJ) [5] (Figure 1.1). Should repair utilize the dHJ pathway, one of two processes, either resolution or dissolution, separates the conjoined DNA molecules and forms the products [14] (Figure 1.1).

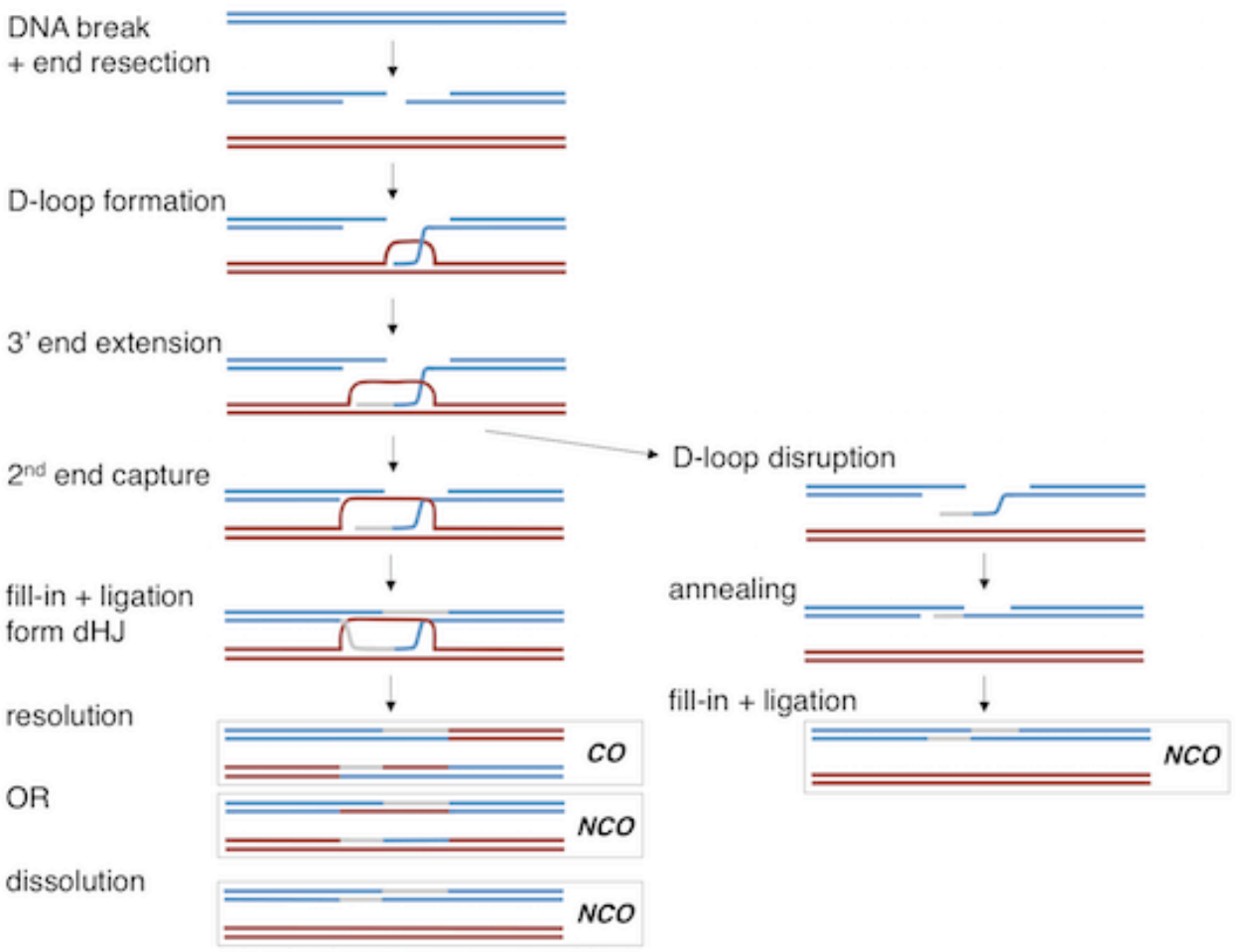


**Figure 1.1** Steps in the homologous recombination pathway. Following break formation, 5'-3' nucleolytic resection generates a 3' ssDNA tail (end resection) onto which the recombinase loads and forms a filament. It searches for a homologous dsDNA to use to template the repair event, and, once a dsDNA donor has been found, mediates strand invasion to form the D-loop. DNA synthesis extends the D-loop, and leads to one of two pathways, the double Holliday junction (dHJ) pathway (left) or the synthesis dependent strand annealing pathway (right). The dHJ pathway can be (a) resolved into a crossover (CO) or a non-crossover (NCO); or (b) dissolved into a NCO, whereas the SDSA pathway always leads to the formation of a NCO.

Historically, recombination has been conceptually divided into three phases: (1) pre-synapsis, consisting of end resection and nucleoprotein filament formation; (2) synapsis, which is composed of homology search and strand invasion; and (3) post-synapsis, including removal of the recombinase from the heteroduplex DNA formed by

the strand invasion, DNA synthesis, and resolution (Figure 1) [15]. Each of these stages can be further subdivided into a series of ordered and regulated events. The fact that HR relies on a template to prime DNA repair synthesis, whereas NHEJ and MMEJ do not, may give the impression that this is the sole cause of the high fidelity of HR. In reality, HR owes its accuracy to the fact that it is highly regulated, and that several of the key steps in the process are reversible, thereby allowing for these steps to be "proof-read" [16]. These two steps are: (1) the formation of the nucleoprotein filament by the recombinase, and (2) the formation of the nascent D-loop prior to DNA synthesis. The work presented here deals largely with the regulation of the formation of the nucleoprotein filament by the meiosis-specific recombinase Dmc1. Hence this review will focus on filament formation and disassembly in *Saccharomyces cerevisiae* ("budding yeast"), with emphasis on how results from somatic and meiotic studies can inform one another. A summary of the proteins discussed in this review is provided in Figure 1.2.

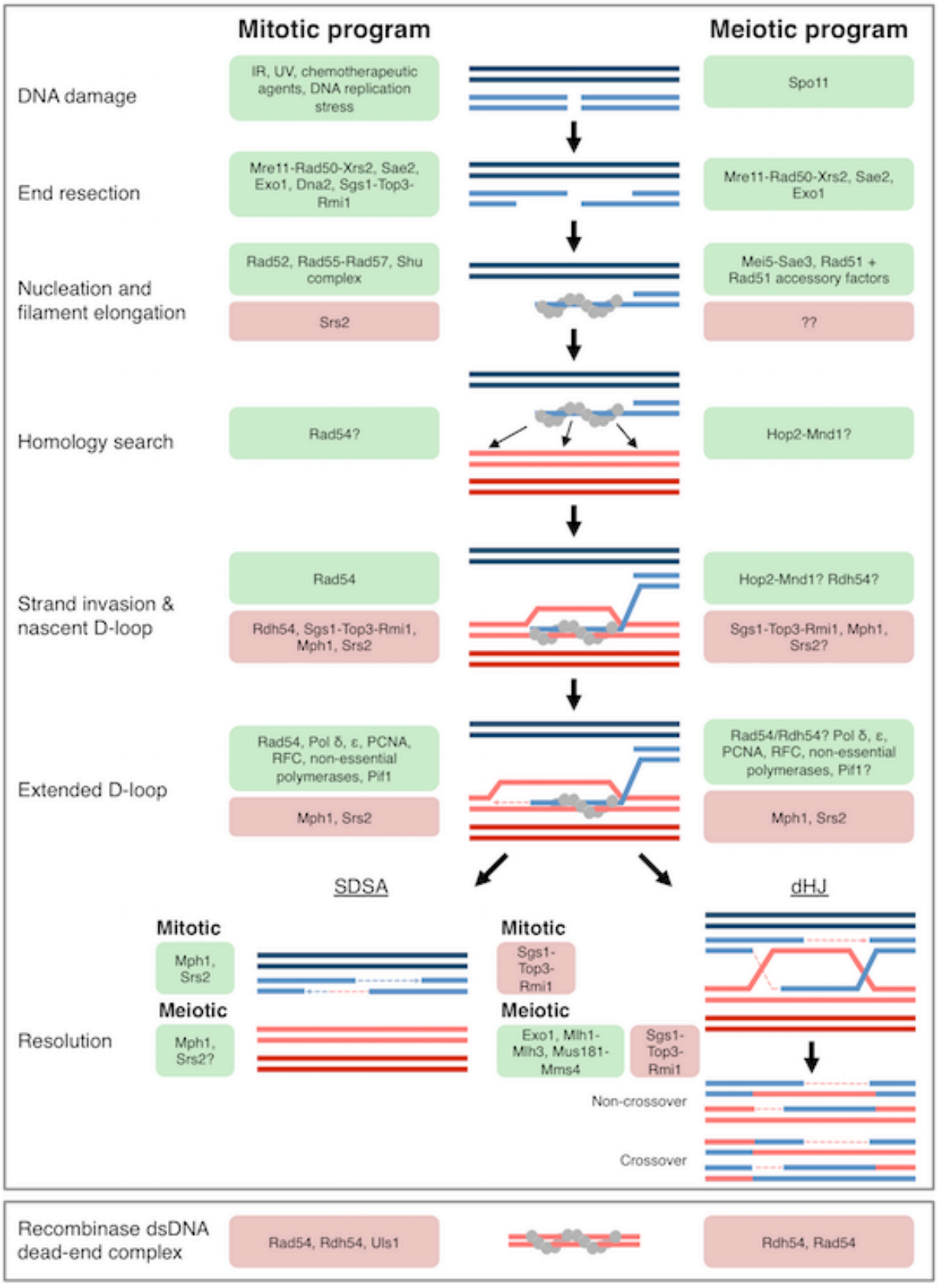


**Figure 1.2** Proteins involved in homologous recombination in budding yeast. Factors

**Figure 1.2 (continued)** that promote the formation of a recombination intermediate are shown in green, while those that prevent or disassemble the intermediate are shown in red.

## 1.2 Genetic and biochemical methods used to study HR

Here I provide a brief overview of several of the most important genetic and biochemical assays for the study of recombination. These assays form the basis for much of our current knowledge regarding the activities of recombination proteins.

### 1.2.1 One- and two-dimensional gel electrophoresis

One- (1D) and two-dimensional (2D) gel electrophoresis assays have formed the basis for many studies of homologous recombination intermediates, including DSBs, extended D-loops (or SEIs), and dHJs, as well as products, such as crossovers (COs), non-crossovers (NCOs), and ectopic recombination events [13,17,18].

1D gel electrophoresis allows for the detection of DSBs as well as recombination products. Typically, 1D gel electrophoresis is used in conjunction with a specific recombination test locus in which the broken strand and the donor, or the homologous "Mom" and "Dad" chromosomes, carry restriction enzyme site polymorphisms that allow each to be distinguished from one another [19]. Following DSB formation, samples are withdrawn from a culture, and the DNA is extracted and restriction enzyme digested. The restriction digested DNA is then run out on an agarose gel, separating it by size and allowing the resected DSBs as well as recombination products between the broken strand and the donor to be differentiated from the parental bands through differences in mass. Southern blotting by alkaline transfer is then used to detect the recombination test locus.

2D gel electrophoresis is similar to 1D gel electrophoresis, but differs in it utilizes DNA in which the joint molecules that are intermediates in the HR pathway have been preserved. The most common way that this is achieved is through covalent inter-strand crosslinking by psoralen, though other methods have also been described [20]. Because these joint molecules have a specific structure, separation of enzymatically digested DNA first by molecular weight using low voltage and a low percentage agarose gel, followed by shape using high voltage and a high percentage agarose gel, allows for the segregation of these species away from linear dsDNA [21,22]. As with 1D gel electrophoresis, 2D gel electrophoresis is usually used in combination with a specific recombination test locus. 2D gel electrophoresis has been particularly important to the study of recombination partner choice (see section on “Mediators and filament stability factors”) during meiosis [22-27], as well as to identify novel recombination intermediates [28,29], but similar assay systems have also been used to study recombination in somatic cells
[30,31].

### 1.2.2 Three-strand and displacement-loop assays

Three-strand and displacement-loop (“D-loop”) assays are both used to assess the ability of a recombinase to perform homology-dependent strand assimilation. The primary difference between these two reactions is that in the D-loop assay, the region of homology on the donor is internal, thus requiring the recombinase to mediate strand invasion and displace the complementary strand. D-loops are the *in vivo* product of Rad51/Dmc1-mediated strand exchange, formed when the recombinase nucleoprotein filament invades a homologous template. The broken strand pairs with the

complementary strand of the donor, forming heteroduplex DNA and displacing the opposite strand.

The three-strand DNA strand exchange reaction was first introduced as a means to study RecA-mediated recombination, and it utilizes a circular ssDNA in conjunction with a linear dsDNA [32]. A common and widely recognized artifact associated with the three-strand reaction involves nucleolytic resection (by a contaminating nuclease) followed by strand annealing [15]. In contrast to the three-strand reaction, the D-loop assay utilizes a linear ssDNA and a supercoiled dsDNA substrate [15,33]. In the commonly used modern version of the D-loop assay, a recombinase protein is first incubated with an ssDNA oligonucleotide to allow for the formation of a nucleoprotein filament, then a homologous supercoiled dsDNA is added to act as the target. The product of the reaction is then deproteinized and separated from the labeled ssDNA on an agarose gel to allow for detection and quantification [34]. Conventional D-loop assays use a radiolabeled ssDNA oligo to visualize the formation of the strand invasion [35]. However, recently a modification of this method that uses a fluorescently labeled ssDNA has been introduced [36].

## 1.3 Pre-Synapsis

### 1.3.1 End resection

The first pre-synaptic event is DNA end resection. End resection via nucleolytic degradation of the ssDNA strand ending 5’ at the site of the DSB is required to generate the ssDNA tail onto which the recombinase will load to carry out the recombination reaction. It consists of two steps; the first involves the cleavage of the broken DNA

molecule to generate a short ssDNA tract, followed by more extensive end resection to generate a long ssDNA tail. End resection prevents the use of NHEJ to repair the damaged DNA, thus it is a highly regulated process, particularly in higher eukaryotes [37]. The initial step in end resection process is carried out by Mre11, Rad50, and Xrs2/Nbs1, which together form a heterohexameric complex (MRX/N), consisting of dimers of each of the factors, and Sae2/CtIP [7]. MRX/N and Sae2/CtIP make an endonucleolytic cut of the 5' end internal to the break, leading to the formation of short 3'-ssDNA tails [37]. The cleavage releases the damaged DNA, and, if applicable, the associated proteins. MRX/N also signals to the cell that there is damaged DNA.

The short 3'-ssDNA tails generated by MRX/N and Sae2/CtIP are then subject to more extensive resection by one of two parallel pathways involving either the Exo1 5'-3' dsDNA exonuclease or the Dna2 endonuclease in conjunction with the Sgs1-Top3-Rmi1 (STR) complex [38,39]. The ssDNA tracts generated by long-range resection are typically ~800 nucleotides in length in meiotic cells [19,40,41], and vary in length in somatic cells, from a few hundred bases to several kilobases [42]. Resection tract lengths can be made much longer (i.e. "hyper-resected") if a recombinase fails to load or if homology search fails to find a suitable region of homology with which to template the repair event [40,42-45]. In mitotically cycling cells, in the *exo1 sgs1* background, resection tracts are very short and mediated entirely by Sae2/CtIP, indicating that these proteins delineate the two pathways that are responsible for all long-range DNA end resection [38,46]. Absent either pathway, end resection is less efficient, and the length of the ssDNA tracts generated is dramatically reduced, suggesting that one pathway cannot fully substitute for the other in its absence [38]. In contrast, in meiotic cells, the

Exo1 pathway predominates, and the Dna2-STR pathway is only required for hyper-resection when recombination fails [41,45,47].

In addition to MRX/N, Sae2/CtIP, Exo1, Dna2, and STR, another factor, known as replication protein A (RPA), also plays a recently appreciated role in end resection [48]. In fact, RPA plays a central role throughout the recombination pathway, in addition to its important functions in replication and alternate mechanisms of DNA repair. RPA is a ubiquitous high affinity ssDNA-binding protein composed of three subunits (Rfa1, Rfa2, and Rfa3) [49]. It binds non-specifically and cooperatively to ssDNA, and to a much lesser extent dsDNA and RNA [14,49,50]. RPA binding to ssDNA removes secondary structure and prevents the formation of DNA hairpins [48,51,52]. Furthermore, RPA binding to ssDNA is required for activation of the DNA damage checkpoint response to DSBs [53]. RPA is required for long-range end resection, and in somatic cells in which Rfa1 is conditionally deleted (deletion is lethal), no long-range resection is observed [48]. Thus RPA is required for Exo1- and Dna2-STR-mediated end resection both *in vitro* and *in vivo* [48,54,55]. RPA's other functions in HR will be highlighted in the subsequent paragraphs.

### 1.3.2 Nucleation and filament formation

Following end resection, the central enzyme in the recombination reaction, the recombinase, must load onto the ssDNA end and form a nucleoprotein filament in order to carry out homology search and strand exchange. The most well-characterized recombinase is the bacterial RecA [14]. The eukaryotic recombinases, Rad51 and Dmc1, are both homologs of RecA, and arose through duplication and differentiation shortly after the divergence of the pro- and eukaryotic [13]. The two proteins are highly

conserved, and share 45% sequence identity in budding yeast [56]. Rad51 serves as the central recombination protein in somatic (vegetative) cells, and also has important functions in replication fork stability. In contrast, Dmc1 plays the primary, catalytic role in meiotic recombination [26,43]. Their shared and unique properties are discussed below.

Rad51 and Dmc1 share several key structural features that carry out the recombination reaction. Each protein has two DNA binding sites, site I and site II. Site I binds ssDNA tightly and allows the protomers to cooperatively form the nucleoprotein filament. Site II, which binds with low affinity, extends and underwinds dsDNA locally to test for homology by attempting base-pairing with the tightly bound ssDNA [26,57]. At the outset of the strand exchange reaction, Rad51/Dmc1 (the slash is used to indicate that the two proteins are equivalent to one another in this context) will be bound to ssDNA via its site I binding site, but when it has completed strand invasion event, it will have catalyzed the formation of heteroduplex DNA, and will now be bound via this same site to the newly formed dsDNA. As a consequence of their need to bind both ssDNA and dsDNA in order to carry out the strand exchange reaction, Rad51 and Dmc1 have only a slight preference for ssDNA over dsDNA [58,59]. Thus the proteins frequently form filaments off-pathway on dsDNA, and a class of proteins, termed translocases, has evolved in eukaryotes to dissociate these Rad51/Dmc1-dead-end complexes, as well as to remove the recombinase from the invading ssDNA end following strand exchange to allow for DNA synthesis [60-63]. In addition, evidence suggests that at least in the context of Rad54-stimulated Rad51-mediated recombination, translocases may function to disrupt heterologous and homeologous interactions between the nucleoprotein filament and dsDNA during homology search [64].

In addition to their DNA binding activities, Rad51 and Dmc1 each contain an ATPase domain. ATP binding, but not hydrolysis is required for filament formation or for stand exchange [59,65,66]. ATP binding changes the conformation of the protein to a form that has high affinity for DNA, and is thus the active form [67]. The ADP bound form of the protein has lower affinity for DNA than the ATP-bound form, and is inactive in homology search and strand exchange. In prokaryotes, RecA ATP hydrolysis is required for filament disassembly following strand exchange, or when the protein inappropriately assembles on dsDNA [68,69]. In contrast to RecA, the eukaryotic recombinases Rad51 and Dmc1 display relatively weak intrinsic ATPase activity and rely on Rad54 family ATP-dependent dsDNA translocases to promote their dissociation, as discussed previously [58-61,63,70]. The translocases may be of particular importance in eukaryotes because, unlike RecA, *in vitro* single-molecule fluorescence imaging showed that Rad51-ADP dissociation from dsDNA is inefficient and incomplete, suggesting that the activities of the translocases are required even when Rad51 is in the ADP-bound form [71]. Moreover, Rad54 was observed to have an effect on Rad51-K191R, a Rad51 mutant that is completely defective in ATP hydrolysis, implying that the ATPase activity of Rad51 is not required for it to be removed from dsDNA by Rad54 [66,72,73]. Thus ATP/ADP binding modulates the recombinase's affinity for DNA, but hydrolysis is not required for strand exchange.

Rad51 and Dmc1 are some of the only proteins in eukaryotes that are capable of forming nucleoprotein filaments [15]. Rad51/Dmc1 filaments share a number of salient properties. Each recombinase forms filaments that are right-handed, have a pitch of ~10 nm, and a diameter of ~11-12 nm [70,74,75]. Each Rad51/Dmc1 protomer within the

filament binds ~3 nucleotides, and one turn of the filament is composed of ~6 protomers, or ~19 nucleotides [70]. This conformation stretches the DNA ~1.6-fold relative to B-form DNA [13]. Crystallization of the active budding yeast Rad51 filament by Rice and colleagues revealed several additional important features regarding how the protomers are structured within the filaments [57]. First, the ATPase site lies directly in the interface between two protomers. In this arrangement, the ATPase site of one protomer contacts the ATPase site of the adjacent protomer, providing a structural explanation for the observed coordinated ATP hydrolysis within the filament [15,57]. Moreover, the N-terminal DNA binding domain (i.e. site I) of one protomer directly contacts the adjacent protomer, which is thought to be the structural mechanism that mediates the cooperative DNA binding across protomers, and that links DNA binding to ATP hydrolysis [15,57,76]. Thus a detailed understanding of the structure of Rad51/Dmc1 filaments had led to mechanistic insight into the properties of these filaments.

The initial binding event, referred to as “nucleation,” is the rate-limiting step in the formation of the nucleoprotein filament [15,77]. Nucleation consists of 2-3 Rad51/Dmc1 protomers cooperatively binding to the ssDNA to form a nascent filament [78,79]. Following nucleation, monomers can be added to either end to grow the filament.

### 1.3.3 Mediators and filament stability factors

The primary barrier to Rad51/Dmc1 nucleation and filament formation is the fact that the ssDNA will already be bound by RPA, which it will need to displace [14]. RPA has both a higher affinity and a higher specificity for ssDNA than Rad51/Dmc1 [50,58,80-82]. RPA promotes recombination, primarily through removing secondary

structure in the ssDNA, which interferes with Rad51/Dmc1 filament formation [51,52,83]. It also prevents spontaneous annealing between homologous regions of ssDNA *in vitro* [84]. Moreover, RPA interacts with a number of DNA repair proteins, including Rad51 and Dmc1 [52,85]. Two models exist to explain these interactions: (1) the “hand-off” model, in which interactions between RPA and a given protein mediate an exchange and the incoming protein is able to trade places with RPA; and (2) the RPA conformation model, in which the binding of the incoming protein to RPA changes RPA’s conformation from an extended form with high affinity for ssDNA to a compacted form with lower affinity for ssDNA, and in the process gains access to the ssDNA itself [81]. Regardless of the mechanism, an overwhelming number of studies now suggest that RPA’s interactions with various DNA-binding proteins is essential to regulate these activities. Furthermore RPA can influence the mechanism through which the DNA damage is repaired. For instance, Symington and colleagues showed that MMEJ is dramatically elevated in the hypomorphic *rfa1* mutant, *rfa1-D228Y*, implying that RPA normally prevents MMEJ in favor of HR by inhibiting annealing between microhomologies [86,87]. Lastly, RPA binds to the displaced strand of the donor molecule during D-loop formation, preventing it from reversal and thereby stabilizing this important intermediate [88,89].

In spite of RPA’s importance to the recombination reaction, Rad51/Dmc1 interaction with RPA is insufficient to promote nucleation, and instead a separate class of accessory proteins, termed “mediators,” has evolved to promote this step [14,90,91]. Additionally, other accessory proteins are likely to be involved in filament stabilization. Given that loss of either a mediator or a filament stability factor generally leads to loss of

focus formation and the ability to carry out recombination, it can be difficult to distinguish between these two classes of effectors. In conjunction with sophisticated *in vivo* genetic studies, ensemble and single-molecule biochemistry experiments have greatly clarified the roles and mechanisms for various Rad51 and Dmc1 mediators and filament stability factors. I summarize our current understanding of Rad51's and Dmc1's accessory factors below.

Despite their many similarities, Rad51 and Dmc1 are fundamentally different in that Rad51-mediated recombination occurs predominantly between sister chromatids ("sisters") (~1 interhomolog recombination event to every 4 intersister events) [92,93], whereas Dmc1-mediated recombination preferentially utilizes the homologous chromosome as the repair template (~5 interhomolog to 1 intersister) [22]. These preferences reflect the underlying goals of the recombination events carried out by each protein; whereas the objective of recombination in somatic cells is to restore the integrity of the genome and prevent loss of heterozygosity, the purpose of meiotic recombination is to physically link the homologous chromosomes to one another, an aim that can only be achieved via interhomolog (IH) recombination, followed by resolution of the resulting recombination intermediate into a CO event [13]. Given that there are two homologous chromatids and only one sister, in both cases, partner choice during recombination defies the pattern expected by random chance (i.e. 2 interhomolog to 1 intersister) [25]. In somatic cells, the bias towards intersister (IS) recombination is likely mediated largely through sister chromatid cohesion [94]. However, the mechanism through which IH bias is achieved during meiosis is still an area of active research. Importantly, the consensus within the field is that these differences in the activities of Rad51 and Dmc1 are not

inherent, but arise through interactions with their specific accessory factors [70,95].

Moreover, Rad51 repairs certain types of DNA damage that Dmc1 is unlikely to encounter. For instance, Rad51 is recruited to repair not only two-ended DSBs, like Dmc1, but also one-ended DSBs and ssDNA gaps, which can arise during replication. The fact that Rad51 must participate in the repair of multiple types of DNA damage may explain why it appears to require more accessory factors that promote nucleation and filament stability. Thus while Rad51 and Dmc1 both possess accessory factors with similar functional roles (e.g. mediators), one must not equate these accessory factors as each fulfills a subtly different function through its own distinct mechanism.

*Rad52*

Rad52 is composed of an N-terminal RPA-binding domain and a C-terminal Rad51-interacting domain, and it acts as a Rad51 mediator, promoting Rad51 loading onto RPA-coated ssDNA [83,96-99]. In *in vitro* reconstitution experiments, if RPA and Rad51 are added to the ssDNA substrate at the same time to mimic *in vivo* conditions, RPA inhibits Rad51-mediated strand exchange [83,98,99]. Addition of small amounts of Rad52 to the reconstitution reaction restores Rad51's activity, but it does not stimulate Rad51-mediated strand exchange in the absence of RPA [83,100]. Furthermore, Rad51's rate of ATP hydrolysis, which is dependent on DNA binding and filament formation, and thus directly related to ssDNA length, is inhibited by the presence of RPA, and this inhibition is relieved upon addition of Rad52, providing further evidence that Rad52 stimulates Rad51 filament formation on RPA-coated ssDNA [99]. Single-molecule imaging experiments confirm these results, showing that Rad52 binding of RPA-coated ssDNA promotes Rad51 filament formation, and suggesting that all three

proteins may co-occupy the same ssDNA following formation of the pre-synaptic filament [101]. In addition to two-hybrid studies that indicate that Rad52 interacts directly with all three RPA subunits (Rfa1, Rfa2, and Rfa3 in budding yeast) [97], Rad52 cannot mediate Rad51 binding on ssDNA coated with *Escherichia coli* single-strand DNA-binding (SSB) protein, the functional equivalent of RPA in prokaryotes, supporting the inference that Rad52's activity is driven by specific interactions with RPA [98].

*In vivo*, Rad52 colocalizes with RPA, and it is required for normal Rad51 focus formation in mitotically and meiotically cycling cells, in response to DSB formation [102-104]. Consistent with this requirement, *RAD52* expression is induced in response to irradiation, as well as during meiosis [105,106]. In agreement with *in vitro* observations showing that sub-stoichiometric levels of Rad52 are required to stimulate Rad51-mediated strand exchange, and that higher Rad52 concentrations inhibit the reaction, in immunopreciptation experiments from yeast whole cell extract, less than 10% of the total pool of Rad51 protein is thought to be associated with Rad52 [83,98,100]. Overexpression of *RAD51*$^{+}$ allows for bypass of dominant negative *RAD52* alleles [96], again in concurrence with the model that one of Rad52's primary functions is to promote Rad51 filament formation on RPA-coated ssDNA.

Besides acting as a mediator for Rad51, Rad52 also has important additional functions in DNA annealing that are discussed in the "Extended D-loop disruption and synthesis-dependent strand annealing (SDSA)" section [107,108].

*Rad55-Rad57*

Rad55 and Rad57 are both Rad51 paralogs, having identity to the core domain of Rad51 including the Walker A and B motifs, involved in DNA binding, as well as the

ATPase domain [109,110]. Together they form a heterodimer that is involved in stabilizing Rad51 filaments [111,112] and preventing their disassembly by the ssDNA helicase Srs2 (see section on “Filament disassembly and regulation of filament length”) [113]. This stimulatory function is achieved through direct interaction between Rad55 and Rad51, though in contrast to Rad52, no interaction between Rad55-Rad57 and RPA has been reported [111,114].

*RAD55* and *RAD57* were first discovered in a screen for mutations in *Saccharomyces cerevisiae* that lead to X-ray sensitivity [115]. A key early finding as to the unique properties of *rad55* and *rad57* mutants is that they are cold sensitive; that is, their sensitivity to X-rays and γ-irradiation is exacerbated at low temperatures (23°) but partially rescued by high temperatures (36°) [111,114-116]. Cold sensitivity is often associated with mutations that affect the stability of a protein complex: in this case, the cold sensitivity of *rad55* and *rad57* mutants is likely attributable to their role in stabilizing Rad51 filaments [111,113]. Consistent with a role in filament assembly or stabilization, overexpression of *RAD51* or *RAD52* is sufficient to rescue the defects associated with *rad55* and *rad57* [111,114]. Moreover, whereas Rad51 requires Rad52 for recruitment to sites of DSBs, loss of Rad55 or Rad57 slows but does not prevent Rad51 localization to sites of DNA damage [117], and Rad51 foci can form in the absence of Rad55 and Rad57 [103,104]. Further evidence in support of a model whereby Rad55-Rad57 acts to stabilize Rad51 filaments is provided by genetic and biochemical analysis of the *rad51-I345T* mutant, which partially bypasses the requirement for Rad55 and Rad57 *in vivo*, but not Rad52 [118]. Nitrocellulose filter-binding assays revealed that Rad51-I345T binds to both ss- and dsDNA with higher affinity than wild-type Rad51, which, when

taken together with their *in vivo* findings, led the authors to propose that Rad55-Rad57 acts in a step that follows Rad52 targeting of a Rad51 monomer to RPA-coated ssDNA, and that likely involves the promotion of cooperative binding by additional Rad51 monomers.

Biochemical analyses of the function of the Rad55-Rad57 heterodimer show that it binds with high affinity to ssDNA, and that it binds dsDNA to a much lesser extent [112]. In addition, Rad55-Rad57 stimulates Rad51-mediated three-strand reactions. These findings at first suggested that Rad55-Rad57 could act as a Rad51 mediator, akin to Rad52, but such a model was inconsistent with genetic evidence showing that the functions of Rad52 and Rad55-Rad57 were distinct [118]. To resolve this discrepancy, Heyer and colleagues recently undertook a more detailed biochemical analysis as to the role of Rad55-Rad57 in Rad51-mediated strand exchange [113]. Under high salt conditions in which Rad51 alone is unable to form stable filaments, the addition of sub-stoichiometric concentrations of Rad55-Rad57 resulted in the formation of stable Rad51 filaments. The addition of small amounts of Rad55-Rad57 was also sufficient to prevent Rad51 filament disruption by the ssDNA helicase Srs2 (see section on “Filament disassembly and regulation of filament length”) [119,120], leading to the formation of longer Rad51 filaments as assayed by electron microscopy [113]. Moreover, the authors were able to use electron microscopy to observe a direct association between Rad55-Rad57 and Rad51 nucleoprotein filaments. Consistent with their biochemical analyses, deletion of *SRS2* fully suppressed the sensitivity of *rad55* and *rad57* mutants to γ-irradiation [72,113,120]. In summary, these findings support a

model whereby Rad55-Rad57 acts to stabilize Rad51 filaments and promote their elongation.

Important questions as to the mechanism through which Rad55-Rad57 stabilizes Rad51 filaments still remain. For instance, it is not presently known how Rad55-Rad57 associates with Rad51 nucleoprotein filaments, and whether this involves partial or total incorporation of the heterodimer into the Rad51 filament, or whether Rad55-Rad57 associates with the filament laterally [113]. In addition, *rad55 srs2* and *rad57 srs2* mutants are nearly as sensitive as the *rad55* and *rad57* single mutants to MMS, which interferes with DNA replication, indicating that other Rad51 accessory factors, such as the Shu complex (discussed below), could be involved in these types of repair events. Lastly, while Rad55 and Rad57 are both Rad51 paralogs and share the core ATPase domain, little is known about Rad55's and Rad57's ability to hydrolyze ATP, and whether they require ATP hydrolysis to carry out their function in stabilizing Rad51 filaments. Interestingly, mutating the conserved lysine residue within the Walker A-box of Rad55 and Rad57 to prevent the proteins from hydrolyzing ATP resulted in a DNA repair deficiency for *RAD55*, but not for *RAD57* [111].

*Shu1-Shu2-Psy3-Csm2 (Shu complex)*

Shu1, Shu2, Psy3, and Csm2 form a stable heterotetramer *in vivo* referred to as "the Shu complex;" loss of any one of the members of the complex causes similar defects, and there is no additive effect conferred by loss of an additional subunit [121-123]. Genetic analyses of the *shu1*, *shu2*, *psy3*, and *csm2* mutants revealed that loss of the Shu complex results in sensitivity to MMS, an alkylating agent that interferes with DNA replication, but these mutants are not sensitive to IR [121,124]. This finding, in

conjunction with the observations that the Shu complex prevents the formation of inter-sister joint-molecules in the *sgs1* background [125] and that the *shu* mutants accumulate mutations that depend on the translesion DNA polymerase ζ [121,126], has led to the conclusion that one of the primary functions of the Shu1-Shu2-Psy3-Csm2 heterotetramer is to regulate Rad51 filament formation in the context of DNA replication [127]. However, given that its current role in genomic stability is poorly understood, and that it is essential to promoting normal meiotic recombination [128-130], I provide an overview of this Rad51 accessory factor.

Psy3 and Csm2 are both Rad51 paralogs, and, akin to Rad55 and Rad57, the Shu complex was discovered on the basis that its loss suppresses some of the defects associated with the *sgs1* and *top3* mutations [121,130-132]. Yeast two-hybrid and *in vitro* immunoprecipitation experiments indicate that the Shu complex interacts with Rad51 and Rad52 indirectly, through an interaction between Csm2 and Rad55 [133,134]. In addition, biochemical reconstitution experiments have shown that the Shu complex acts synergistically with Rad52 and Rad55-Rad57 to promote Rad51 loading onto RPA-coated ssDNA [134]. Within the heterotetramer, Psy3 and Csm2 form a core heterodimer in which the two proteins' loop 2 domains are closely associated with one another and cooperate to support DNA binding by the complex [132]. This heterodimer forms a structure that closely resembles a Rad51 homodimer, and that binds to both ss- and dsDNA non-specifically and independent of a nucleotide cofactor [130,132]. *In vitro*, the Psy3-Csm2 heterodimer alone stimulates Rad51 loading onto RPA-coated ssDNA [134], and it increases the resistance of Rad51 filaments to salt [130]. Lastly, *in vivo* analyses by Bernstein et al. showed that loss of Shu1 resulted in increased Srs2 foci as

well as increased Srs2 recruitment to a site of an inducible DSB; from this they concluded that the Shu complex may function to prevent Srs2-mediated disassembly of Rad51 filaments in a manner that is analogous to that of Rad51 paralogs Rad55-Rad57 [113,135]. This conclusion is supported by direct interaction between Srs2 and Shu2 by yeast two-hybrid analysis [136].

In meiotic cells, all members of the Shu complex are required for normal progression, spore viability, and Rad51 focus formation [130]. However, the *psy3* and *csm2* mutants have more severe defects than the *shu1* and *shu2* mutants, supporting the biochemical data that the core Psy3-Csm2 heterodimer is required for the complex's ability to bind DNA and stimulate Rad51 filament formation. In contrast to Rad52 and Rad55-Rad57 [102], immunostaining of spread meiotic nuclei for Shu complex components failed to detect these proteins, but Psy3 nonetheless localizes to the *HIS4::LEU2* recombination hotspot during meiosis as evidenced by chromatin-immunoprecipitation experiments, suggesting that the complex is not present in high enough abundance to meet the threshold required for cytological detection [130]. Interestingly, loss of Rad51 or Rad55, the presumed interaction partners of the Shu complex, does not abrogate Psy3 recruitment to the *HIS4::LEU2* DSB hotspot, though conversely, loss of Psy3 is sufficient to prevent Rad51 recruitment. This finding implies that the Shu complex can function independent of Rad55-Rad57, at least during meiosis. In addition, when this finding is considered in conjunction with 2D gel electrophoresis analysis showing that a *csm2* mutant was phenotypically equivalent to a *rad51* mutant, it suggests a more canonical role for this complex in either Rad51 nucleation (i.e. a mediator) or filament stability. Providing further evidence against a

model whereby the sole function of the Shu complex is to prevent Rad51 filament disruption by Srs2 [135], *psy3* and *psy3 srs2* form equivalent numbers of Rad51 foci in meiotic cells [130], and by 2D gel electrophoresis, the *shu1 srs2* double mutant resembles the *shu1* single mutant [128], indicating that Srs2-mediated disruption of Rad51 filaments cannot account for the reduction in Rad51 foci and loss of IH bias observed in *shu* mutants during meiosis.

While the Psy3-Csm2 heterodimer is sufficient to stimulate Rad51 filament formation *in vitro* [130,134], and the *psy3* and *csm2* mutations confer a more severe defect in spore viability and meiotic recombination than the *shu1* and *shu2* mutations [130], all four proteins are required for wild-type spore viability and Rad51 focus formation in meiotic cells, and the *shu1* and *shu2* mutants are phenotypically equivalent to the *psy3* and *csm2* mutants with respect to their role in mitotically cycling cells [121]. These findings raise the possibility that our current biochemical understanding of the function of the Shu complex does not fully recapitulate its *in vivo* function. Moreover, it is not presently understood why the *rad55* and *rad57* mutants are more sensitive to DNA-damaging agents and exhibit more severe deficiencies in mating-type switching, gene conversion, meiotic progression, and sporulation than the *shu1*, *shu2*, *psy3*, and *csm2* mutants [24,107,114,116,130,133,137], yet overexpression of Rad51 rescues many of the defects associated with loss of Rad55-Rad57, but not loss of Csm2 or Psy3 [111,114,130,133]. Finally, the manner in which the Shu complex interacts with Rad51 requires a more detailed analysis; whereas Shinohara and colleagues found that Psy3 could affect Rad51 loading at meiotic DSB hotspots *in vivo* [130], a mutation that prevented Csm2 interaction with Rad55 eliminated the stimulatory effect of Psy3-Csm2

on Rad51 filament formation *in vitro* [134]. Further research is required to acquire a detailed mechanistic understanding of the role this complex plays in the regulation of Rad51 filament dynamics at DSBs and at the replication fork.

*Mei5-Sae3*

In *Saccharomyces cerevisiae*, Mei5-Sae3 is a meiosis-specific accessory factor that interacts with Dmc1 [138-140]. Homologs of Mei5-Sae3 in other organisms include Sfr1-Swi5 in fission yeast and MEI5-SWI5 in higher eukaryotes including mice and humans, with no known homolog in plants [141]. In fission yeast, Sfr1-Swi5 interacts with and promotes both Rad51 and Dmc1 focus formation, while in mice and humans MEI5-SWI5 appears to interact with Rad51 only [142-144]. Here I summarize the genetic and biochemical attributes of Mei5-Sae3 in budding yeast, though a more comprehensive overview of Mei5-Sae3 and its homologs in other organisms is presented in Chapter 3.

Mei5 and Sae3 are meiosis-specific proteins that together form an obligate heterodimer, Mei5-Sae3 [138,139,145]. Mei5-Sae3 forms immunostaining foci during meiosis, and colocalizes with Dmc1 and other components of the HR pathway [139,145]. In addition to requiring one another for recruitment to chromatin, Mei5-Sae3 foci fail to form in *dmc1* mutants, and likewise Dmc1 requires Mei5-Sae3 for recruitment to chromatin. As follows from Dmc1's requirement for Mei5-Sae3 for recruitment to chromatin, recombination in *mei5*, sae3, and *mei5 sae3* mutants is absent by 2D gel electrophoresis [80], very few COs are formed, and DSBs persist and become hyper-resected [138,139,145]. Given these serious deficiencies in meiotic recombination, it follows that meiotic progression is severely delayed in *mei5*, *sae3*, and *mei5 sae3*

mutants, and few viable spores are formed [138,139,145,146]. These findings indicate that Mei5-Sae3 is involved in Dmc1 filament formation and/or stabilization. Mei5-Sae3 promotes Dmc1 filament formation/stabilization through direct interaction with Dmc1, through the N-terminal portion of Mei5 [139].

Purification of Mei5-Sae3 showed that the complex binds both ss- and dsDNA, with a strong preference for the former [147]. The DNA binding activity of the complex is afforded by Mei5, with no contribution by Sae3 [148]. Mei5-Sae3 also interacts with RPA [52,147], and, consistent with genetic data, it promotes Dmc1 loading onto RPA-coated ssDNA [147], and stimulates Dmc1-mediated strand exchange in D-loop assays [26,52]. Purified Mei5-Sae3 and Rad51 interact with one another through Mei5's N-terminal domain, similar to Mei5-Sae3 and Dmc1, however the biological relevance of this activity remains unclear. It has been suggested that Mei5-Sae3 prefers to bind a DNA fork structure *in vitro* [148], though again no *in vivo* significance for this finding has been shown.

Whereas Mei5 is required for the complex's interaction with Dmc1 and ssDNA [139,148], little is known about the role of Sae3 in promoting Dmc1-mediated recombination. In addition, the molecular mechanism through which Mei5-Sae3 stimulates Dmc1 filament formation/stability was unclear, but we provide evidence in Chapter 3 that Mei5-Sae3 functions to maintain filaments in the active, ATP-bound form by promoting ADP release, believed to be the rate-limiting step in the RecA/Rad51/Dmc1 ATPase cycle.

*Rad51*

This section focuses on Rad51's function as a Dmc1 accessory factor during meiosis. Rad51's genetic and biochemical attributes as a strand exchange protein in somatic cells are discussed elsewhere.

During meiosis, the strand exchange activity of Rad51 is inhibited by the meiosis-specific protein Hed1 [140,149], converting it into a Dmc1 accessory factor [26,150]. In its capacity as a Dmc1 accessory factor, Rad51 is required for the formation of bright Dmc1 immunostaining foci [150], though dim Dmc1 foci are detectable in the *rad51* background [151]. It is also required for the formation of bright Mei5-Sae3 foci [139], and we offer further insight into the significance of this finding in Chapter 3. While both Rad51 and Dmc1 are RecA homologs, and organize into filaments, evidence suggests that the two proteins form homo-polymeric filaments that are directly adjacent to one another on the same strand of ssDNA rather than forming a single (i.e. mixed) filament containing both Dmc1 and Rad51 protomers [152,153]. Furthermore, *rad51* mutants are defective in HR, displaying high levels of IS joint molecules at the expense of IH joint molecules as assayed by 2D gel electrophoresis [24]. Likely as a result of the decrease in IH recombination, CO formation is reduced in the *rad51* background, as shown by 1D gel electrophoresis, and DSBs become hyper-resected [44,151]. Curiously, meiotic ectopic recombination, which can be visualized on 1D gels at the *HIS4::LEU2* hotspot as a recombination event that involves the native *LEU2* locus [17], is increased in *rad51* strains [154]. Importantly, using the *rad51-II3A* allele, in which three alanine substitutions were made in DNA binding site II of Rad51, preventing it from carrying out homology search and thus strand invasion, Bishop and colleagues showed that Rad51's strand exchange activity is completely dispensable for the formation of normal double

Holliday junction recombination intermediates during meiosis [26]. In conjunction with prior genetic evidence, such as the fact that *dmc1* strains are totally defective in meiotic recombination [27,43] whereas recombination still occurs in *rad51* strains, albeit with severe deficiencies, the work by Cloud et al. showed conclusively that Dmc1 is the primary recombinase during meiosis, and that Rad51 serves as its accessory factor [26,155]. Rad51's function as a Dmc1 accessory factor involves direct interactions between the two proteins, as we demonstrate in Chapter 3. Taken together, these studies suggest that Rad51 is involved in stabilizing, but not nucleating, Dmc1 filaments *in vivo*.

In *in vitro* reconstitution experiments, Rad51 stimulates Dmc1's strand exchange activity, alone [26], and in conjunction with Dmc1's other accessory factors [52], consistent with its proposed *in vivo* function of promoting Dmc1 filament formation. Interestingly, single molecule imaging studies show that when mixed together, Rad51 and Dmc1 self-segregate into discrete, side-by-side filaments [95], supporting *in vivo* cytological observations [153]. When purified Rad51 and Mei5-Sae3 are mixed together, the two proteins interact with one another through Mei5, though Mei5-Sae3 does not stimulate Rad51-mediated recombination [148]. Given that Mei5-Sae3 [139] and Rad51 (results presented in Chapter 3) each interact with Dmc1 directly, and that Rad51 is competent to influence Dmc1 activity independent of Mei5-Sae3 (results presented in Chapter 3), the biological significance of the interaction between budding yeast Rad51 and Mei5-Sae3 is ambiguous.

As a result of Rad51's function as a Dmc1 accessory factor during meiosis, Rad51's accessory proteins, including Rad52, Rad55-Rad57, and the Shu complex are

also required for normal Rad51 DNA binding dynamics [102,130] and therefore also required for normal Dmc1-mediated recombination. Mutants lacking one or more of these Rad51 accessory factors display a severe defect in meiotic IH recombination, and instead perform recombination predominantly between sisters, akin to the *rad51* mutant [24,129,130,156]. It should be noted, however, that analysis of the *rad52* mutant is complicated by its additional function in annealing complementary ssDNA strands (see section on “Extended D-loop disruption and SDSA”) [157]. Consistent with their defects in Rad51 and Dmc1 focus formation during meiotic prophase I, and with their loss of IH bias in Dmc1-mediated recombination, *rad52*, *rad55*, *rad57*, and *shu* mutants display low spore viability and decreased meiotic progression [116,130,137]. The role of Rad54, another Rad51 accessory factor, in meiotic and somatic cells is discussed below. While some authors have interpreted these results to mean that Rad51 accessory factors are directly involved in promoting IH recombination, it is much more likely that the loss of IH bias in these mutants reflects decreased recruitment of Dmc1 accessory factor Rad51 to sites of meiotic recombination.

The importance of Rad51 to Dmc1-mediated strand exchange, and in particular to IH bias, cannot be understated. While there are other positive regulators of IH bias, including the DNA damage signaling checkpoint proteins [17,158], components of the synaptonemal complex [159], and Mek1, a meiosis-specific kinase [27,158,160-162], the role of these factors in promoting IH bias is likely to be indirect. For instance, at least one of the ways that Mek1 promotes IH bias is through phosphorylating and thereby activating Hed1, the protein that inhibits Rad51’s strand exchange activity [163]. In contrast, Rad51, in addition to Dmc1, likely has a direct role in achieving IH bias during

meiosis [25]. Importantly, neither Dmc1 [24] nor Rad51 [27] on its own is competent to perform the meiotic recombination that is observed in wild-type cells (i.e. that has a ~5:1 ratio of IH to IS recombination events). IH bias is thus an emergent property of cooperation between the two recombinases [13]. While models invoking nuclear architecture reorganization as a means to favor IH recombination over IS strand invasion are intriguing, these models fail to explain why each recombinase on its own fails to achieve IH bias, and why meiotic recombination frequently occurs between sister chromatids (V. Böerner unpublished results) [162]. Negative regulation of IS recombination is also important to IH bias [13]. In addition to Hed1, Dmc1 itself [27,164], inhibit Rad51-mediated strand exchange during meiosis, representing an important means of suppressing IS recombination. Furthermore, new evidence suggests that IS recombination is prevented through the disassembly of nascent IS exchanges (see section on “Nascent D-loop disruption”) (V. Böerner unpublished results).

Thus Rad51’s and Dmc1’s accessory factor

### 1.3.4 Translocases

The translocases Rad54 and Rdh54 (Tid1) function at multiple stages in the HR pathway, with established functions in pre- and post-synaptic events, and possible functions during synapsis. I provide an overview of their activities here, and briefly mention their role in later stages where appropriate.

As previously mentioned (see section on “Nucleation and filament formation”), translocases are important effectors of Rad51/Dmc1 activity because Rad51 and Dmc1 have relatively little preference for ssDNA over dsDNA [58,59], and dsDNA is the far more abundant species in the nucleus. Their propensity to bind dsDNA causes Rad51

and Dmc1 to form non-productive, off-pathway structures on dsDNA, a phenomenon that is particularly apparent in the absence of the translocases, whose role it is to disassemble Rad51- and Dmc1-dsDNA complexes [61,63,165]. Thee off-pathway structures formed by Rad51 and Dmc1 on dsDNA interfere with Rad51/Dmc1 recruitment to sites of DSBs, and impose a barrier to normal chromosome segregation [61,63,152]. In addition, the activity of the translocases is required to remove Rad51/Dmc1 from the 3'-OH end following strand invasion to allow for end extension by various DNA polymerases [62,117] (see section on "End extension"). Lastly, Rdh54 has a newly discovered non-enzymatic function in regulating nascent D-loop disassembly [166].

Rad54 and Rdh54 are both members of the helicase-like superfamily 2, which have a core structure that bears homology to the central region of RecA, consistent with the observation that both these classes of proteins undergo conformational changes in response to ATP binding and hydrolysis [167,168]. Rad54 and Rdh54 share a core domain, but have substantially different N-terminal domains [169], explaining why the two proteins can only partially substitute for one another. In particular, the N-terminal domain of Rad54 has been demonstrated to be important for its interaction with Rad51, and with ssDNA [64,170-172]. Both proteins are dsDNA-specific ATPases that are able to quickly and processively translocate along dsDNA, but they differ from classical DNA helicases in that they are unable to separate dsDNA strands [173-176]. With respect to Rad54, this dsDNA-dependent ATPase activity is enhanced through interactions with Rad51, and by ssDNA containing branched molecules, such as a D-loop [60,172,177].

Given their structural and functional similarities, Rdh54 likely shares many of these properties with Rad54.

Rad54 and Rdh54 can stimulate both Rad51- and Dmc1-mediated D-loop formation *in vitro*, though Rad54 has a greater stimulatory effect on Rad51 and conversely Rdh54 has a larger effect on Dmc1 [172,173,176,178]. This stimulatory effect is mediated through direct interactions between Rad54 and Rdh54 with Dmc1 and Rad51 [170,171,173,176]. Though conventional D-loop assays use a super-coiled dsDNA plasmid as the donor, Rad54 has been shown to promote Rad51 D-loop formation with a relaxed dsDNA plasmid [179] and even linear dsDNA [64]. Negative supercoiling is thought to promote homology search and strand invasion because as the donor DNA is stretched, the supercoils relax, releasing energy that drives pairing between the broken strand and the complementary strand of the donor [180]. Importantly, these findings rule out the possibility that Rad54 stimulates Rad51 D-loop formation through affecting the topology of the target dsDNA. While many models have been proposed to explain the stimulatory activities of Rad54 and Rdh54 on Rad51/Dmc1 D-loop formation, a unifying model in which Rad54 translocates along the nascent D-loop, removing Rad51 and forming heteroduplex DNA simultaneously, has only been proposed recently [64].

Somatic cells require the activity of at least three translocases, Rad54, Rdh54, and Uls1, each of which act partially redundantly with one another [63,115,181-183], but that likely have subtly different primary functions [166,176]. Recombination is somewhat impaired in the absence of any one of the translocases, though the double and triple mutants are generally more severe than the single mutants, again pointing to their

functional redundancy [63,182,184]. Similarly, meiotic yeast requires the activities of both Rad54 and Rdh54, but like the somatic program the phenotypes associated with each of the single mutants are mild [61,184]. Genetic observations suggest that Rad54's activity is more important in somatic cells than Rdh54, and conversely that Rdh54 is more important during meiosis [152,184,185], mirroring the *in vitro* observations.

In sum, the activities of the translocases are essential throughout the recombination program, and though genetic and biochemical observations support the conclusion that the proteins act partially redundantly with one another, each likely has specialized functions.

### 1.3.5 Filament disassembly and regulation of filament length

Srs2 is a member of the helicase superfamily 1 group of proteins. It translocates along ssDNA in the 3' to 5' direction, and has DNA-dependent ATPase activity [186]. Like other members of the helicase superfamily 1, Srs2's DNA unwinding activity, in contrast to its ssDNA translocase activity, requires oligomerization [187]. Srs2 interacts directly with Rad51, triggering Rad51 nucleoprotein filament disassembly and suppressing D-loop formation by a mechanism that is independent of its ability to disrupt extended D-loops [119,120,188]. This anti-recombinogenic activity of Srs2 has been labeled as Srs2's "strippase" activity to distinguish it from its pro-recombinogenic role in promoting synthesis-dependent strand annealing (SDSA). It is thought that Srs2's function as a Rad51 strippase is important when later steps in the HR pathway, such as homology search and strand invasion, are impaired, because dismantling the filaments allows the cell to utilize other methods of DNA repair, such as single-strand annealing or

MMEJ [120]. Its activity is directly opposed by Rad55-Rad57 [113], and may also be inhibited by the Shu complex [135] and Rad52 [189]. While *in vitro* studies indicated that Srs2 may destabilize filaments through the triggering of Rad51's ATPase activity [190], *in vivo* studies showed that the Srs2 mutant that should be defective for this function is competent to dismantle Rad51 filaments [123]. Similar to Rad54/Rdh54, Srs2 likely disrupts Rad51 filaments by knocking them off as it translocates along ssDNA. Importantly, Srs2 can only act on Rad51, and not Dmc1 [123].

In spite of the fact the resection tract lengths can be quite long in somatic and meiotic cells, Rad51/Dmc1 filaments visualized by conventional light microscopy are typically shorter than 200 nanometers in length, which corresponds with the resolution limit of visible light [13]. Assuming that these Rad51/Dmc1 foci represent filaments with properties as described (see section on "Nucleation and filament formation") such that one 10 nanometer turn of the helical filament correlates with ~19 nucleotides, this implies that a Rad51/Dmc1 focus contains less than 400 nucleotides. Moreover, super-resolution imaging of meiotic Rad51 and Dmc1 foci by direct stochastic optical reconstruction microscopy (dSTRORM) showed that these foci are on average ~100 nucleotides long in wild-type cells, and that multiple foci can form on one side of a DSB [153]. Though these measurements in wild-type cells indicate that Rad51/Dmc1 filaments are relatively short, Dmc1 filaments become elongated in the *mnd1* background when there is no strand exchange (see section on "Rad51/Dmc1 accessory factors in homology search and strand invasion") and DSBs become hyper-resected, indicating that the formation of longer structures is possible [153]. Thus cytological observations of Rad51/Dmc1 filaments in somatic and meiotic cells indicate that these

filaments are typically much shorter than the total length of ssDNA generated by end resection.

Supporting this inference, genetic analyses of mutants deficient for long-range resection, such as *exo1* and *exo1 sgs1*, support normal levels of recombination in somatic and meiotic cells alike, in spite of the fact that only 100-600 nucleotides of ssDNA are exposed in these backgrounds [38,41,46]. Taken together, these results support the claim that long Rad51/Dmc1 filaments do not form in wild-type cells, and are not required for the normal HR program. Despite these observations, long Rad51/Dmc1 filaments are frequently used in biochemical reconstitution and single-molecule imaging experiments.

What factors could function to control Rad51/Dmc1 filament lengths *in vivo*? Obvious positive regulators of filament length include Rad52, Rad55-Rad57, and the Shu complex for Rad51, and Mei5-Sae3 and Rad51 for Dmc1. Rad55-Rad57, the Shu complex, and Rad51 may be of particular interest because they are not strictly required for Rad51/Dmc1 focus formation, yet dimmer foci are formed in their absence (see section on “Mediators and filament stability factors”), implying that these filaments are shorter. Mediator activity may be important not only in allowing the filament to form, but also in its organization. For instance, frequent independent nucleation events would lead to the formation of short filaments, because each Rad51/Dmc1 protomer binds 3 nucleotides, meaning that there is a two out of three chance that two independent nucleation events will be out of register with one another [15]. Moreover, Rad55-Rad57 and the Shu complex been shown to have a role in preventing Srs2-driven Rad51 filament disassembly (see section on “Mediators and filament stability factors”). The fact

that multiple Rad51 accessory factors have been implicated in preventing Srs2-mediated disruption of Rad51 nucleoprotein filaments suggests that there may be a more subtle interplay between these accessory factors and Srs2 than one that strictly involves Rad51 filament disassembly. The only candidate for negative regulators of filament length is Srs2, which may not only disassemble Rad51 filaments in cases where recombination is non-productive, but engage in a regulatory balance with Rad51 accessory factors to maintain filaments at appropriate lengths *in vivo*. No Srs2-like activity has been identified yet for Dmc1, making it an important area where future research should be focused.

## 1.4 Synapsis

### 1.4.1 Homology search mechanism

DNA DSBs, arising either spontaneously or through the meiotic program, trigger rearrangements to the nuclear architecture that are thought to facilitate homology search [4,191,192]. In addition, in meiotic cells, the sister chromatids are configured into a linear array of chromatin loops connected by a central axis that is made up of meiosis-specific proteins [193]. This organization promotes homologous recombination and the pairing of homologous chromosomes.

Homology search is the process through which RecA/Rad51/Dmc1 filaments rapidly scan the genome through transient binding and unbinding of dsDNA to identify an intact donor dsDNA with homology to the ssDNA onto which they are loaded. Studying homology search *in vivo* or *in vitro* is quite difficult because homology recognition is transitory, and immediately triggers strand invasion. Multiple mechanisms

through which RecA/Rad51/Dmc1 could carry out homology search have been proposed, though these models are not mutually exclusive [194,195].

### 1.4.2 Rad51/Dmc1 accessory factors in homology search and strand invasion

*Rad54*

Rad54 has been shown to disassemble Rad51-mediated D-loops in *in vitro* reconstitution experiments (see section on “Nascent D-loop disruption”) [196]. While this activity is suppressed by use of ssDNA oligos that mimic physiological substrates, Wright and Heyer suggested that its purpose may be to disrupt interactions between the Rad51 nucleoprotein filament and homeologous sequences during homology search [64]. Rad54’s activity has also been implicated in Rad51 homology search via several other mechanisms [197-200]. For instance, Alexeev et al. showed that Rad54 can engage in nucleosome remodeling, which could in principle stimulate Rad51 homology search *in vivo*, but this model fails to explain why Rad54 stimulates Rad51 in D-loop assays in which the dsDNA target is not chromatinized [198].

*Hop2-Mnd1*

Hop2-Mnd1, the last of Dmc1’s accessory factors, is notable in that it is not required for presynaptic events. Hop2 and Mnd1 are both meiosis-specific proteins, and they form an obligate heterodimer, depending on one another for recruitment to chromatin [201-203]. Surprisingly, the two proteins do not depend on DSBs for focus formation, nor do they colocalize with Dmc1, Rad51, or other components of the recombination machinery [201,204,205]. Similarly, chromatin immunoprecipitation experiments found that Hop2-Mnd1 does not associate preferentially with recombination hotspots, which are regions of the genome that are very likely to incur a Spo11-induced

DSB, and thus undergo recombination [204]. Dmc1 and Rad51 foci form normally in the absence of Hop2 and Mnd1, though they persist [204,205] and Dmc1 foci become elongated in the *mnd1* background [153]. In *hop2* and *mnd1* mutants, Dmc1-mediated recombination is totally defective, and no joint molecules are formed by 2D gel electrophoresis, leading DSBs to persist and become hyper-resected, and for CO formation to be reduced [27,202,204-207]. Meiotic progression is thus very low in the *hop2* and *mnd1* backgrounds [27,146,205,207]. Together, this genetic data has led to the conclusion that Hop2-Mnd1 is involved in Dmc1-mediated strand invasion at a stage that comes after filament formation and elongation.

*In vitro*, Hop2-Mnd1 has a strong preference for binding dsDNA over ssDNA [203], consistent with its *in vivo* pattern of focus formation. The N-terminal regions of both Hop2 and Mnd1 are responsible for this dsDNA binding activity [207]. Mouse Hop2-Mnd1 has been shown to interact directly with mouse Dmc1 [208], likely through the N-terminal portion of Mnd1 [207]. Hop2-Mnd1 greatly stimulates Dmc1-mediated D-loop formation, and strand assimilation is optimal when Hop2-Mnd1 is pre-incubated with the dsDNA donor [52,203,209]. Unlike Rad54/Rdh54, which also stimulates Rad51/Dmc1-mediated recombination, Hop2-Mnd1 does not contain an ATP-binding domain, nor has ATPase activity been detected for this complex [203].

The role of Hop2-Mnd1 in Dmc1-mediated recombination remains elusive. One interesting model for Hop2-Mnd1's role in Dmc1-promoted strand invasion is that Hop2-Mnd1 functions in Dmc1 homology search by non-specifically altering the structure of duplex DNA, ultimately leading to IH bias [204,210,211]. However, more research is

required to determine whether this model fully explains Dmc1's requirement for Hop2-Mnd1 in promoting HR.

## 1.5 Post-synapsis

### 1.5.1 Nascent D-loop disruption

D-loop formation is catalyzed by Rad51/Dmc1 invasion of a homologous dsDNA template, followed by pairing of the broken strand with the complementary strand of the donor, which displaces the opposite strand and leads to the formation of heteroduplex DNA (Figure 1.1). A nascent D-loop is one that has not yet been extended by a DNA polymerase. Nascent D-loop disassembly thus returns the substrates to their original form and allows for re-initiation of homology search. Besides the disassembly of aberrant recombination intermediates containing mismatches (reviewed in [212]) and involving more than one donor ("multi-invasions") [213], the role of nascent D-loop disassembly remains poorly understood. However, recent work by Piazza et al. shows that nascent D-loop disassembly is pervasive, even between perfectly matched sequences [166]. To explain this seemingly paradoxical and wasteful activity, it has been proposed that nascent D-loop disruption may (1) promote homology search; and (2) prohibit the formation of dHJs, which are disfavored is somatic cells, through preventing D-loop formation and extension on both strands [214].

A major barrier to studying nascent D-loop disruption is that these intermediates cannot be visualized by 2D gel electrophoresis [13,25,193,214]. As such, many genetic studies of D-loop disassembly factors have relied on genetic endpoint analysis [30,215], in which it is difficult to distinguish the roles of each of these factors on nascent and

extended D-loops. To address this problem, Piazza et al. has recently developed the D-loop capture assay, which uses the principle of proximity ligation to detect nascent D-loops [166]. This novel assay system was the basis for their findings reported in Piazza et al. 2019, discussed below.

In somatic cells, genetic analyses of recombination intermediates and products in conjunction with *in vitro* reconstitution studies have provided evidence that the helicases Mph1 and Srs2, as well as the helicase-topoisomerase complex Sgs1-Top3-Rmi1 (STR), mediate nascent D-loop disruption [166,216-218]. Furthermore, use of the D-loop capture assay in combination with genetic analysis provided evidence for the existence of two nascent D-loop disassembly mechanisms, a primary pathway that involves the concerted activity of Mph1 and STR, and a minor pathway that relies on Srs2, which are delineated by an ATPase-independent function of Rdh54 [166]. These three factors, Mph1, STR, and Srs2, are also all implicated in disassembling aberrant multi-invasion recombination events [213]. Both Rad54 and Rdh54 were also shown to disrupt D-loops [175,196], even as they promote their formation in other reconstitution experiments. However, this activity is eliminated for Rad54 if ssDNA oligos are modified to mimic *in vivo* substrates by increasing their length from ~90 nucleotides to ~600-1200 nucleotides, and by adding a dsDNA tail [64].

Studies that have implicated D-loop disassembly factors directly in nascent D-loop disruption during meiosis are limited, in large part due to the difficulties associated with nascent D-loop with detection. However, the activities of STR, Mph1, and Srs2 have all been shown to be necessary for wild-type recombination in meiotic cells, and at least some of this requirement is likely due to their processing of nascent D-loops (V.

Böerner unpublished results) [29,128,219-225]. For instance, Böerner and colleagues have shown a role for Mph1 in preventing IS recombination in meiotic cells, which likely acts at the nascent D-loop stage to disassemble strand invasion events that occur between sisters (V. Böerner unpublished results). Multiple studies have reached conflicting conclusions as to whether *srs2* increases the formation of abnormal multi-chromatid structures in meiotic cells, but agree that *srs2* cells have decreased formation of both COs and NCOs [128,130,225]. In addition, cytological observations of *srs2* mutants have provided evidence that Srs2's Rad51 filament disassembly activity does not extend to Dmc1, and that large Rad51 aggregates form in its absence, likely as a result of Rad51 strand exchange following the normal meiotic recombination program [123,225]. These results highlight the need for a more detailed analysis of the role of nascent D-loop disassembly in meiotic recombination. Though obstacles exist to adapting the D-loop capture assay to use in meiotic cells, including the fact that the assay measures recombination between a broken site and an ectopic donor, adaptation of the D-loop capture assay to measure nascent D-loop formation between sister chromatids and homologous chromosomes would greatly expand the scope of information that one could obtain from its use in meiotic and somatic cells alike [166].

### 1.5.2 End extension

Following strand invasion and the formation of a nascent D-loop, D-loop extension by a DNA polymerase, templated by the homologous strand of the intact duplex with which the broken strand is now paired, irreversibly transitions the recombination intermediate to a later stage in the HR pathway (Figure 1.1). Because it is an irreversible reaction, D-loop extension is likely highly regulated, though little is

known about these events. Only D-loops in which the 3’ end of the broken strand is incorporated into the D-loop are competent to be extended, though internal D-loops are readily formed both *in vitro* and *in vivo* [64,213]. Prior to end extension, Rad54 must remove Rad51 from the 3’ end of the D-loop to allow access by the DNA polymerase, or alternatively, structure-selective nucleases can cleave an internal D-loop to create a *de novo* 3’ end [62,117,180].

Recombination-associated first end synthesis requires strand displacement activity, meaning that the polymerase must be able to displace downstream DNA that it encounters during synthesis, similar to the DNA synthesis that is associated with replication of the lagging strand [226]. Second end synthesis, in the context of the gap-filling reaction that is required during the formation of a dHJ or during SDSA, may or may not require strand displacement. These two modes of second end synthesis differ from one another in that in the former pathway (dHJ formation) the template will be topologically constrained, whereas in the latter pathway (SDSA), there is no such barrier. Surprisingly, recombination-associated DNA synthesis is less processive and more mutagenic than replicative DNA synthesis, making it an important area of research [227,228].

The primary polymerase implicated in recombination-associated first end synthesis is DNA polymerase δ, the preferred lagging strand polymerase during DNA replication [229-235]. Pol δ is highly processive, and this processivity depends on its interaction with proliferating cell nuclear antigen (PCNA), a DNA sliding clamp that encircles the DNA and anchors the polymerase to it [233,236]. In addition, Pol δ has a 3’-5’ exonuclease activity that allows it to perform proofreading, improving its fidelity and

allowing it to engage mismatched primer templates [237]. The low-fidelity non-essential polymerases, including η, κ, Rev1, ν, and ζ, have also been implicated in recombination-associated DNA synthesis, likely playing roles that are context dependent [226,236,238-241]. Importantly, the mutagenicity of the synthesis reaction is determined by the involvement of the low-fidelity polymerases, thus underlining the importance of determining which polymerases are involved and under what circumstances [226]. Little is currently known regarding recombination-associated second end synthesis, though evidence suggests that Pol ε may be involved [226,230].

### 1.5.3. Second end capture and resolution

Second end capture, the engagement of the second end of the DNA DSB, can happen through one of two pathways (Figure 1.1). First, the extended D-loop can be disrupted by a helicase in a process referred to as SDSA. If the end that has formed the invasion has been sufficiently extended, it will now contain significant homology to the other end of the DSB, the two ends will be able to pair with one another, and gap filling and ligation will complete the break repair process. SDSA always leads to the formation of a NCO, the preferred outcome in somatic cells because it prevents loss of heterozygosity and potential genome rearrangements that could arise through CO formation. However, SDSA is also a common outcome during meiosis and gives rise to the majority of NCO events [242]. Second, the other end of the break can be engaged by pairing with the displaced strand of the duplex, forming a structure referred to as a dHJ. DHJs can also arise through independent invasion and extension of both ends of the DSB into the same donor. DHJs can be processed to form a CO, leading to the physical connections between homologous chromosomes that are the ultimate goal of

the meiotic recombination program. However, these structures are generally regarded as potentially deleterious in somatic cells, and in this context mechanisms have evolved to promote their dissolution and resolution into NCOs.

In addition to its previously described role as a Rad51 mediator, Rad52 also functions to promote annealing between complementary strands of RPA-coated ssDNA, and is likely important to both mechanisms of second end capture [84,157,243,244]. This function is essential both during HR, as described, as well as during SSA, a separate homology-dependent DNA repair pathway, whose relevance is thought to be limited to DSBs that occur between two direct repeats. The fact that Rad52 functions in multiple DNA repair pathways is thought to explain why loss of *RAD52* confers the most severe DNA repair defects out of all of the *RAD52* epistasis group genes, which also include *RAD51*, *RAD54*, *MRE11*, *RAD50*, *XRS2*, *RAD55*, and *RAD57* [245]. Rad52 is aided in this capacity by a second protein with similar biochemical attributes, Rad59 [246-248].

*Extended D-loop disruption and SDSA*

SDSA must always proceed through a step that involves helicase-mediated disruption of an extended D-loop. Genetic and biochemical data provide evidence for the function of at least two helicases that are capable of disrupting extended D-loops in somatic cells, Mph1 and Srs2, with Mph1 processing the majority of extended D-loops and Srs2 making a minor contribution [166,188,215,217,249]. In addition to promoting SDSA, emerging research suggests that extended D-loop disruption is pervasive and that it can facilitate template switching, even during the normal repair process.

*Double Holliday junctions and their resolution*

DHJs are disfavored in somatic cells because they have the potential to lead to the formation of a CO product, which could result in loss of heterozygosity [180]. In contrast, given that the goal of the meiotic recombination program is to physically link the homologous chromosomes via the formation of a reciprocal CO, dHJs are the preferred outcome during meiosis [13].

DHJs can be resolved either by nucleolytic processing (“resolution”), or by dissolution (Figure 1.1). DHJ resolution is catalyzed by the structure-selective endonucleases Mus81-Mms4, Slx1-Slx4, and Yen1 in somatic cells, and, in addition to these factors, Exo1 and Mlh1-Mlh3 in meiotic cells [250]. Symmetrical cleavage of the two phosphodiester bonds across the Holliday junction resolves the intertwined strands into nicked duplex DNA that can then be ligated to complete the break repair process [180]. They can either cleave the two junctions in the same plane, resulting in the formation of a NCO, or in opposite planes, leading to the formation of CO. During dHJ dissolution, STR acts to promote branch migration of the two Holliday junctions toward one another, forming a hemicatenane, and then this structure is dissolved into a NCO [251]. DHJ resolution and dissolution both occur during the normal somatic and meiotic repair programs.

Due to their significance to the meiotic recombination program, the formation of dHJs and their subsequent resolution into a CO prodruct are highly regulated. First, the Msh4-Msh5 heterodimer specifically recognizes Holliday junctions and encircles them, stabilizing the nascent joint molecule and protecting it from dissolution, and the meiosis-specific Mer3 helicase may promote their formation [193]. Second, the majority of COs in meiotic cells are formed through a pathway that involves Sgs1, Mlh1-Mlh3, and Exo1

[250]. Though the mechanism through which these proteins cooperate to preferentially form COs is poorly understood, Mlh1-Mlh3 is an endonuclease, and it can recognize and bind Holliday junctions *in vitro* [193].

In sum, these two pathways, SDSA and dHJ resolution or dissolution, allow the second end of the break to be engaged, resulting in the formation of recombination products.

References


1. Halazonetis TD, Gorgoulis VG, Bartek J. An oncogene-induced DNA damage model for cancer development. Science. American Association for the Advancement of Science; 2008;319: 1352–1355. doi:10.1126/science.1140735

2. Mehta A, Haber JE. Sources of DNA double-strand breaks and models of recombinational DNA repair. Cold Spring Harb Perspect Biol. Cold Spring Harbor Lab; 2014;6: a016428–a016428. doi:10.1101/cshperspect.a016428

3. Kowalczykowski SC. Initiation of genetic recombination and recombination-dependent replication. Trends Biochem Sci. 2000;25: 156–165. doi:10.1016/s0968-0004(00)01569-3

4. Symington LS, Rothstein R, Lisby M. Mechanisms and regulation of mitotic recombination in Saccharomyces cerevisiae. Genetics. Genetics; 2014;198: 795–835. doi:10.1534/genetics.114.166140

5. Shrivastav M, De Haro LP, Nickoloff JA. Regulation of DNA double-strand break repair pathway choice. Cell Res. Nature Publishing Group; 2008;18: 134–147. doi:10.1038/cr.2007.111

6. Keeney S. Spo11 and the Formation of DNA Double-Strand Breaks in Meiosis. Genome Dyn Stab. Berlin, Heidelberg: Springer Berlin Heidelberg; 2008;2: 81–123. doi:10.1007/7050_2007_026

7. Symington LS, Gautier J. Double-strand break end resection and repair pathway choice. Annu Rev Genet. 2011;45: 247–271. doi:10.1146/annurev-genet-110410-132435

8. McVey M, Lee SE. MMEJ repair of double-strand breaks (director's cut): deleted sequences and alternative endings. Trends Genet. 2008;24: 529–538. doi:10.1016/j.tig.2008.08.007

9. Wang H, Xu X. Microhomology-mediated end joining: new players join the team. Cell Biosci. BioMed Central; 2017;7: 6–6. doi:10.1186/s13578-017-0136-8

10. Delacôte F, Han M, Stamato TD, Jasin M, Lopez BS. An xrcc4 defect or Wortmannin stimulates homologous recombination specifically induced by double-strand breaks in mammalian cells. Nucleic Acids Res. 2002;30: 3454–3463. doi:10.1093/nar/gkf452

11. Haber JE. DNA recombination: the replication connection. Trends Biochem Sci. 1999;24: 271–275. doi:10.1016/s0968-0004(99)01413-9

12. Willis NA, Panday A, Duffey EE, Scully R. Rad51 recruitment and exclusion of non-homologous end joining during homologous recombination at a Tus/Ter mammalian replication fork barrier. Malkova A, editor. PLoS Genet. Public Library of Science; 2018;14: e1007486. doi:10.1371/journal.pgen.1007486

13. Brown MS, Bishop DK. DNA Strand Exchange and RecA Homologs in Meiosis. Cold Spring Harb Perspect Biol. 2015;7: a016659–31. doi:10.1101/cshperspect.a016659

14. Kowalczykowski SC. An Overview of the Molecular Mechanisms of Recombinational DNA Repair. Cold Spring Harb Perspect Biol. 2015;7. doi:10.1101/cshperspect.a016410

15. Heyer W-D. Biochemistry of eukaryotic homologous recombination. Aguilera A, Rothstein R, editors. Top Curr Genet. Berlin, Heidelberg: Springer Berlin Heidelberg; 2007;17: 95–133. doi:10.1007/978-3-540-71021-9

16. Heyer W-D. Regulation of recombination and genomic maintenance. Cold Spring Harb Perspect Biol. 2015;7: a016501. doi:10.1101/cshperspect.a016501

17. Grushcow JM, Holzen TM, Park KJ, Weinert T, Lichten M, Bishop DK. Saccharomyces cerevisiae checkpoint genes MEC1, RAD17 and RAD24 are required for normal meiotic recombination partner choice. Genetics. Genetics Society of America; 1999;153: 607–620.

18. Murakami H, Borde V, Nicolas A, Keeney S. Gel electrophoresis assays for analyzing DNA double-strand breaks in Saccharomyces cerevisiae at various spatial resolutions. Methods Mol Biol. Totowa, NJ: Humana Press; 2009;557: 117–142. doi:10.1007/978-1-59745-527-5_9

19. Cao L, Alani E, Kleckner N. A pathway for generation and processing of double-strand breaks during meiotic recombination in S. cerevisiae. Cell. 1990;61: 1089–1101.

20. Oh SD, Jessop L, Lao JP, Allers T, Lichten M, Hunter N. Stabilization and electrophoretic analysis of meiotic recombination intermediates in Saccharomyces cerevisiae. Methods Mol Biol. Totowa, NJ: Humana Press; 2009;557: 209–234. doi:10.1007/978-1-59745-527-5_14

21. Bell L, Byers B. Separation of branched from linear DNA by two-dimensional gel electrophoresis. Anal Biochem. 1983;130: 527–535. doi:10.1016/0003-2697(83)90628-0

22. Schwacha A, Kleckner N. Identification of joint molecules that form frequently between homologs but rarely between sister chromatids during

yeast meiosis. Cell. 1994;76: 51–63.

23. Schwacha A, Kleckner N. Identification of double Holliday junctions as intermediates in meiotic recombination. Cell. 1995;83: 783–791. doi:10.1016/0092-8674(95)90191-4

24. Schwacha A, Kleckner N. Interhomolog bias during meiotic recombination: meiotic functions promote a highly differentiated interhomolog-only pathway. Cell. 1997;90: 1123–1135.

25. Lao JP, Hunter N. Trying to avoid your sister. PLoS Biol. Public Library of Science; 2010;8: e1000519. doi:10.1371/journal.pbio.1000519

26. Cloud V, Chan Y-L, Grubb J, Budke B, Bishop DK. Rad51 is an accessory factor for Dmc1-mediated joint molecule formation during meiosis. Science. 2012;337: 1222–1225. doi:10.1126/science.1219379

27. Lao JP, Cloud V, Huang C-C, Grubb J, Thacker D, Lee C-Y, et al. Meiotic Crossover Control by Concerted Action of Rad51-Dmc1 in Homolog Template Bias and Robust Homeostatic Regulation. Lichten M, editor. PLoS Genet. 2013;9: e1003978–22. doi:10.1371/journal.pgen.1003978

28. Hunter N, Kleckner N. The single-end invasion: an asymmetric intermediate at the double-strand break to double-holliday junction transition of meiotic recombination. Cell. 2001;106: 59–70.

29. Oh SD, Lao JP, Hwang PY-H, Taylor AF, Smith GR, Hunter N. BLM ortholog, Sgs1, prevents aberrant crossing-over by suppressing formation of multichromatid joint molecules. Cell. 2007;130: 259–272. doi:10.1016/j.cell.2007.05.035

30. Mazón G, Symington LS. Mph1 and Mus81-Mms4 prevent aberrant processing of mitotic recombination intermediates. Molecular Cell. 2013;52: 63–74. doi:10.1016/j.molcel.2013.09.007

31. Elango R, Sheng Z, Jackson J, DeCata J, Ibrahim Y, Pham NT, et al. **Break-induced replication promotes formation of lethal joint molecules dissolved by Srs2**

. Nat Commun. Nature Publishing Group; 2017;8: 1790–13. doi:10.1038/s41467-017-01987-2

32. Rao BJ, Dutreix M, Radding CM. Stable three-stranded DNA made by RecA protein. Proc Natl Acad Sci USA. National Academy of Sciences; 1991;88: 2984–2988. doi:10.1073/pnas.88.8.2984

33. Shibata T, DasGupta C, Cunningham RP, Radding CM. Purified Escherichia

coli recA protein catalyzes homologous pairing of superhelical DNA and single-stranded fragments. Proc Natl Acad Sci USA. 1979;76: 1638–1642. doi:10.1073/pnas.76.4.1638

34. Konforti BB, Davis RW. 3' homologous free ends are required for stable joint molecule formation by the RecA and single-stranded binding proteins of Escherichia coli. Proc Natl Acad Sci USA. National Academy of Sciences; 1987;84: 690–694. doi:10.1073/pnas.84.3.690

35. Kwon Y, Daley JM, Sung P. Reconstituted System for the Examination of Repair DNA Synthesis in Homologous Recombination. Meth Enzymol. Elsevier; 2017;591: 307–325. doi:10.1016/bs.mie.2017.03.021

36. Chan Y-L, Bishop DK. Purification of Saccharomyces cerevisiae Homologous Recombination Proteins Dmc1 and Rdh54/Tid1 and a Fluorescent D-Loop Assay. Meth Enzymol. Elsevier; 2018;600: 307–320. doi:10.1016/bs.mie.2017.12.003

37. Symington LS. End resection at double-strand breaks: mechanism and regulation. Cold Spring Harb Perspect Biol. Cold Spring Harbor Lab; 2014;6: a016436–a016436. doi:10.1101/cshperspect.a016436

38. Zhu Z, Chung W-H, Shim EY, Lee SE, Ira G. Sgs1 helicase and two nucleases Dna2 and Exo1 resect DNA double-strand break ends. Cell. 2008;134: 981–994. doi:10.1016/j.cell.2008.08.037

39. Mimitou EP, Symington LS. Ku prevents Exo1 and Sgs1-dependent resection of DNA ends in the absence of a functional MRX complex or Sae2. EMBO J. 2010;29: 3358–3369. doi:10.1038/emboj.2010.193

40. Mimitou EP, Yamada S, Keeney S. A global view of meiotic double-strand break end resection. Science. American Association for the Advancement of Science; 2017;355: 40–45. doi:10.1126/science.aak9704

41. Zakharyevich K, Ma Y, Tang S, Hwang PY-H, Boiteux S, Hunter N. Temporally and biochemically distinct activities of Exo1 during meiosis: double-strand break resection and resolution of double Holliday junctions. Molecular Cell. 2010;40: 1001–1015. doi:10.1016/j.molcel.2010.11.032

42. Chung W-H, Zhu Z, Papusha A, Malkova A, Ira G. Defective resection at DNA double-strand breaks leads to de novo telomere formation and enhances gene targeting. Lichten M, editor. PLoS Genet. Public Library of Science; 2010;6: e1000948. doi:10.1371/journal.pgen.1000948

43. Bishop DK, Park D, Xu L, Kleckner N. DMC1: a meiosis-specific yeast homolog of E. coli recA required for recombination, synaptonemal complex formation, and cell cycle progression. Cell. 1992;69: 439–456.

44. Shinohara A, Ogawa H, Ogawa T. Rad51 protein involved in repair and recombination in S. cerevisiae is a RecA-like protein. Cell. 1992;69: 457–470.

45. Manfrini N, Guerini I, Citterio A, Lucchini G, Longhese MP. Processing of meiotic DNA double strand breaks requires cyclin-dependent kinase and multiple nucleases. J Biol Chem. American Society for Biochemistry and Molecular Biology; 2010;285: 11628–11637. doi:10.1074/jbc.M110.104083

46. Mimitou EP, Symington LS. Sae2, Exo1 and Sgs1 collaborate in DNA double-strand break processing. Nature. 2008;455: 770–774. doi:10.1038/nature07312

47. Keelagher RE, Cotton VE, Goldman ASH, Borts RH. Separable roles for Exonuclease I in meiotic DNA double-strand break repair. DNA Repair. 2011;10: 126–137. doi:10.1016/j.dnarep.2010.09.024

48. Chen H, Lisby M, Symington LS. RPA coordinates DNA end resection and prevents formation of DNA hairpins. Molecular Cell. 2013;50: 589–600. doi:10.1016/j.molcel.2013.04.032

49. Wold MS. Replication protein A: a heterotrimeric, single-stranded DNA-binding protein required for eukaryotic DNA metabolism. Annu Rev Biochem. 1997;66: 61–92. doi:10.1146/annurev.biochem.66.1.61

50. Alani E, Thresher R, Griffith JD, Kolodner RD. Characterization of DNA-binding and strand-exchange stimulation properties of y-RPA, a yeast single-strand-DNA-binding protein. J Mol Biol. 1992;227: 54–71. doi:10.1016/0022-2836(92)90681-9

51. Sugiyama T, Zaitseva EM, Kowalczykowski SC. A single-stranded DNA-binding protein is needed for efficient presynaptic complex formation by the Saccharomyces cerevisiae Rad51 protein. Journal of Biological Chemistry. American Society for Biochemistry and Molecular Biology; 1997;272: 7940–7945. doi:10.1074/jbc.272.12.7940

52. Chan Y-L, Zhang A, Weissman BP, Bishop DK. RPA resolves conflicting activities of accessory proteins during reconstitution of Dmc1-mediated meiotic recombination. Nucleic Acids Res. 2019;47: 747–761. doi:10.1093/nar/gky1160

53. Zou L, Elledge SJ. Sensing DNA damage through ATRIP recognition of RPA-ssDNA complexes. Science. American Association for the Advancement of Science; 2003;300: 1542–1548. doi:10.1126/science.1083430

54. Cejka P, Cannavo E, Polaczek P, Masuda-Sasa T, Pokharel S, Campbell

JL, et al. DNA end resection by Dna2-Sgs1-RPA and its stimulation by Top3-Rmi1 and Mre11-Rad50-Xrs2. Nature. Nature Publishing Group; 2010;467: 112–116. doi:10.1038/nature09355

55. Niu H, Chung W-H, Zhu Z, Kwon Y, Zhao W, Chi P, et al. Mechanism of the ATP-dependent DNA end-resection machinery from Saccharomyces cerevisiae. Nature. Nature Publishing Group; 2010;467: 108–111. doi:10.1038/nature09318

56. Masson JY, West SC. The Rad51 and Dmc1 recombinases: a non-identical twin relationship. Trends Biochem Sci. 2001;26: 131–136.

57. Conway AB, Lynch TW, Zhang Y, Fortin GS, Fung CW, Symington LS, et al. Crystal structure of a Rad51 filament. Nat Struct Mol Biol. 2004;11: 791–796. doi:10.1038/nsmb795

58. Zaitseva EM, Zaitsev EN, Kowalczykowski SC. The DNA binding properties of Saccharomyces cerevisiae Rad51 protein. Journal of Biological Chemistry. American Society for Biochemistry and Molecular Biology; 1999;274: 2907–2915. doi:10.1074/jbc.274.5.2907

59. Hong EL, Shinohara A, Bishop DK. Saccharomyces cerevisiae Dmc1 protein promotes renaturation of single-strand DNA (ssDNA) and assimilation of ssDNA into homologous super-coiled duplex DNA. Journal of Biological Chemistry. 2001;276: 41906–41912. doi:10.1074/jbc.M105563200

60. Solinger JA, Kiianitsa K, Heyer W-D. Rad54, a Swi2/Snf2-like recombinational repair protein, disassembles Rad51:dsDNA filaments. Molecular Cell. 2002;10: 1175–1188.

61. Holzen TM, Shah PP, Olivares HA, Bishop DK. Tid1/Rdh54 promotes dissociation of Dmc1 from nonrecombinogenic sites on meiotic chromatin. Genes Dev. 2006;20: 2593–2604. doi:10.1101/gad.1447106

62. Li X, Heyer W-D. RAD54 controls access to the invading 3'-OH end after RAD51-mediated DNA strand invasion in homologous recombination in Saccharomyces cerevisiae. Nucleic Acids Res. 2009;37: 638–646. doi:10.1093/nar/gkn980

63. Shah PP, Zheng X, Epshtein A, Carey JN, Bishop DK, Klein HL. Swi2/Snf2-related translocases prevent accumulation of toxic Rad51 complexes during mitotic growth. Molecular Cell. 2010;39: 862–872. doi:10.1016/j.molcel.2010.08.028

64. Wright WD, Heyer W-D. Rad54 functions as a heteroduplex DNA pump modulated by its DNA substrates and Rad51 during D loop formation. Molecular Cell. 2014;53: 420–432. doi:10.1016/j.molcel.2013.12.027

65. Sung P, Stratton SA. Yeast Rad51 recombinase mediates polar DNA strand exchange in the absence of ATP hydrolysis. Journal of Biological Chemistry. American Society for Biochemistry and Molecular Biology; 1996;271: 27983–27986. doi:10.1074/jbc.271.45.27983

66. Morgan EA, Shah N, Symington LS. The requirement for ATP hydrolysis by Saccharomyces cerevisiae Rad51 is bypassed by mating-type heterozygosity or RAD54 in high copy. Mol Cell Biol. 2002;22: 6336–6343. doi:10.1128/mcb.22.18.6336-6343.2002

67. Namsaraev EA, Berg P. Binding of Rad51p to DNA. Interaction of Rad51p with single- and double-stranded DNA. Journal of Biological Chemistry. American Society for Biochemistry and Molecular Biology; 1998;273: 6177–6182. doi:10.1074/jbc.273.11.6177

68. Gataulin DV, Carey JN, Li J, Shah P, Grubb JT, Bishop DK. The ATPase activity of E. coli RecA prevents accumulation of toxic complexes formed by erroneous binding to undamaged double stranded DNA. Nucleic Acids Res. 2018;46: 9510–9523. doi:10.1093/nar/gky748

69. Campbell MJ, Davis RW. Toxic mutations in the recA gene of E. coli prevent proper chromosome segregation. J Mol Biol. 1999;286: 417–435. doi:10.1006/jmbi.1998.2456

70. Sheridan SD, Yu X, Roth R, Heuser JE, Sehorn MG, Sung P, et al. A comparative analysis of Dmc1 and Rad51 nucleoprotein filaments. Nucleic Acids Res. 2008;36: 4057–4066. doi:10.1093/nar/gkn352

71. Hilario J, Amitani I, Baskin RJ, Kowalczykowski SC. Direct imaging of human Rad51 nucleoprotein dynamics on individual DNA molecules. Proc Natl Acad Sci USA. 2009;106: 361–368. doi:10.1073/pnas.0811965106

72. Fung CW, Fortin GS, Peterson SE, Symington LS. The rad51-K191R ATPase-defective mutant is impaired for presynaptic filament formation. Mol Cell Biol. 2006;26: 9544–9554. doi:10.1128/MCB.00599-06

73. Li X, Zhang X-P, Solinger JA, Kiianitsa K, Yu X, Egelman EH, et al. Rad51 and Rad54 ATPase activities are both required to modulate Rad51-dsDNA filament dynamics. Nucleic Acids Res. 2007;35: 4124–4140. doi:10.1093/nar/gkm412

74. Ogawa T, Yu X, Shinohara A, Egelman EH. Similarity of the yeast RAD51 filament to the bacterial RecA filament. Science. American Association for the Advancement of Science; 1993;259: 1896–1899. doi:10.1126/science.8456314

75. Yu X, Jacobs SA, West SC, Ogawa T, Egelman EH. Domain structure and

dynamics in the helical filaments formed by RecA and Rad51 on DNA. Proc Natl Acad Sci USA. National Academy of Sciences; 2001;98: 8419–8424. doi:10.1073/pnas.111005398

76. Galkin VE, Wu Y, Zhang X-P, Qian X, He Y, Yu X, et al. The Rad51/RadA N-terminal domain activates nucleoprotein filament ATPase activity. Structure. 2006;14: 983–992. doi:10.1016/j.str.2006.04.001

77. Galletto R, Amitani I, Baskin RJ, Kowalczykowski SC. Direct observation of individual RecA filaments assembling on single DNA molecules. Nature. Nature Publishing Group; 2006;443: 875–878. doi:10.1038/nature05197

78. Bell JC, Plank JL, Dombrowski CC, Kowalczykowski SC. Direct imaging of RecA nucleation and growth on single molecules of SSB-coated ssDNA. Nature. Nature Publishing Group; 2012;491: 274–278. doi:10.1038/nature11598

79. Lu C-H, Yeh H-Y, Su G-C, Ito K, Kurokawa Y, Iwasaki H, et al. Swi5-Sfr1 stimulates Rad51 recombinase filament assembly by modulating Rad51 dissociation. Proc Natl Acad Sci USA. National Academy of Sciences; 2018;115: E10059–E10068. doi:10.1073/pnas.1812753115

80. Cho H-R, Kong Y-J, Hong S-G, Kim KP. Hop2 and Sae3 Are Required for Dmc1-Mediated Double-Strand Break Repair via Homolog Bias during Meiosis. Molecules and Cells. 2016;39: 550–556. doi:10.14348/molcells.2016.0069

81. Fanning E, Klimovich V, Nager AR. A dynamic model for replication protein A (RPA) function in DNA processing pathways. Nucleic Acids Res. 2006;34: 4126–4137. doi:10.1093/nar/gkl550

82. Chen R, Wold MS. Replication protein A: single-stranded DNA's first responder: dynamic DNA-interactions allow replication protein A to direct single-strand DNA intermediates into different pathways for synthesis or repair. Bioessays. John Wiley & Sons, Ltd; 2014;36: 1156–1161. doi:10.1002/bies.201400107

83. Sung P. Function of yeast Rad52 protein as a mediator between replication protein A and the Rad51 recombinase. Journal of Biological Chemistry. American Society for Biochemistry and Molecular Biology; 1997;272: 28194–28197. doi:10.1074/jbc.272.45.28194

84. Sugiyama T, New JH, Kowalczykowski SC. DNA annealing by RAD52 protein is stimulated by specific interaction with the complex of replication protein A and single-stranded DNA. Proc Natl Acad Sci USA. National Academy of Sciences; 1998;95: 6049–6054. doi:10.1073/pnas.95.11.6049

85. Stauffer ME, Chazin WJ. Physical interaction between replication protein A and Rad51 promotes exchange on single-stranded DNA. Journal of Biological Chemistry. American Society for Biochemistry and Molecular Biology; 2004;279: 25638–25645. doi:10.1074/jbc.M400029200

86. Smith J, Rothstein R. A mutation in the gene encoding the Saccharomyces cerevisiae single-stranded DNA-binding protein Rfa1 stimulates a RAD52-independent pathway for direct-repeat recombination. Mol Cell Biol. American Society for Microbiology Journals; 1995;15: 1632–1641. doi:10.1128/mcb.15.3.1632

87. Deng SK, Gibb B, de Almeida MJ, Greene EC, Symington LS. RPA antagonizes microhomology-mediated repair of DNA double-strand breaks. Nat Struct Mol Biol. Nature Publishing Group; 2014;21: 405–412. doi:10.1038/nsmb.2786

88. Lavery PE, Kowalczykowski SC. A postsynaptic role for single-stranded DNA-binding protein in recA protein-promoted DNA strand exchange. Journal of Biological Chemistry. 1992;267: 9315–9320.

89. Eggler AL, Inman RB, Cox MM. The Rad51-dependent pairing of long DNA substrates is stabilized by replication protein A. Journal of Biological Chemistry. American Society for Biochemistry and Molecular Biology; 2002;277: 39280–39288. doi:10.1074/jbc.M204328200

90. Krejci L, Altmannova V, Spirek M, Zhao X. Homologous recombination and its regulation. Nucleic Acids Res. 2012;40: 5795–5818. doi:10.1093/nar/gks270

91. Zelensky A, Kanaar R, Wyman C. Mediators of homologous DNA pairing. Cold Spring Harb Perspect Biol. Cold Spring Harbor Lab; 2014;6: a016451–a016451. doi:10.1101/cshperspect.a016451

92. Kadyk LC, Hartwell LH. Sister chromatids are preferred over homologs as substrates for recombinational repair in Saccharomyces cerevisiae. Genetics. Genetics Society of America; 1992;132: 387–402.

93. Bzymek M, Thayer NH, Oh SD, Kleckner N, Hunter N. Double Holliday junctions are intermediates of DNA break repair. Nature. 2010;464: 937–941. doi:10.1038/nature08868

94. Sjögren C, Ström L. S-phase and DNA damage activated establishment of sister chromatid cohesion--importance for DNA repair. Exp Cell Res. 2010;316: 1445–1453. doi:10.1016/j.yexcr.2009.12.018

95. Crickard JB, Greene EC. Biochemical attributes of mitotic and meiotic presynaptic complexes. DNA Repair. 2018;71: 148–157.

doi:10.1016/j.dnarep.2018.08.018

96. Milne GT, Weaver DT. Dominant negative alleles of RAD52 reveal a DNA repair/recombination complex including Rad51 and Rad52. Genes Dev. Cold Spring Harbor Lab; 1993;7: 1755–1765. doi:10.1101/gad.7.9.1755

97. Hays SL, Firmenich AA, Massey P, Banerjee R, Berg P. Studies of the interaction between Rad52 protein and the yeast single-stranded DNA binding protein RPA. Mol Cell Biol. American Society for Microbiology Journals; 1998;18: 4400–4406. doi:10.1128/mcb.18.7.4400

98. New JH, Sugiyama T, Zaitseva E, Kowalczykowski SC. Rad52 protein stimulates DNA strand exchange by Rad51 and replication protein A. Nature. Nature Publishing Group; 1998;391: 407–410. doi:10.1038/34950

99. Shinohara A, Ogawa T. Stimulation by Rad52 of yeast Rad51-mediated recombination. Nature. Nature Publishing Group; 1998;391: 404–407. doi:10.1038/34943

100. Song B, Sung P. Functional interactions among yeast Rad51 recombinase, Rad52 mediator, and replication protein A in DNA strand exchange. Journal of Biological Chemistry. American Society for Biochemistry and Molecular Biology; 2000;275: 15895–15904. doi:10.1074/jbc.M910244199

101. Gibb B, Ye LF, Kwon Y, Niu H, Sung P, Greene EC. Protein dynamics during presynaptic-complex assembly on individual single-stranded DNA molecules. Nat Struct Mol Biol. Nature Publishing Group; 2014;21: 893–900. doi:10.1038/nsmb.2886

102. Gasior SL, Wong AK, Kora Y, Shinohara A, Bishop DK. Rad52 associates with RPA and functions with rad55 and rad57 to assemble meiotic recombination complexes. Genes Dev. Cold Spring Harbor Lab; 1998;12: 2208–2221. doi:10.1101/gad.12.14.2208

103. Gasior SL, Olivares H, Ear U, Hari DM, Weichselbaum R, Bishop DK. Assembly of RecA-like recombinases: distinct roles for mediator proteins in mitosis and meiosis. Proc Natl Acad Sci USA. National Academy of Sciences; 2001;98: 8411–8418. doi:10.1073/pnas.121046198

104. Lisby M, Barlow JH, Burgess RC, Rothstein R. Choreography of the DNA damage response: spatiotemporal relationships among checkpoint and repair proteins. Cell. 2004;118: 699–713. doi:10.1016/j.cell.2004.08.015

105. Cole GM, Schild D, Lovett ST, Mortimer RK. Regulation of RAD54- and RAD52-lacZ gene fusions in Saccharomyces cerevisiae in response to DNA damage. Mol Cell Biol. American Society for Microbiology Journals; 1987;7: 1078–1084. doi:10.1128/mcb.7.3.1078

106. Cole GM, Schild D, Mortimer RK. Two DNA repair and recombination genes in Saccharomyces cerevisiae, RAD52 and RAD54, are induced during meiosis. Mol Cell Biol. American Society for Microbiology Journals; 1989;9: 3101–3104. doi:10.1128/mcb.9.7.3101

107. Rattray AJ, Symington LS. Use of a chromosomal inverted repeat to demonstrate that the RAD51 and RAD52 genes of Saccharomyces cerevisiae have different roles in mitotic recombination. Genetics. Genetics Society of America; 1994;138: 587–595.

108. Mortensen UH, Bendixen C, Sunjevaric I, Rothstein R. DNA strand annealing is promoted by the yeast Rad52 protein. Proc Natl Acad Sci USA. National Academy of Sciences; 1996;93: 10729–10734. doi:10.1073/pnas.93.20.10729

109. Kans JA, Mortimer RK. Nucleotide sequence of the RAD57 gene of Saccharomyces cerevisiae. Gene. 1991;105: 139–140. doi:10.1016/0378-1119(91)90527-i

110. Lovett ST. Sequence of the RAD55 gene of Saccharomyces cerevisiae: similarity of RAD55 to prokaryotic RecA and other RecA-like proteins. Gene. 1994;142: 103–106. doi:10.1016/0378-1119(94)90362-x

111. Johnson RD, Symington LS. Functional differences and interactions among the putative RecA homologs Rad51, Rad55, and Rad57. Mol Cell Biol. American Society for Microbiology Journals; 1995;15: 4843–4850. doi:10.1128/mcb.15.9.4843

112. Sung P. Yeast Rad55 and Rad57 proteins form a heterodimer that functions with replication protein A to promote DNA strand exchange by Rad51 recombinase. Genes Dev. Cold Spring Harbor Lab; 1997;11: 1111–1121. doi:10.1101/gad.11.9.1111

113. Liu J, Renault L, Veaute X, Fabre F, Stahlberg H, Heyer W-D. Rad51 paralogues Rad55-Rad57 balance the antirecombinase Srs2 in Rad51 filament formation. Nature. 2011;479: 245–248. doi:10.1038/nature10522

114. Hays SL, Firmenich AA, Berg P. Complex formation in yeast double-strand break repair: participation of Rad51, Rad52, Rad55, and Rad57 proteins. Proc Natl Acad Sci USA. National Academy of Sciences; 1995;92: 6925–6929. doi:10.1073/pnas.92.15.6925

115. Game JC, Mortimer RK. A genetic study of x-ray sensitive mutants in yeast. Mutat Res. 1974;24: 281–292. doi:10.1016/0027-5107(74)90176-6

116. Lovett ST, Mortimer RK. Characterization of null mutants of the RAD55 gene of Saccharomyces cerevisiae: effects of temperature, osmotic strength and

mating type. Genetics. Genetics Society of America; 1987;116: 547–553.

117. Sugawara N, Wang X, Haber JE. In vivo roles of Rad52, Rad54, and Rad55 proteins in Rad51-mediated recombination. Molecular Cell. 2003;12: 209–219. doi:10.1016/s1097-2765(03)00269-7

118. Fortin GS, Symington LS. Mutations in yeast Rad51 that partially bypass the requirement for Rad55 and Rad57 in DNA repair by increasing the stability of Rad51-DNA complexes. EMBO J. EMBO Press; 2002;21: 3160–3170. doi:10.1093/emboj/cdf293

119. Krejci L, Van Komen S, Li Y, Villemain J, Reddy MS, Klein H, et al. DNA helicase Srs2 disrupts the Rad51 presynaptic filament. Nature. Nature Publishing Group; 2003;423: 305–309. doi:10.1038/nature01577

120. Veaute X, Jeusset J, Soustelle C, Kowalczykowski SC, Le Cam E, Fabre F. The Srs2 helicase prevents recombination by disrupting Rad51 nucleoprotein filaments. Nature. 2003;423: 309–312. doi:10.1038/nature01585

121. Shor E, Weinstein J, Rothstein R. A genetic screen for top3 suppressors in Saccharomyces cerevisiae identifies SHU1, SHU2, PSY3 and CSM2: four genes involved in error-free DNA repair. Genetics. Genetics; 2005;169: 1275–1289. doi:10.1534/genetics.104.036764

122. Ball LG, Zhang K, Cobb JA, Boone C, Xiao W. The yeast Shu complex couples error-free post-replication repair to homologous recombination. Mol Microbiol. John Wiley & Sons, Ltd (10.1111); 2009;73: 89–102. doi:10.1111/j.1365-2958.2009.06748.x

123. Sasanuma H, Furihata Y, Shinohara M, Shinohara A. Remodeling of the Rad51 DNA strand-exchange protein by the Srs2 helicase. Genetics. Genetics; 2013;194: 859–872. doi:10.1534/genetics.113.150615

124. Hanway D, Chin JK, Xia G, Oshiro G, Winzeler EA, Romesberg FE. Previously uncharacterized genes in the UV- and MMS-induced DNA damage response in yeast. Proc Natl Acad Sci USA. National Academy of Sciences; 2002;99: 10605–10610. doi:10.1073/pnas.152264899

125. Mankouri HW, Ngo H-P, Hickson ID. Esc2 and Sgs1 act in functionally distinct branches of the homologous recombination repair pathway in Saccharomyces cerevisiae. Zheng Y, editor. Mol Biol Cell. 2009;20: 1683–1694. doi:10.1091/mbc.e08-08-0877

126. Huang M-E, Rio A-G, Nicolas A, Kolodner RD. A genomewide screen in Saccharomyces cerevisiae for genes that suppress the accumulation of mutations. Proc Natl Acad Sci USA. National Academy of Sciences;

2003;100: 11529–11534. doi:10.1073/pnas.2035018100

127. Martino J, Bernstein KA. The Shu complex is a conserved regulator of homologous recombination. Lisby M, editor. FEMS Yeast Res. 2016;16: fow073. doi:10.1093/femsyr/fow073

128. Hong S, Kim KP. Shu1 promotes homolog bias of meiotic recombination in Saccharomyces cerevisiae. Molecules and Cells. 2013;36: 446–454. doi:10.1007/s10059-013-0215-6

129. Hong S, Sung Y, Yu M, Lee M, Kleckner N, Kim KP. The Logic and Mechanism of Homologous Recombination Partner Choice. Molecular Cell. Elsevier Inc; 2013;51: 440–453. doi:10.1016/j.molcel.2013.08.008

130. Sasanuma H, Tawaramoto MS, Lao JP, Hosaka H, Sanda E, Suzuki M, et al. A new protein complex promoting the assembly of Rad51 filaments. Nat Commun. Nature Publishing Group; 2013;4: 1676–13. doi:10.1038/ncomms2678

131. Shor E, Gangloff S, Wagner M, Weinstein J, Price G, Rothstein R. Mutations in homologous recombination genes rescue top3 slow growth in Saccharomyces cerevisiae. Genetics. Genetics Society of America; 2002;162: 647–662.

132. Tao Y, Li X, Liu Y, Ruan J, Qi S, Niu L, et al. Structural analysis of Shu proteins reveals a DNA binding role essential for resisting damage. J Biol Chem. American Society for Biochemistry and Molecular Biology; 2012;287: 20231–20239. doi:10.1074/jbc.M111.334698

133. Godin S, Wier A, Kabbinavar F, Bratton-Palmer DS, Ghodke H, Van Houten B, et al. The Shu complex interacts with Rad51 through the Rad51 paralogues Rad55-Rad57 to mediate error-free recombination. Nucleic Acids Res. 2013;41: 4525–4534. doi:10.1093/nar/gkt138

134. Gaines WA, Godin SK, Kabbinavar FF, Rao T, VanDemark AP, Sung P, et al. Promotion of presynaptic filament assembly by the ensemble of S. cerevisiae Rad51 paralogues with Rad52. Nat Commun. Nature Publishing Group; 2015;6: 7834–7. doi:10.1038/ncomms8834

135. Bernstein KA, Reid RJD, Sunjevaric I, Demuth K, Burgess RC, Rothstein R. The Shu complex, which contains Rad51 paralogues, promotes DNA repair through inhibition of the Srs2 anti-recombinase. Bloom KS, editor. Mol Biol Cell. 2011;22: 1599–1607. doi:10.1091/mbc.E10-08-0691

136. Ito T, Chiba T, Ozawa R, Yoshida M, Hattori M, Sakaki Y. A comprehensive two-hybrid analysis to explore the yeast protein interactome. Proc Natl Acad Sci USA. National Academy of Sciences; 2001;98: 4569–4574.

doi:10.1073/pnas.061034498

137. Game JC, Zamb TJ, Braun RJ, Resnick M, Roth RM. The Role of Radiation (rad) Genes in Meiotic Recombination in Yeast. Genetics. Genetics Society of America; 1980;94: 51–68.

138. McKee AH, Kleckner N. Mutations in Saccharomyces cerevisiae that block meiotic prophase chromosome metabolism and confer cell cycle arrest at pachytene identify two new meiosis-specific genes SAE1 and SAE3. Genetics. Genetics Society of America; 1997;146: 817–834.

139. Hayase A, Takagi M, Miyazaki T, Oshiumi H, Shinohara M, Shinohara A. A Protein Complex Containing Mei5 and Sae3 Promotes the Assembly of the Meiosis-Specific RecA Homolog Dmc1. Cell. 2004;119: 927–940. doi:10.1016/j.cell.2004.10.031

140. Tsubouchi H, Roeder GS. Budding yeast Hed1 down-regulates the mitotic recombination machinery when meiotic recombination is impaired. Genes Dev. Cold Spring Harbor Lab; 2006;20: 1766–1775. doi:10.1101/gad.1422506

141. Argunhan B, Murayama Y, Iwasaki H. The differentiated and conserved roles of Swi5-Sfr1 in homologous recombination. FEBS Lett. 2017;591: 2035–2047. doi:10.1002/1873-3468.12656

142. Haruta N, Kurokawa Y, Murayama Y, Akamatsu Y, Unzai S, Tsutsui Y, et al. The Swi5-Sfr1 complex stimulates Rhp51/Rad51- and Dmc1-mediated DNA strand exchange in vitro. Nat Struct Mol Biol. 2006;13: 823–830. doi:10.1038/nsmb1136

143. Yuan J, Chen J. The role of the human SWI5-MEI5 complex in homologous recombination repair. J Biol Chem. 2011;286: 9888–9893. doi:10.1074/jbc.M110.207290

144. Su G-C, Chung C-I, Liao C-Y, Lin S-W, Tsai C-T, Huang T, et al. Enhancement of ADP release from the RAD51 presynaptic filament by the SWI5-SFR1 complex. Nucleic Acids Res. 2014;42: 349–358. doi:10.1093/nar/gkt879

145. Tsubouchi H, Roeder GS. The budding yeast mei5 and sae3 proteins act together with dmc1 during meiotic recombination. Genetics. 2004;168: 1219–1230. doi:10.1534/genetics.103.025700

146. Rabitsch KP, Tóth A, Gálová M, Schleiffer A, Schaffner G, Aigner E, et al. A screen for genes required for meiosis and spore formation based on whole-genome expression. Curr Biol. 2001;11: 1001–1009. doi:10.1016/s0960-9822(01)00274-3

147. Ferrari SR, Grubb J, Bishop DK. The Mei5-Sae3 Protein Complex Mediates Dmc1 Activity in Saccharomyces cerevisiae. Journal of Biological Chemistry. 2009;284: 11766–11770. doi:10.1074/jbc.C900023200

148. Say AF, Ledford LL, Sharma D, Singh AK, Leung W-K, Sehorn HA, et al. The budding yeast Mei5–Sae3 complex interacts with Rad51 and preferentially binds a DNA fork structure. DNA Repair. 2011;10: 586–594. doi:10.1016/j.dnarep.2011.03.006

149. Busygina V, Sehorn MG, Shi IY, Tsubouchi H, Roeder GS, Sung P. Hed1 regulates Rad51-mediated recombination via a novel mechanism. Genes Dev. 2008;22: 786–795. doi:10.1101/gad.1638708

150. Bishop DK. RecA homologs Dmc1 and Rad51 interact to form multiple nuclear complexes prior to meiotic chromosome synapsis. Cell. 1994;79: 1081–1092.

151. Shinohara A, Gasior S, Ogawa T, Kleckner N, Bishop DK. Saccharomyces cerevisiae recA homologues RAD51 and DMC1 have both distinct and overlapping roles in meiotic recombination. Genes Cells. 1997;2: 615–629.

152. Shinohara M, Gasior SL, Bishop DK, Shinohara A. Tid1/Rdh54 promotes colocalization of rad51 and dmc1 during meiotic recombination. Proc Natl Acad Sci USA. National Academy of Sciences; 2000;97: 10814–10819. doi:10.1073/pnas.97.20.10814

153. Brown MS, Grubb J, Zhang A, Rust MJ, Bishop DK. Small Rad51 and Dmc1 Complexes Often Co-occupy Both Ends of a Meiotic DNA Double Strand Break. Lichten M, editor. PLoS Genet. Public Library of Science; 2015;11: e1005653. doi:10.1371/journal.pgen.1005653

154. Shinohara M, Shinohara A. Multiple pathways suppress non-allelic homologous recombination during meiosis in Saccharomyces cerevisiae. PLoS ONE. 2013;8: e63144. doi:10.1371/journal.pone.0063144

155. Bishop DK. Rad51, the lead in mitotic recombinational DNA repair, plays a supporting role in budding yeast meiosis. Cell Cycle. 2012;11: 4105–4106. doi:10.4161/cc.22396

156. Borts RH, Lichten M, Haber JE. Analysis of meiosis-defective mutations in yeast by physical monitoring of recombination. Genetics. Genetics Society of America; 1986;113: 551–567.

157. Lao JP, Oh SD, Shinohara M, Shinohara A, Hunter N. **Rad52 promotes post-invasion steps of meiotic double-strand-break repair**. Molecular Cell. 2008;29: 517–524. doi:10.1016/j.molcel.2007.12.014

158. Thompson DA, Stahl FW. Genetic control of recombination partner preference in yeast meiosis. Isolation and characterization of mutants elevated for meiotic unequal sister-chromatid recombination. Genetics. Genetics Society of America; 1999;153: 621–641.

159. Ho H-C, Burgess SM. Pch2 acts through Xrs2 and Tel1/ATM to modulate interhomolog bias and checkpoint function during meiosis. McKim KS, editor. PLoS Genet. Public Library of Science; 2011;7: e1002351. doi:10.1371/journal.pgen.1002351

160. Rockmill B, Roeder GS. A meiosis-specific protein kinase homolog required for chromosome synapsis and recombination. Genes Dev. Cold Spring Harbor Lab; 1991;5: 2392–2404. doi:10.1101/gad.5.12b.2392

161. Niu H, Wan L, Baumgartner B, Schaefer D, Loidl J, Hollingsworth NM. Partner choice during meiosis is regulated by Hop1-promoted dimerization of Mek1. Mol Biol Cell. 2005;16: 5804–5818. doi:10.1091/mbc.E05-05-0465

162. Goldfarb T, Lichten M. Frequent and efficient use of the sister chromatid for DNA double-strand break repair during budding yeast meiosis. Hawley RS, editor. PLoS Biol. Public Library of Science; 2010;8: e1000520. doi:10.1371/journal.pbio.1000520

163. Callender TL, Laureau R, Wan L, Chen X, Sandhu R, Laljee S, et al. Mek1 Down Regulates Rad51 Activity during Yeast Meiosis by Phosphorylation of Hed1. Lichten M, editor. PLoS Genet. Public Library of Science; 2016;12: e1006226. doi:10.1371/journal.pgen.1006226

164. Liu Y, Gaines WA, Callender T, Busygina V, Oke A, Sung P, et al. Down-regulation of Rad51 activity during meiosis in yeast prevents competition with Dmc1 for repair of double-strand breaks. Lichten M, editor. PLoS Genet. 2014;10: e1004005. doi:10.1371/journal.pgen.1004005

165. Chi P, Kwon Y, Seong C, Epshtein A, Lam I, Sung P, et al. Yeast recombination factor Rdh54 functionally interacts with the Rad51 recombinase and catalyzes Rad51 removal from DNA. Journal of Biological Chemistry. 2006;281: 26268–26279. doi:10.1074/jbc.M602983200

166. Piazza A, Shah SS, Wright WD, Gore SK, Koszul R, Heyer W-D. Dynamic Processing of Displacement Loops during Recombinational DNA Repair. Molecular Cell. 2019;73: 1255–1266.e4. doi:10.1016/j.molcel.2019.01.005

167. Subramanya HS, Bird LE, Brannigan JA, Wigley DB. Crystal structure of a DExx box DNA helicase. Nature. Nature Publishing Group; 1996;384: 379–383. doi:10.1038/384379a0

168. Flaus A, Martin DMA, Barton GJ, Owen-Hughes T. Identification of multiple

distinct Snf2 subfamilies with conserved structural motifs. Nucleic Acids Res. 2006;34: 2887–2905. doi:10.1093/nar/gkl295

169. Ceballos SJ, Heyer W-D. Functions of the Snf2/Swi2 family Rad54 motor protein in homologous recombination. Biochim Biophys Acta. 2011;1809: 509–523. doi:10.1016/j.bbagrm.2011.06.006

170. Jiang H, Xie Y, Houston P, Stemke-Hale K, Mortensen UH, Rothstein R, et al. Direct association between the yeast Rad51 and Rad54 recombination proteins. Journal of Biological Chemistry. American Society for Biochemistry and Molecular Biology; 1996;271: 33181–33186. doi:10.1074/jbc.271.52.33181

171. Clever B, Interthal H, Schmuckli-Maurer J, King J, Sigrist M, Heyer WD. Recombinational repair in yeast: functional interactions between Rad51 and Rad54 proteins. EMBO J. John Wiley & Sons, Ltd; 1997;16: 2535–2544. doi:10.1093/emboj/16.9.2535

172. Mazin AV, Bornarth CJ, Solinger JA, Heyer WD, Kowalczykowski SC. Rad54 protein is targeted to pairing loci by the Rad51 nucleoprotein filament. Molecular Cell. 2000;6: 583–592. doi:10.1016/s1097-2765(00)00057-5

173. Petukhova G, Stratton S, Sung P. Catalysis of homologous DNA pairing by yeast Rad51 and Rad54 proteins. Nature. Nature Publishing Group; 1998;393: 91–94. doi:10.1038/30037

174. Amitani I, Baskin RJ, Kowalczykowski SC. Visualization of Rad54, a chromatin remodeling protein, translocating on single DNA molecules. Molecular Cell. 2006;23: 143–148. doi:10.1016/j.molcel.2006.05.009

175. Nimonkar AV, Amitani I, Baskin RJ, Kowalczykowski SC. Single molecule imaging of Tid1/Rdh54, a Rad54 homolog that translocates on duplex DNA and can disrupt joint molecules. Journal of Biological Chemistry. American Society for Biochemistry and Molecular Biology; 2007;282: 30776–30784. doi:10.1074/jbc.M704767200

176. Nimonkar AV, Dombrowski CC, Siino JS, Stasiak AZ, Stasiak A, Kowalczykowski SC. Saccharomyces cerevisiae Dmc1 and Rad51 proteins preferentially function with Tid1 and Rad54 proteins, respectively, to promote DNA strand invasion during genetic recombination. J Biol Chem. American Society for Biochemistry and Molecular Biology; 2012;287: 28727–28737. doi:10.1074/jbc.M112.373290

177. Mazina OM, Rossi MJ, Thomaä NH, Mazin AV. Interactions of human rad54 protein with branched DNA molecules. Journal of Biological Chemistry. American Society for Biochemistry and Molecular Biology; 2007;282: 21068–21080. doi:10.1074/jbc.M701992200

178. Petukhova G, Sung P, Klein H. Promotion of Rad51-dependent D-loop formation by yeast recombination factor Rdh54/Tid1. Genes Dev. Cold Spring Harbor Lab; 2000;14: 2206–2215. doi:10.1101/gad.826100

179. Van Komen S, Petukhova G, Sigurdsson S, Stratton S, Sung P. Superhelicity-driven homologous DNA pairing by yeast recombination factors Rad51 and Rad54. Molecular Cell. 2000;6: 563–572. doi:10.1016/s1097-2765(00)00055-1

180. Wright WD, Shah SS, Heyer W-D. Homologous recombination and the repair of DNA double-strand breaks. J Biol Chem. 2018;293: 10524–10535. doi:10.1074/jbc.TM118.000372

181. Cole GM, Mortimer RK. Failure to induce a DNA repair gene, RAD54, in Saccharomyces cerevisiae does not affect DNA repair or recombination phenotypes. Mol Cell Biol. American Society for Microbiology Journals; 1989;9: 3314–3322. doi:10.1128/mcb.9.8.3314

182. Klein HL. RDH54, a RAD54 homologue in Saccharomyces cerevisiae, is required for mitotic diploid-specific recombination and repair and for meiosis. Genetics. Genetics Society of America; 1997;147: 1533–1543.

183. Cal-Bakowska M, Litwin I, Bocer T, Wysocki R, Dziadkowiec D. The Swi2-Snf2-like protein Uls1 is involved in replication stress response. Nucleic Acids Res. 3rd ed. 2011;39: 8765–8777. doi:10.1093/nar/gkr587

184. Shinohara M, Shita-Yamaguchi E, Buerstedde JM, Shinagawa H, Ogawa H, Shinohara A. Characterization of the roles of the Saccharomyces cerevisiae RAD54 gene and a homologue of RAD54, RDH54/TID1, in mitosis and meiosis. Genetics. 1997;147: 1545–1556.

185. Heyer W-D, Li X, Rolfsmeier M, Zhang X-P. Rad54: the Swiss Army knife of homologous recombination? Nucleic Acids Res. 2006;34: 4115–4125. doi:10.1093/nar/gkl481

186. Rong L, Klein HL. Purification and characterization of the SRS2 DNA helicase of the yeast Saccharomyces cerevisiae. Journal of Biological Chemistry. 1993;268: 1252–1259.

187. Lohman TM, Tomko EJ, Wu CG. Non-hexameric DNA helicases and translocases: mechanisms and regulation. Nat Rev Mol Cell Biol. Nature Publishing Group; 2008;9: 391–401. doi:10.1038/nrm2394

188. Liu J, Ede C, Wright WD, Gore SK, Jenkins SS, Freudenthal BD, et al. Srs2 promotes synthesis-dependent strand annealing by disrupting DNA polymerase δ-extending D-loops. Elife. 2017;6: 105. doi:10.7554/eLife.22195

189. Ma E, Dupaigne P, Maloisel L, Guerois R, Le Cam E, Coïc E. Rad52-Rad51 association is essential to protect Rad51 filaments against Srs2, but facultative for filament formation. Elife. 2018;7: 3224. doi:10.7554/eLife.32744

190. Antony E, Tomko EJ, Xiao Q, Krejci L, Lohman TM, Ellenberger T. Srs2 disassembles Rad51 filaments by a protein-protein interaction triggering ATP turnover and dissociation of Rad51 from DNA. Molecular Cell. 2009;35: 105–115. doi:10.1016/j.molcel.2009.05.026

191. Agmon N, Liefshitz B, Zimmer C, Fabre E, Kupiec M. Effect of nuclear architecture on the efficiency of double-strand break repair. Nat Cell Biol. Nature Publishing Group; 2013;15: 694–699. doi:10.1038/ncb2745

192. Estrem C, Moore JK. Astral microtubule forces alter nuclear organization and inhibit DNA repair in budding yeast. Bloom KS, editor. Mol Biol Cell. 2019;30: 2000–2013. doi:10.1091/mbc.E18-12-0808

193. Hunter N. Meiotic Recombination: The Essence of Heredity. Cold Spring Harb Perspect Biol. Cold Spring Harbor Lab; 2015;7: a016618–35. doi:10.1101/cshperspect.a016618

194. Danilowicz C, Feinstein E, Conover A, Coljee VW, Vlassakis J, Chan Y-L, et al. RecA homology search is promoted by mechanical stress along the scanned duplex DNA. Nucleic Acids Res. 2012;40: 1717–1727. doi:10.1093/nar/gkr855

195. Forget AL, Kowalczykowski SC. Single-molecule imaging of DNA pairing by RecA reveals a three-dimensional homology search. Nature. Nature Publishing Group; 2012;482: 423–427. doi:10.1038/nature10782

196. Bugreev DV, Hanaoka F, Mazin AV. Rad54 dissociates homologous recombination intermediates by branch migration. Nat Struct Mol Biol. Nature Publishing Group; 2007;14: 746–753. doi:10.1038/nsmb1268

197. Ristic D, Wyman C, Paulusma C, Kanaar R. The architecture of the human Rad54-DNA complex provides evidence for protein translocation along DNA. Proc Natl Acad Sci USA. National Academy of Sciences; 2001;98: 8454–8460. doi:10.1073/pnas.151056798

198. Alexeev A, Mazin A, Kowalczykowski SC. Rad54 protein possesses chromatin-remodeling activity stimulated by the Rad51-ssDNA nucleoprotein filament. Nat Struct Biol. Nature Publishing Group; 2003;10: 182–186. doi:10.1038/nsb901

199. Renkawitz J, Lademann CA, Kalocsay M, Jentsch S. Monitoring homology search during DNA double-strand break repair in vivo. Molecular Cell.

2013;50: 261–272. doi:10.1016/j.molcel.2013.02.020

200. Tavares EM, Wright WD, Heyer W-D, Le Cam E, Dupaigne P. In vitro role of Rad54 in Rad51-ssDNA filament-dependent homology search and synaptic complexes formation. Nat Commun. Nature Publishing Group; 2019;10: 4058–12. doi:10.1038/s41467-019-12082-z

201. Tsubouchi H, Roeder GS. The Mnd1 protein forms a complex with hop2 to promote homologous chromosome pairing and meiotic double-strand break repair. Mol Cell Biol. American Society for Microbiology; 2002;22: 3078–3088. doi:10.1128/MCB.22.9.3078-3088.2002

202. Henry JM, Camahort R, Rice DA, Florens L, Swanson SK, Washburn MP, et al. Mnd1/Hop2 facilitates Dmc1-dependent interhomolog crossover formation in meiosis of budding yeast. Mol Cell Biol. 2006;26: 2913–2923. doi:10.1128/MCB.26.8.2913-2923.2006

203. Chen Y-K, Leng C-H, Olivares H, Lee M-H, Chang Y-C, Kung W-M, et al. Heterodimeric complexes of Hop2 and Mnd1 function with Dmc1 to promote meiotic homolog juxtaposition and strand assimilation. Proc Natl Acad Sci USA. National Acad Sciences; 2004;101: 10572–10577. doi:10.1073/pnas.0404195101

204. Zierhut C, Berlinger M, Rupp C, Shinohara A, Klein F. Mnd1 Is Required for Meiotic Interhomolog Repair. Current Biology. 2004;14: 752–762. doi:10.1016/j.cub.2004.04.030

205. Leu JY, Chua PR, Roeder GS. The meiosis-specific Hop2 protein of S. cerevisiae ensures synapsis between homologous chromosomes. Cell. 1998;94: 375–386. doi:10.1016/s0092-8674(00)81480-4

206. Tsubouchi H, Roeder GS. The Mnd1 protein forms a complex with hop2 to promote homologous chromosome pairing and meiotic double-strand break repair. Mol Cell Biol. American Society for Microbiology; 2002;22: 3078–3088. doi:10.1128/MCB.22.9.3078-3088.2002

207. Gerton JL, DeRisi JL. Mnd1p: an evolutionarily conserved protein required for meiotic recombination. Proc Natl Acad Sci USA. National Academy of Sciences; 2002;99: 6895–6900. doi:10.1073/pnas.102167899

208. Petukhova GV, Pezza RJ, Vanevski F, Ploquin M, Masson J-Y, Camerini-Otero RD. The Hop2 and Mnd1 proteins act in concert with Rad51 and Dmc1 in meiotic recombination. Nat Struct Mol Biol. 2005;12: 449–453. doi:10.1038/nsmb923

209. Chan Y-L, Brown MS, Qin D, Handa N, Bishop DK. The third exon of the budding yeast meiotic recombination gene HOP2 is required for calcium-

dependent and recombinase Dmc1-specific stimulation of homologous strand assimilation. J Biol Chem. American Society for Biochemistry and Molecular Biology; 2014;289: 18076–18086. doi:10.1074/jbc.M114.558601

210. Pezza RJ, Voloshin ON, Vanevski F, Camerini-Otero RD. Hop2/Mnd1 acts on two critical steps in Dmc1-promoted homologous pairing. Genes Dev. 2007;21: 1758–1766. doi:10.1101/gad.1562907

211. Pezza RJ, Camerini-Otero RD, Bianco PR. Hop2-Mnd1 condenses DNA to stimulate the synapsis phase of DNA strand exchange. Biophys J. 2010;99: 3763–3772. doi:10.1016/j.bpj.2010.10.028

212. Spies M, Fishel R. Mismatch repair during homologous and homeologous recombination. Cold Spring Harb Perspect Biol. 2015;7: a022657. doi:10.1101/cshperspect.a022657

213. Piazza A, Wright WD, Heyer W-D. Multi-invasions Are Recombination Byproducts that Induce Chromosomal Rearrangements. Cell. 2017;170: 760–773.e15. doi:10.1016/j.cell.2017.06.052

214. Piazza A, Heyer W-D. Moving forward one step back at a time: reversibility during homologous recombination. Current Genetics. Springer Berlin Heidelberg; 2019;: 1–8. doi:10.1007/s00294-019-00995-7

215. Mitchel K, Lehner K, Jinks-Robertson S. Heteroduplex DNA Position Defines the Roles of the Sgs1, Srs2, and Mph1 Helicases in Promoting Distinct Recombination Outcomes. Symington LS, editor. PLoS Genet. 2013;9: e1003340–13. doi:10.1371/journal.pgen.1003340

216. Gangloff S, Soustelle C, Fabre F. Homologous recombination is responsible for cell death in the absence of the Sgs1 and Srs2 helicases. Nat Genet. Nature Publishing Group; 2000;25: 192–194. doi:10.1038/76055

217. Prakash R, Satory D, Dray E, Papusha A, Scheller J, Kramer W, et al. Yeast Mph1 helicase dissociates Rad51-made D-loops: implications for crossover control in mitotic recombination. Genes Dev. Cold Spring Harbor Lab; 2009;23: 67–79. doi:10.1101/gad.1737809

218. Fasching CL, Cejka P, Kowalczykowski SC, Heyer W-D. Top3-Rmi1 dissolve Rad51-mediated D loops by a topoisomerase-based mechanism. Molecular Cell. 2015;57: 595–606. doi:10.1016/j.molcel.2015.01.022

219. Jessop L, Lichten M. Mus81/Mms4 endonuclease and Sgs1 helicase collaborate to ensure proper recombination intermediate metabolism during meiosis. Molecular Cell. 2008;31: 313–323. doi:10.1016/j.molcel.2008.05.021

220. Oh SD, Lao JP, Taylor AF, Smith GR, Hunter N. RecQ helicase, Sgs1, and XPF family endonuclease, Mus81-Mms4, resolve aberrant joint molecules during meiotic recombination. Molecular Cell. 2008;31: 324–336. doi:10.1016/j.molcel.2008.07.006

221. Crismani W, Girard C, Froger N, Pradillo M, Santos JL, Chelysheva L, et al. FANCM limits meiotic crossovers. Science. American Association for the Advancement of Science; 2012;336: 1588–1590. doi:10.1126/science.1220381

222. Knoll A, Higgins JD, Seeliger K, Reha SJ, Dangel NJ, Bauknecht M, et al. The Fanconi anemia ortholog FANCM ensures ordered homologous recombination in both somatic and meiotic cells in Arabidopsis. Plant Cell. American Society of Plant Biologists; 2012;24: 1448–1464. doi:10.1105/tpc.112.096644

223. Lorenz A, Osman F, Sun W, Nandi S, Steinacher R, Whitby MC. The fission yeast FANCM ortholog directs non-crossover recombination during meiosis. Science. American Association for the Advancement of Science; 2012;336: 1585–1588. doi:10.1126/science.1220111

224. Tang S, Wu MKY, Zhang R, Hunter N. Pervasive and essential roles of the Top3-Rmi1 decatenase orchestrate recombination and facilitate chromosome segregation in meiosis. Molecular Cell. 2015;57: 607–621. doi:10.1016/j.molcel.2015.01.021

225. Hunt LJ, Ahmed EA, Kaur H, Ahuja JS, Hulme L, Chou T-C, et al. S. cerevisiae Srs2 helicase ensures normal recombination intermediate metabolism during meiosis and prevents accumulation of Rad51 aggregates. Chromosoma; 2019;: 1–17. doi:10.1007/s00412-019-00705-9

226. McVey M, Khodaverdian VY, Meyer D, Cerqueira PG, Heyer W-D. Eukaryotic DNA Polymerases in Homologous Recombination. Annu Rev Genet. 2016;50: 393–421. doi:10.1146/annurev-genet-120215-035243

227. Strathern JN, Shafer BK, McGill CB. DNA synthesis errors associated with double-strand-break repair. Genetics. Genetics Society of America; 1995;140: 965–972.

228. Hicks WM, Kim M, Haber JE. Increased mutagenesis and unique mutation signature associated with mitotic gene conversion. Science. American Association for the Advancement of Science; 2010;329: 82–85. doi:10.1126/science.1191125

229. Fabre F, Boulet A, Faye G. Possible involvement of the yeast POLIII DNA polymerase in induced gene conversion. Mol Gen Genet. Springer-Verlag; 1991;229: 353–356. doi:10.1007/bf00267455

230. Holmes AM, Haber JE. Double-strand break repair in yeast requires both leading and lagging strand DNA polymerases. Cell. 1999;96: 415–424. doi:10.1016/s0092-8674(00)80554-1

231. Maloisel L, Bhargava J, Roeder GS. A role for DNA polymerase delta in gene conversion and crossing over during meiosis in Saccharomyces cerevisiae. Genetics. Genetics; 2004;167: 1133–1142. doi:10.1534/genetics.104.026260

232. Maloisel L, Fabre F, Gangloff S. DNA polymerase delta is preferentially recruited during homologous recombination to promote heteroduplex DNA extension. Mol Cell Biol. American Society for Microbiology Journals; 2008;28: 1373–1382. doi:10.1128/MCB.01651-07

233. Li X, Stith CM, Burgers PM, Heyer W-D. PCNA is required for initiation of recombination-associated DNA synthesis by DNA polymerase delta. Molecular Cell. 2009;36: 704–713. doi:10.1016/j.molcel.2009.09.036

234. Wilson MA, Kwon Y, Xu Y, Chung W-H, Chi P, Niu H, et al. Pif1 helicase and Polδ promote recombination-coupled DNA synthesis via bubble migration. Nature. Nature Publishing Group; 2013;502: 393–396. doi:10.1038/nature12585

235. Sebesta M, Burkovics P, Haracska L, Krejci L. Reconstitution of DNA repair synthesis in vitro and the role of polymerase and helicase activities. DNA Repair. 2011;10: 567–576. doi:10.1016/j.dnarep.2011.03.003

236. Li J, Holzschu DL, Sugiyama T. PCNA is efficiently loaded on the DNA recombination intermediate to modulate polymerase δ, η, and ζ activities. Proc Natl Acad Sci USA. National Academy of Sciences; 2013;110: 7672–7677. doi:10.1073/pnas.1222241110

237. Shcherbakova PV, Pavlov YI. 3“-->5” exonucleases of DNA polymerases epsilon and delta correct base analog induced DNA replication errors on opposite DNA strands in Saccharomyces cerevisiae. Genetics. Genetics Society of America; 1996;142: 717–726.

238. Holbeck SL, Strathern JN. A role for REV3 in mutagenesis during double-strand break repair in Saccharomyces cerevisiae. Genetics. Genetics Society of America; 1997;147: 1017–1024.

239. Kawamoto T, Araki K, Sonoda E, Yamashita YM, Harada K, Kikuchi K, et al. Dual roles for DNA polymerase eta in homologous DNA recombination and translesion DNA synthesis. Molecular Cell. 2005;20: 793–799. doi:10.1016/j.molcel.2005.10.016

240. Pomerantz RT, Goodman MF, O'Donnell ME. DNA polymerases are error-

prone at RecA-mediated recombination intermediates. Cell Cycle. 2013;12: 2558–2563. doi:10.4161/cc.25691

241. Meyer D, Fu BXH, Chavez M, Loeillet S, Cerqueira PG, Nicolas A, et al. Cooperation between non-essential DNA polymerases contributes to genome stability in Saccharomyces cerevisiae. DNA Repair. 2019;76: 40–49. doi:10.1016/j.dnarep.2019.02.004

242. McMahill MS, Sham CW, Bishop DK. Synthesis-dependent strand annealing in meiosis. Lichten M, editor. PLoS Biol. Public Library of Science; 2007;5: e299. doi:10.1371/journal.pbio.0050299

243. Mortensen UH, Bendixen C, Sunjevaric I, Rothstein R. DNA strand annealing is promoted by the yeast Rad52 protein. Proc Natl Acad Sci USA. National Academy of Sciences; 1996;93: 10729–10734. doi:10.1073/pnas.93.20.10729

244. Shinohara A, Shinohara M, Ohta T, Matsuda S, Ogawa T. Rad52 forms ring structures and co-operates with RPA in single-strand DNA annealing. Genes Cells. 1998;3: 145–156.

245. Symington LS. Role of RAD52 epistasis group genes in homologous recombination and double-strand break repair. Microbiol Mol Biol Rev. American Society for Microbiology; 2002;66: 630–70– table of contents. doi:10.1128/mmbr.66.4.630-670.2002

246. Petukhova G, Stratton SA, Sung P. Single strand DNA binding and annealing activities in the yeast recombination factor Rad59. Journal of Biological Chemistry. American Society for Biochemistry and Molecular Biology; 1999;274: 33839–33842. doi:10.1074/jbc.274.48.33839

247. Sugawara N, Ira G, Haber JE. DNA length dependence of the single-strand annealing pathway and the role of Saccharomyces cerevisiae RAD59 in double-strand break repair. Mol Cell Biol. American Society for Microbiology Journals; 2000;20: 5300–5309. doi:10.1128/mcb.20.14.5300-5309.2000

248. Davis AP, Symington LS. The yeast recombinational repair protein Rad59 interacts with Rad52 and stimulates single-strand annealing. Genetics. Genetics Society of America; 2001;159: 515–525.

249. Ira G, Malkova A, Liberi G, Foiani M, Haber JE. Srs2 and Sgs1-Top3 suppress crossovers during double-strand break repair in yeast. Cell. 2003;115: 401–411. doi:10.1016/s0092-8674(03)00886-9

250. Zakharyevich K, Tang S, Ma Y, Hunter N. Delineation of joint molecule resolution pathways in meiosis identifies a crossover-specific resolvase. Cell. 2012;149: 334–347. doi:10.1016/j.cell.2012.03.023

251. Bizard AH, Hickson ID. The dissolution of double Holliday junctions. Cold Spring Harb Perspect Biol. Cold Spring Harbor Lab; 2014;6: a016477–a016477. doi:10.1101/cshperspect.a016477

Chapter 2: Materials and methods

* Douglas Bishop and Jennifer Grubb performed some of the meiotic time course experiments. Jennifer Grubb was responsible for the meiotic two-hybrid analysis. In addition, Douglas Bishop prepared and stained spread yeast nuclei for analysis by wide-field microscopy for one experiment. Super-resolution imaging by stimulated emission depletion (STED) microscopy was performed at the University of Chicago microscopy core with technical assistance from Vytas Bindokas and Christine Labno.

## 2.1 Chapter overview

The methods used in the preparation of the data contained within this dissertation are described.

## 2.2 Materials and methods

### 2.2.1 Yeast strains

The yeast strains used in this study are listed in Table 2.1. All yeast strains are isogenic derivatives of strain SK-1.

| Name | Strain | Genotype |
|---|---|---|
| wild-type | DKB3698 | *ho::hisG/", leu2::hisG/", ura3(ΔSma-Pst)/", HIS4::LEU2-(BamHI; +ori)/his4-X::LEU2-(NgoMIV; +ori)-URA3* |
| *dmc1-E157D* | DKB6342 | *lys2/", ho::hisG/ho::LYS2, leu2::hisG, ura3/", HIS4::LEU2-(BamHI; +ori)/his4-X::LEU2-(NgoMIV; +ori)-URA3, dmc1-E157D-NATMX4/"* |
| *DMC1$^{+}$/dmc1-E157D* | DKB6398 | *LYS2/lys2 or LYS2, ho::hisG/ho::hisG or ho::LYS2, leu2::hisG/", ura3/", HIS4::LEU2-(BamHI; +ori)/", dmc1-E157D-NATMX4/DMC1$^{+}$* |

**Table 2.1** Yeast strains used in this study.

| Name | Strain | Genotype |
|---|---|---|
| *DMC1$^{+}$/dmc1-E157D* | DKB6399 | *LYS2/lys2 or LYS2, ho::hisG/ho::hisG or ho::LYS2, leu2::hisG/", ura3/", HIS4::LEU2-(BamHI; +ori)/", dmc1-E157D-NATMX4/DMC1$^{+}$* |
| *mei5* | DKB6320 | *ho::hisG/", leu2::hisG/", ura3/", HIS4::LEU2-(BamHI; +ori)/his4-X::LEU2-(NgoMIV; +ori)-URA3, mei5::KANMX/"* |
| *ndt80* | DKB3428 | *ho::hisG/", leu2::hisG/", ura3(ΔPst-Sma)/", HIS4X::LEU2-(BamHI)-ura3/his4::LEU2(NgoMIV; +ori)-URA3, ndt80::KANMX4/"* |
| *rad51* | DKB3710 | *ho::hisG or LYS2/", ura3/", leu2::hisG/", HIS4::LEU2-(BamHI; +ori)/his4X::LEU2-(NgoMIV; +ori)-URA3, rad51::hisG/"* |
| *rad51-II3A* | DKB3689 | *ho::hisG/", leu2::hisG/", ura3(ΔSma-Pst)/",HIS4-X::LEU2-(BamHI; +ori)-ura3/his4X::LEU2-(NgoMIV; +or)-URA3, RAD51-R188A, K361A, K371A-KANMX6/"* |
| *rdh54* | DKB2526 | *ho::LYS2/", lys2/", leu2::hisG/", his4-X::LEU2/", trp1::hisG/", tid1::LEU2/"* |
| *spo11* | DKB2123 | *ho::LYS2/", lys2/", leu2::hisG/", ura3/", his4-X/his4B, spo11::hisG-URA3-hisG/"* |
| *spo11* | DKB2524 | *ho::LYS2/", lys2/", leu2::hisG/", trp1::hisG/", ura3/", his4X::LEU2/", spo11::hisG-URA3-hisG/"* |
| *dmc1-E157D mei5* | DKB6299 | *ho::LYS2/ho::hisG, ura3/", leu2::hisG/", HIS4::LEU2-(BamHI; +ori)/his4-X::LEU2-(NgoMIV; +ori)-URA3, dmc1-E157D-NATMX4/", mei5::KANMX/"* |
| *dmc1-E157D mei5* | DKB6300 | *ho::LYS2/ho::hisG, ura3/", leu2::hisG/", HIS4::LEU2-(BamHI; +ori)/his4-X::LEU2-(NgoMIV; +ori)-URA3, dmc1-E157D-NATMX4/", mei5::KANMX/"* |
| *DMC1/dmc1-E157D mei5* | DKB6406 | *ho::hisG, leu2::hisG, ura3, his4-X::LEU2-(NgoMIV; +ori)-URA3/HIS4::LEU2-(BamHI; +ori), mei5::KANMX/", dmc1-E157D-NATMX4/DMC1$^{+}$* |
| *DMC1/dmc1-E157D mei5* | DKB6407 | *ho::hisG, leu2::hisG, ura3, his4-X::LEU2-(NgoMIV; +ori)-URA3/HIS4::LEU2-(BamHI; +ori), mei5::KANMX/", dmc1-E157D-NATMX4/DMC1$^{+}$* |
| *dmc1-E157D ndt80* | DKB6676 | *ho::hisG/", lys2/", leu2::hisG/", ura3/", HIS4X::LEU2-(BamHI)-ura3/his4::LEU2(NgoMIV; +ori)-URA3, ndt80::KANMX4/", dmc1-E157D-NATMX4/"* |
| *dmc1-E157D ndt80* | DKB6682 | *LYS2/lys2 or LYS2, ho::hisG/ho::hisG or ho::LYS2, leu2::hisG/", ura3/", HIS4X::LEU2-(BamHI)-ura3/his4::LEU2(NgoMIV; +ori)-URA3, ndt80::KANMX4/", dmc1-E157D-NATMX4/"* |
| *dmc1-E157D rad51* | DKB6393 | *lys2* or *LYS2/", ho::hisG* or *ho::LYS2/", ura3/", leu2::hisG/", arg4-nsp/ARG4, his4-X::LEU2-(NgoMIV; +ori)--URA3/HIS4::LEU2-(BamHI; +ori), dmc1-E157D-NATMX4/", rad51::hisG/"* |
| *dmc1-E157D rad51-II3A* | DKB6400 | *ho::hisG/", leu2::hisG/", ura3/", HIS4::LEU2-(BamHI; +ori)/his4-X::LEU2-(NgoMIV; +ori)-URA, RAD51-R188A, K361A, K371-A-KANMX6/", dmc1-E157D-NATMX4/"* |

**Table 2.1 (continued)** Yeast strains used in this study.

| Name | Strain | Genotype |
|---|---|---|
| *dmc1-E157D rdh54* | DKB6583 | *ho::LYS2/", lys2/", leu2::hisG/", his4-X::LEU2/", TRP1/trp1::hisG, tid1::LEU2/", dmc1-E157D-NATMX4/"* |
| *dmc1-E157D sae3* | DKB6539 | *lys2/", ho::LYS2/", leu2 or LEU2/", ura3/", HIS4::LEU2-(BamHI; +ori)/his4-X::LEU2-(NgoMIV; +ori)-URA3, dmc1-E157D-NATMX4/", sae3::hisG-URA3-hisG/"* |
| *dmc1-E157D sae3* | DKB6540 | *lys2/", ho::LYS2/", leu2 or LEU2/", ura3/", HIS4::LEU2-(BamHI; +ori)/his4-X::LEU2-(NgoMIV; +ori)-URA3, dmc1-E157D-NATMX4/", sae3::hisG-URA3-hisG/"* |
| *spo11 dmc1-E157D* | DKB6419 | *ho::hisG* or *ho::LYS2/ho::hisG, LYS2* or *lys2/lys2, leu2::hisG/", ura3/", his4-X::LEU2-(NgoMIV; +ori)-URA3/HIS4::LEU2-(BamHI; +ori), dmc1-E157D-NATMX4/", spo11::hisG-URA3-hisG/"* |
| *spo11 rdh54* | DKB2523 | *ho::LYS2/", lys2/", ura3/", leu2::hisG/", his4-X::LEU2/", trp1::hisG/", tid1::LEU2/", spo11::hisG-URA3-hisG/"* |
| *dmc1-E157D mei5 rad51* | DKB6412 | *lys2 or LYS2/", ho::hisG or ho::LYS2/", ura3/", leu2::hisG/", arg4-nsp or ARG4/ARG4, HIS4::LEU2-(BamHI; +ori)/his4-X::LEU2-(NgoMIV; +ori), rad51::hisG/", dmc1-E157D-NATMX4/", mei5::KANMX/"* |
| *dmc1-E157D mei5 rad51* | DKB6413 | *lys2* or *LYS2/", ho::hisG* or *ho::LYS2/", ura3/", leu2::hisG/", arg4-nsp/ARG4, HIS4::LEU2-(BamHI; +ori)/his4-X::LEU2-(NgoMIV; +ori), rad51::hisG/", dmc1-E157D-NATMX4/", mei5::KANMX/"* |
| *spo11 dmc1-E157D mei5* | DKB6425 | *ho::hisG or ho::LYS2/", lys2 or LYS2, leu2::hisG/", ura3/", HIS4::LEU2-(BamHI; +ori)/his4-X::LEU2-(NgoMIV; +ori)-URA3, dmc1-E157D-NATMX4/", spo11::hisG-URA3-hisG/", mei5::KANMX/"* |
| *spo11 mei5 rdh54* | DKB6571 | *ho::LYS2/", lys2/", ura3/", leu2::hisG/", his4-X::LEU2/", trp1::hisG/", tid1::LEU2/", spo11::hisG-URA3-hisG/", mei5::KANMX/"* |
| two-hybrid strain | DKB6501 | *lys2/", ho::LYS2/", URA3/", leu2:hisG/", his4-X/HIS4, trp1::hisG/", arg4-nsp or ARG4/", dmc1::ARG4/", rad51::hisG/", ndt80::KANMX/", LexA(op)-lacZ::URA3/" +pNRB729 +pNRB271* |
| two-hybrid strain | DKB6503 | *lys2/", ho::LYS2/", URA3/", leu2:hisG/", his4-X/HIS4, trp1::hisG/", arg4-nsp or ARG4/", dmc1::ARG4/", rad51::hisG/", ndt80::KANMX/", LexA(op)-lacZ::URA3/" +pNRB727 +pNRB688* |
| two-hybrid strain | DKB6508 | *lys2/", ho::LYS2/", URA3/", leu2:hisG/", HIS4/his4-X, trp1::hisG/", arg4-nsp or ARG4/", dmc1::ARG4/", :mei5:KANMX/", rad51::hisG/", ndt80::KANMX/", LexA(op)-lacZ::URA3/" +pNRB727 +pNRB271* |
| two-hybrid strain | DKB6509 | *lys2/", ho::LYS2/", URA3/", leu2:hisG/", his4-X/HIS4, trp1::hisG/", arg4-nsp or ARG4/", dmc1::ARG4/", rad51::hisG/", ndt80::KANMX/", LexA(op)-lacZ::URA3/" +pNRB727 +pNRB271* |
| two-hybrid strain | DKB6513 | *lys2/", ho::LYS2/", URA3/", leu2:hisG/", his4-X/HIS4, trp1::hisG/", arg4-nsp or ARG4/", dmc1::ARG4/", rad51::hisG/", ndt80::KANMX/", LexA(op)-lacZ::URA3/" +pNRB728 +pNRB271* |

**Table 2.1 (continued)** Yeast strains used in this study.

| Name | Strain | Genotype |
|---|---|---|
| two-hybrid strain | DKB6515 | *lys2/", ho::LYS2/", URA3/", leu2:hisG/", his4-X/HIS4, trp1::hisG/", arg4-nsp or ARG4/", dmc1::ARG4/", rad51::hisG/", ndt80::KANMX/", LexA(op)-lacZ::URA3/" +pNRB727 +pNRB267* |

**Table 2.1 (continued)** Yeast strains used in this study.

To construct the *dmc1* point mutants, DKB plasmid pNRB628 containing the *DMC1* open reading frame, a 701 base pair upstream homology arm, the *TEF1* promoter, the *natMX4* open reading frame, the *ADH1* terminator, and a 40 base pair downstream homology arm, was modified by Gibson assembly to include the desired point mutations. *dmc1::LEU2-URA3-KAN* haploid yeast (DKB129, DKB130) were transformed with a linear PCR fragment containing the homology arms, the mutated *dmc1* open reading frame, and the *natMX4* (for resistance to nourseothricin sulfate, or cloNAT) selectable marker. Yeast were outgrown in 5 milliliters liquid YPDA for 4.5 hours at 30°C in a culture rotator, then plated on selective media and allowed to grow at 30°C for 3 days. After 3 days, colonies were struck out on the selective media and on 5-fluoroorotic acid (5-FOA), which selects against *URA3*$^{+}$ yeast and therefore identifies clones that have lost the *dmc1::LEU2-URA3-KAN* allele. Those colonies that grew on the cloNAT media and did not grow on the 5-FOA plates were tested to confirm proper targeting by polymerase chain reaction, and then confirmed via sequencing.

### 2.2.2 Meiotic time courses

Yeast cultures were induced to undergo synchronous meiosis as described previously [1]. Appropriate samples were collected at time points indicated in figures.

### 2.2.3 Spore viability

Spore viability was determined by tetrad dissection as the percent of spores that germinate and form a colony on a YPDA plate relative to the number expected if all dissected spores had lived.

### 2.2.4 Preparation and staining of spread yeast nuclei

Surface-spreading and immunostaining of meiotic yeast chromosomes on glass slides was performed as described previously [2]. Primary antibodies were used at the following dilutions: purified anti-goat Dmc1 bleed #4 DKB antibody #192 (1:800), anti-rabbit Rad51 bleed #2 DKB antibody #159 (1:1000), anti-rabbit RFA2 (1:1000), and anti-rabbit Hop2 bleed #3 DKB antibody #143 (1:1000). Secondary antibodies were used at a dilution of 1:1000 and included: Alexa Fluor 488 chicken anti-goat (Invitrogen by ThermoFisher Scientific), Alexa Fluor 594 donkey anti-rabbit (Invitrogen by ThermoFisher Scientific), Alexa Fluor 594 donkey anti-goat (Invitrogen by ThermoFisher Scientific) and Alexa Fluor 488 donkey anti-rabbit (Invitrogen by ThermoFisher Scientific). Images were collected on a Zeiss Axiovision 4.6 wide-field fluorescence microscope at 100X magnification. The same imaging parameters were used for all samples.

### 2.2.5 Wide-field microscopy analysis

For each strain, 50 or more adjacent and randomly selected nuclei were imaged. A field of nuclei was chosen for analysis based on the DAPI staining pattern. Nuclei were scored as focus positive if there were 3 or more immunostaining foci in a given nucleus. Due to focus crowding in wide-field images, it was not possible to generate reliable focus counts using automated methods. Therefore, focus counts were determined by eye for the experiments reported in Supplemental Figure 8.

### 2.2.6 One-dimensional gel electrophoresis

One-dimensional gel electrophoresis at the *HIS4::LEU2* meiotic hotspot was performed as follows. 15 milliliter sporulation media samples were collected at time points indicated from meiotic cultures. Sodium azide was added to a final concentration of 0.1%. Cells were spun down at 3000 rpm in tabletop clinical centrifuges for 5 minutes, then the supernatant was removed and the pellet was frozen at -20°C. DNA was then purified as described previously [3]. Approximately 2 micrograms DNA per sample was then digested with XhoI or PstI (as indicated in figure legend) restriction enzyme (New England BioLabs) and processed as described previously [3]. Samples were then run on a 0.6% (XhoI) or 0.7% (PstI) agarose gel at 2V/cm for 24 (XhoI) or 18 (PstI) hours, followed by Southern blotting as described previously [4].

### 2.2.7 Two-dimensional gel electrophoresis

Two-dimensional gel electrophoresis at the *HIS4:LEU2* meiotic hotspot was performed as previously described [5].

### 2.2.8 Meiotic two-hybrid analysis

Analysis of Rad51-Dmc1 interaction in meiotic cells was performed using the meiotic two-hybrid method [6]. DNA binding domain constructs were transformed into *MATa* haploid strains DKB6431 (*MEI5*$^{+}$) and DKB6429 (*mei5*) and activation domain constructs were transformed into *MATα* haploid strains DKB6430 (*MEI5*$^{+}$) and DKB6428 (*mei5*). Independent transformants were mated to generate the diploid strains used for meiotic two hybrid experiments. 5 ml cultures were grown for 72 hours in synthetic tryptophan leucine dropout media to maintain 2μ plasmids and then transferred to YPD medium at OD600=0.2, and then grown for two generations before being transferred to

SPS medium overnight, after which sporulation was induced on SPM-1/5COM medium. Recipes for media are as described previously [1]. Samples were prepared for β-galactosidase assays after 6 hours and 18 hours. The plasmids used for the two-hybrid studies were derived from pGAD-C1 [7] for activation domain fusions, and from pCA1 a gift from Scott Keeney [6] for DNA binding domain fusions. Note that this system uses *E. coli lexA* as DNA binding domain for hybrid constructs in combination with a *lex-op::lacZ* reporter construct [6]. Plasmid designations and the markers carried by the plasmids were as follows: Dmc1BD=pNRB729 *2μ, TRP1, $P_{DMC1}$-DMC1-lexA, ampR, ori; Dmc1AD=pNRB271 2μ, LEU2, $P_{ADH}$-GAL4-AD::DMC1, ampR, ori*; Rad51BD=pNRB727 *2μ, TRP1, $P_{DMC1}$-lexA-Rad51, ampR, ori*; Rad51AD=pNRB688 *2μ, LEU2, $P_{ADH}$-GAL4-AD::RAD51, ampR, ori*; ∆BD=pNRB728 *2μ, TRP1, $P_{DMC1}$-lexA, ampR, ori*; and ∆AD=pNRB267 *2μ, LEU2, $P_{ADH}$-GAL4, ampR, ori.* Plasmid sequences are available on request.

**2.2.9 Immunofluorescence imaging by STED microscopy**

Spreads were stained using a protocol described previously [2] with the following modifications. Spreads were dipped in 0.2% Photo-Flo (Kodak) for 30 seconds, the excess was tapped off, and then the slides were washed in 1X TBS for 5 minutes. Spreads were then blocked with 300μL 3% BSA in 1X TBS. Following blocking, spreads were incubated with anti-goat Dmc1 (1:800) and anti-Rabbit RPA (1:1000) for ≥16 hours at 4°C. Slides were then washed in 1X TBS + 0.05% Triton X-100 for 5 minutes with gentle rocking 7 times. Spreads were incubated with fluorochrome-conjugated secondary antibodies Alexa Fluor 594 donkey anti-goat and Alex Fluor 488 donkey anti-rabbit (1:1000) (ThermoFisher Scientific) for 2 hours at 4°C, followed by washes as

described. Slides were allowed to dry completely in fume hood, then 35μL Vectashield (Vector Laboratories, Inc.) was added, a coverslip was placed atop the slide, and the coverslip was sealed with nail polish.

Imaging was conducted on a Leica SP8 3D, 3-color Stimulated Emission Depletion (STED) Laser Scanning Confocal Microscope at the University of Chicago Integrated Light Microscopy Core Facility. The same imaging parameters were used for all strains. Images were deconvolved using Huygens software and applying the same settings for each image. Resolution is reported based on measurements taken from deconvolved images.

### 2.2.10 STED microscopy analysis

To quantitate the number of foci in each nucleus, the image channels were separated, and each channel image was converted to a binary image in ImageJ. The "Analyze Particles" function was used to obtain information regarding the number of foci in an image, the coordinates of the center of each focus, and the major length of each focus. The same settings were used to analyze all images. Colocalization between Dmc1 and RPA was scored in R using the coordinates given by ImageJ to calculate the distance between a given Dmc1 focus and all RPA foci in the nucleus. A Dmc1 focus was scored as colocalizing with a RPA focus if the nearest RPA focus was less than the length of that Dmc1 focus plus a preset RPA value that was calculated for each strain. The RPA value was calculated based on one half of the average length of all RPA foci in that sample plus one half of two standard deviations of that RPA length. This means that if a given Dmc1 focus is sitting side-by-side with an RPA focus, the distance between it and the center of the nearest RPA focus can be the length of that Dmc1

focus plus one half the average length of all RPA foci in that strain background, plus one half of two standard deviations of the RPA focus lengths. This calculation attempts to take into account the fact that both RPA foci and Dmc1 focus lengths vary from sample to sample. Plots and statistical tests were carried out in R using the ggplot and ggpubr packages.

### 2.2.11 Meiotic whole cell lysate, SDS-PAGE, and Western blotting

4 milliliters of meiotic culture was collected at the appropriate time point. Tricholoroacetic acid was added to a final concentration of 10% weight/volume. Samples were placed in a 60°C water bath for 5 minutes, then placed on ice for 5 minutes. Next, samples were spun down at 3000 rotations per minute in a low-speed centrifuge, the supernatant removed by aspiration, and pellet then washed in $ddH_2O$. The pellet was then re-suspended in 1X-SDS-PAGE (60 mM TrisHCl pH 6.8, 0.05% SDS, 100 mM DTT, 5% glycerol) buffer supplemented with 50 mM sodium PIPES pH 7.5 to the appropriate concentration according to the optical density of cells in the sample. The samples were then boiled for 10 minutes, spun down, and pellets stored at -20°C.

A 12% SDS-polyacrylamide gel was prepared, and 30 microliters of each sample was run at 120V for 1.5 hours alongside 20 nanograms purified Dmc1 protein. Samples were then transferred to Merck Millipore Limited Immobilon-P Transfer Membrane for 16 hours at 50V at 4°C. The membrane was then blotted using anti-goat Dmc1 (1:1000) primary antibody and an anti-goat HRP-conjugated secondary antibody (1:1000).

### 2.2.12 Meiotic progression and MI segregation imaging

Differential interference contrast (DIC) and epifluorescence images were collected on an IX-81 microscope (Olympus, Tokyo, Japan) controlled by MetaMorph software (Molecular Devices, Sunnyvale, CA) and fitted with an Orca-ER camera (Hamamatsu, Bridgewater, NJ) and a 60X, 1.4 NA Plan Apo objective. Nuclear divisions were monitored by DAPI staining. Cells with two DAPI-staining bodies or a single DAPI-staining body that was stretched were scored as having initiated MI; cells with three or more DAPI bodies or an "X" shape were scored as undergoing meiosis II division.

### 2.2.13 Protein purification

All proteins used in this study are *Saccharomyces cerevisiae* proteins. His6-tagged Dmc1 was expressed and purified as described previously with the following modifications [8,9]. Quick change PCR was used to introduce the E157D mutation into *DMC1* overexpression plasmid pNRB150, generating plasmid pNRB756. This plasmid was introduced into the *E. coli* strain Rosetta(DE3)pLysS by transformation. Cells were then selected on agar plates containing 100 µg/mL ampicillin, 34 µg/mL chloramphenicol, and 1% glucose at 37°C. The next morning, many individual colonies were used to inoculate one liter LB supplemented with 1% glucose, 100 µg/mL ampicillin, and 17 µg/mL chloramphenicol in a 2.8-L baffled flask. Cells were then grown in a shaker at 37°C (230–250 rpm) until $A_{600}$ reaches 0.5–0.7. *DMC1-E157D* expression was then induced by adding IPTG to a final concentration of 0.5 mM. Cells were harvested after 1.5 hours.

### 2.2.14 D-loop assays

D-loop assays were carried out as previously described [9,10].

References


1. Bishop DK. RecA homologs Dmc1 and Rad51 interact to form multiple nuclear complexes prior to meiotic chromosome synapsis. Cell. 1994;79: 1081–1092.

2. Grubb J, Brown MS, Bishop DK. Surface Spreading and Immunostaining of Yeast Chromosomes. J Vis Exp. 2015;: e53081. doi:10.3791/53081

3. Lao JP, Tang S, Hunter N. Native/Denaturing two-dimensional DNA electrophoresis and its application to the analysis of recombination intermediates. Methods Mol Biol. Totowa, NJ: Humana Press; 2013;1054: 105–120. doi:10.1007/978-1-62703-565-1_6

4. Oh SD, Jessop L, Lao JP, Allers T, Lichten M, Hunter N. Stabilization and electrophoretic analysis of meiotic recombination intermediates in Saccharomyces cerevisiae. Methods Mol Biol. Totowa, NJ: Humana Press; 2009;557: 209–234. doi:10.1007/978-1-59745-527-5_14

5. Cloud V, Chan Y-L, Grubb J, Budke B, Bishop DK. Rad51 is an accessory factor for Dmc1-mediated joint molecule formation during meiosis. Science. 2012;337: 1222–1225. doi:10.1126/science.1219379

6. Arora C, Kee K, Maleki S, Keeney S. Antiviral protein Ski8 is a direct partner of Spo11 in meiotic DNA break formation, independent of its cytoplasmic role in RNA metabolism. Molecular Cell. 2004;13: 549–559.

7. James P, Halladay J, Craig EA. Genomic Libraries and a Host Strain Designed for Highly Efficient Two-Hybrid Selection in Yeast. Genetics. Genetics Society of America; 1996;144: 1425–1436.

8. Hong EL, Shinohara A, Bishop DK. Saccharomyces cerevisiae Dmc1 protein promotes renaturation of single-strand DNA (ssDNA) and assimilation of ssDNA into homologous super-coiled duplex DNA. Journal of Biological Chemistry. 2001;276: 41906–41912. doi:10.1074/jbc.M105563200

9. Chan Y-L, Bishop DK. Purification of Saccharomyces cerevisiae Homologous Recombination Proteins Dmc1 and Rdh54/Tid1 and a Fluorescent D-Loop Assay. Meth Enzymol. Elsevier; 2018;600: 307–320. doi:10.1016/bs.mie.2017.12.003

10. Chan Y-L, Zhang A, Weissman BP, Bishop DK. RPA resolves conflicting activities of accessory proteins during reconstitution of Dmc1-mediated meiotic recombination. Nucleic Acids Res. 2019;47: 747–761. doi:10.1093/nar/gky1160

# Chapter 3: A mutant form of Dmc1 that bypasses the requirement for accessory protein Mei5-Sae3 reveals independent activities of Mei5-Sae3 and Rad51 in Dmc1 filament stability

* This chapter is a slightly modified version of a manuscript that we submitted to PLoS Genetics and that is currently under revision: Reitz, D., Grubb, J., Bishop, D.K. A mutant form of Dmc1 that bypasses the requirement for accessory protein Mei5-Sae3 reveals independent activities of Mei5-Sae3 and Rad51 in Dmc1 filament stability (submitted 2019). Jennifer Grubb performed the meiotic two-hybrid analysis (Supplemental Figure 3.7) and the imaging associated with the MI segregation analysis (Supplemental Figure 3.3a). Douglas Bishop contributed the time course analysis of *dmc1-E157D*, *rdh54*, and *dmc1-E157D rdh54* strains (Supplemental Figure 3.9), as well as the experiment to look at the dependency of Dmc1 focus formation on Mei5-Sae3 in the *spo11 rdh54* background (Supplemental Figure 3.10).

## 3.1 Chapter overview

During meiosis, two rounds of division follow a single round of DNA replication to create the gametes for biparental reproduction. The first round of division requires that the homologous chromosomes become physically linked to one another to create the tension that is necessary for their segregation. This linkage is achieved through DNA recombination between the two homologous chromosomes, followed by resolution of the recombination intermediate into a crossover. Central to this process is the meiosis-specific recombinase Dmc1, and its accessory factors, which provide important

regulatory functions to ensure that recombination is accurate, efficient, and occurs predominantly between homologous chromosomes, and not sister chromatids. To gain insight into the regulation of Dmc1 by its accessory factors, we mutated Dmc1 such that it was no longer dependent on its accessory factor Mei5-Sae3. Our analysis reveals that Dmc1 accessory factors Mei5-Sae3 and Rad51 have independent roles in stabilizing Dmc1 filaments. Furthermore, we find that although Rad51 is required for promoting recombination between homologous chromosomes, Mei5-Sae3 is not. Lastly, we show that our Dmc1 mutant forms abnormally long filaments, and high levels of aberrant recombination intermediates and products. These findings suggest that filaments are actively maintained at short lengths to prevent deleterious genome rearrangements.

## 3.2 Introduction

Homologous recombination (HR) is a high-fidelity mechanism of repair of DNA double strand breaks (DSBs), interstrand cross-links, and stalled or collapsed replication forks in mitotically dividing cells. In addition, during meiosis, most eukaryotes rely on reciprocal crossover recombination (CO) to physically link the maternal and paternal chromosomes via chiasmata, thereby making it possible for the meiosis I (MI) spindle to create the tension between homolog pairs that is required for their reductional segregation [1]. The RecA homolog Dmc1 is specifically expressed in meiotic cells and plays the central catalytic role in meiotic recombination in budding yeast [2,3]. A second RecA homolog, Rad51, plays the central catalytic role in mitotic recombination [4,5], but is converted to an accessory protein that regulates Dmc1's catalytic activity in meiotic cells [3].

Meiotic recombination is initiated by programmed DSBs formed by the activity of the transesterase Spo11 [6]. Following meiotic DSB formation and end resection, Dmc1 forms a helical nucleoprotein filament on the single-stranded DNA (ssDNA) tracts created by the resection machinery [7]. The nucleoprotein filament then searches the genome for a sequence of duplex DNA that is homologous to the ssDNA onto which it is loaded [8]. This region of homology can be an allelic site on one of the two homologous chromatids or on the sister chromatid. In addition, if a DSB is in a region that is repeated at more than one chromosomal locus, this can result in ectopic recombination between the two chromosomal loci [9-12]. Meiotic recombination normally favors the use of the homologous chromosome rather than the sister chromatid, consistent with the biological requirement for interhomolog (IH) COs for reductional segregation; this phenomenon is known as “IH bias” [13,14]. Once a homologous region of double-stranded DNA (dsDNA) is found, strand exchange occurs to form a tract of hybrid DNA, pairing the ssDNA with the complementary strand of the duplex. Hybrid DNA formation displaces the opposite strand of the donor dsDNA, forming a displacement loop (D-loop) [15]. The repair process then uses the intact donor duplex DNA as a template to direct recombination-associated DNA synthesis [16]. Processing of extended D-loops by helicases gives rise to non-crossover recombinants by a pathway referred to as synthesis-dependent strand annealing [17-19]. The subset of D-loops destined to become COs are stabilized to form a joint molecule (JM) species that can be detected on two-dimensional (2D) gels as a so-called single-end invasion (SEI) [20]. SEIs are then converted to double Holliday Junction intermediates (dHJs) by the capture of the

second end of the DSB and further repair synthesis to generate full length dsDNA [21]. Finally dHJs are resolved by Exo1 and the MutL $\gamma$ complex to give rise to COs [22].

HR is highly regulated to ensure its accuracy and avoid potentially deleterious consequences of the process. Two key steps in HR, nucleoprotein filament formation and the initial invasion event, are reversible and therefore subject to this regulation [23]. Nucleoprotein filament formation, or nucleation, involves the recruitment of the strand exchange protein to sites of ssDNA tracts, followed by displacement of the high affinity ssDNA binding protein RPA. Next, filaments elongate in a process that is driven by cooperative interactions between strand exchange protomers. A class of accessory proteins collectively referred to as “mediator” proteins can act to promote the displacement of RPA and/or to stabilize nascent filaments, allowing them to elongate [24,25]. Mutants lacking one of these assembly proteins display defects in formation of filaments on ssDNA, which can be detected by immunostaining or other cytological methods following DNA damaging treatment, or during the normal meiotic program. UvrD family helicases, including UvrD in prokaryotes and Srs2 in budding yeast, antagonize recombination at this step by disassembling ssDNA nucleoprotein filaments [26-29]. Though the strippase function of Srs2 with respect to Rad51 filaments has been well documented, Srs2 does not disassemble Dmc1 filaments, and in fact Dmc1 may inhibit Srs2 activity on ssDNA [30,31]. It is currently unknown whether there exists an ssDNA “strippase” that acts on Dmc1.

Under normal circumstances *in vivo*, RecA family proteins form nucleoprotein filaments that are shorter than the resolution limit of conventional light microscopy (~200 nanometers). This is true for RecA, and for both eukaryotic RecA homologs, Rad51 and

Dmc1 [32-35]. Super-resolution microscopy imaging of Dmc1 filaments formed during meiosis indicates that Dmc1 filaments are typically about 120 nanometers (nm) long, a length that corresponds to roughly 100 nucleotides when taking into account the fact that RecA family proteins stretch the DNA ~1.5 fold when assembled into a filament [36,37]. Furthermore, in the *exo1-D173A* mutant, in which DNA end resection is impaired during meiosis, JMs are formed at a level that is equivalent to wild-type, implying that short ssDNA tracts support normal meiotic recombination [38]. In contrast, longer than normal Dmc1 filaments accumulate in the absence of Mnd1, a Dmc1 accessory protein that is required for Dmc1 activity after the filament formation stage [36]. Taken together, these results suggest that while RecA family proteins are competent to form long filaments, they are regulated such that they form relatively short filaments *in vivo*. The significance of this regulation and the factors that influence filament length are presently not well understood.

RecA family recombinases are DNA-dependent ATPases, but their ATPase activity is not required for filament formation or for stand exchange [39-42]. Instead, ATP binding changes the conformation of the protein to a form that has high affinity for DNA, and is thus the active form [39,43]. The ADP bound form of the protein has lower affinity for DNA than the ATP-bound form, and is inactive in homology search and strand exchange. In prokaryotes, RecA ATP hydrolysis is required for filament disassembly following strand exchange, or when the protein inappropriately assembles on dsDNA [35,42]. In contrast to RecA, the eukaryotic recombinases Rad51 and Dmc1 display relatively weak intrinsic ATPase activity and rely on Rad54 family ATP-dependent dsDNA translocases to promote their dissociation [44-48]. Translocase driven

dissociation is required to clear strand exchange proteins from D-loops to allow completion of recombination events [49]. Translocases also prevent accumulation of off-pathway complexes formed by filament nucleation on unbroken dsDNA [47,49-53]. A previous study of human Rad51 used *in vitro* single-molecule fluorescence imaging to show that Rad51-ADP dissociation from dsDNA is inefficient and incomplete, suggesting that the activity of the translocases is required even when Rad51 is in the ADP-bound form [54]. Moreover, Rad54 overexpression was observed to suppress the defects associated with Rad51-K191R, a *rad51* mutant that is completely defective in ATP hydrolysis, implying that the ATPase activity of Rad51 is not required for it to be removed from dsDNA by Rad54 [55-57]. Finally, in the context of the nucleoprotein filament, the ATPase domain of one protomer directly contacts the N-terminal binding domain of the adjacent protomer; this observation is believed to be the structural basis for the finding that ATP-binding promotes protomer-protomer cooperativity [58,59].

We are interested in understanding how accessory proteins regulate the activity of the meiotic RecA homolog Dmc1. In *Saccharomyces cerevisiae*, Dmc1's activity is regulated by at least five key accessory proteins including RPA, Mei5-Sae3, Hop2-Mnd1, Rad51, and the translocase Rdh54 (a.k.a. Tid1). RPA rapidly binds to tracts of ssDNA and serves to coordinate the interactions between Dmc1's other accessory proteins and ssDNA [60]. *In vivo*, Mei5-Sae3 and Rad51 are required for normal Dmc1 filament formation at tracts of RPA coated ssDNA, suggesting that these factors are involved in nucleation and/or filament elongation [61-63]. Conversely, Hop2-Mnd1 is required for strand exchange, but not for filament nucleation or stability [64,65]. Rdh54

is a Rad54 family translocase implicated in promoting dissociation of Dmc1 from dsDNA, as discussed above.

Budding yeast Mei5-Sae3 is a homolog of *Schizosaccharomyces pombe* and mammalian Sfr1-Swi5/MEI5-SWI5, with no known homolog in plants [66]. In budding yeast, Mei5-Sae3 is Dmc1-specific, whereas in fission yeast Sfr1-Swi5 is an accessory factor to both Dmc1 and Rad51 [67]. In mammals, MEI5-SWI5 protein is reported to function with RAD51, but there is no known interaction with DMC1, and an effort to detect DMC1 stimulatory activity *in vitro* yielded negative results [68,69]. Biochemical studies have suggested several functions for Mei5-Sae3. First, studies using fission yeast proteins have shown that Sfr1-Swi5 stimulates fission yeast Rad51 (referred to as Rhp51) and Dmc1 in three-stranded DNA exchange reactions, and it helps Rhp51 overcome the inhibitory effect of RPA [67]. Studies using purified budding yeast Mei5-Sae3 and Dmc1 similarly concluded that Mei5-Sae3 promotes Dmc1 loading onto RPA-coated ssDNA, and that it enhances Dmc1-mediated D-loop formation when used alone, or in combination with Rad51 [3,60,70]. In addition to this mediator activity, Haruta et al. also reported that Sfr1-Swi5 enhances Rhp51's ATPase activity; this result was subsequently confirmed and extended by work from Su et al. using purified *Mus musculus* proteins [67,69]. Su et al. showed that SWI5-MEI5 stimulates RAD51 by promoting ADP release, the step in ATP hydrolysis that is believed to be the slowest and thus rate-limiting [69,71]. Enhancement of ADP release is thought to have a stabilizing effect on Rad51 filaments by maintaining them in the ATP-bound state. In addition, later studies using single-molecule fluorescence resonance energy transfer, concluded that mouse SWI5-MEI5 promotes RAD51 nucleation by preventing

dissociation, effectively reducing the number of protomers required for a nucleation event from three to two [72]. The same study also found that fission yeast Sfr1-Swi5 prevents Rhp51 disassembly, suggesting a conserved role for this complex in stabilizing Rad51 filaments.

*In vivo*, *Saccharomyces cerevisiae* Dmc1 and Mei5-Sae3 are interdependent for focus formation, and the foci formed by the two proteins co-localize with one another, and with other DSB-dependent proteins such as Rad51 [62,63]. Moreover, Dmc1 and Mei5-Sae3 both depend on Rad51 for normal meiotic focus formation; average focus staining intensity is lower in *rad51* mutants than in wild-type [61,62]. Consistent with it being necessary for Dmc1 focus formation, Mei5-Sae3 is also required for Dmc1-mediated recombination. *In vivo,* DSBs form normally in *mei5* or *sae3* mutants, but these intermediates are not converted to D-loops [62,63,73]. Fission yeast Rhp51 differs from Dmc1 in its dependency on Sfr1-Swi5; while loss of Sfr1-Swi5 reduces recombination, recombination is only eliminated when both Sfr1-Swi5 and Rhp55-Rhp57, a heterodimeric accessory protein homologous to budding yeast Rad55-Rad57, are deleted [74]. Similarly, knockdown of MEI5-SWI5 in human cells impairs RAD51 focus formation in response to ionizing radiation and also reduces recombination [68]. In contrast, deletion of mouse *Swi5* and *Sfr1* does not reduce the level of recombination when assayed with a direct-repeat reporter construct, but it does make cells more sensitive to DNA damaging agents that require HR for repair, including ionizing radiation, camptothecin, and poly(ADP-ribose) polymerase (PARP) inhibitor [75]. It is not known whether these differences in the requirement of SWI5-MEI5 by RAD51 in

humans and mouse are due to differences in the cell types used or true biological differences in the human and mouse RAD51 recombinases [68].

Rad51, the RecA homolog that catalyzes homology search and strand exchange during mitotic recombination, is the second accessory protein that plays a role in forming wild-type Dmc1 filaments during meiosis [61]. Although Rad51 is required for normal meiotic recombination, its strand exchange activity is dispensable [3]. In fact, Rad51 strand exchange activity is inhibited during MI by the meiosis-specific protein Hed1 [76,77]. In the absence of Rad51, Dmc1 foci have reduced staining intensity, suggesting that filaments are defective [61,78]. Recombination still occurs in *rad51* mutants, but it is mis-regulated such that D-loop formation occurs predominantly between sister chromatids, instead of between homologous chromosomes [79]. In addition, CO formation is reduced, only a sub-population progresses through meiotic divisions, and the spores formed are not viable [4]. In biochemical reconstitution experiments, Rad51 alone can stimulate Dmc1-mediated D-loop formation, although optimal levels of D-loop formation require both Rad51 and Mei5-Sae3 [3]. In spite of its importance as a Dmc1 accessory factor, very little is known about the molecular mechanisms involved in Rad51's non-catalytic role in meiotic recombination.

One approach to studying the role of accessory proteins is to assume that the activity of the enzyme has evolved to depend on that accessory factor. In this view, beneficial regulation of an enzyme's activity is selected for at the expense of the enzyme's intrinsic activity. If such an evolutionary process is responsible for a particular regulatory mechanism, it should be possible to mutate the core enzyme to eliminate the "built-in" defect, rendering the mutant protein capable of catalyzing its reaction in the

absence of the accessory protein. Comparison of the activities of the mutant and wild-type proteins with and without the accessory protein can then provide mechanistic insight into the processes that accessory protein normally regulates.

We applied this approach to Dmc1 in an attempt to further elucidate the mechanisms through which Mei5-Sae3 influences Dmc1's activity. We identified a gain-of-function *dmc1* mutant whose activity is independent of Mei5-Sae3. Characterization of this Dmc1 mutant provides new insight into the mechanism of action of Mei5-Sae3 *in vivo*, and also sheds light on the functional relationship between Mei5-Sae3 and Rad51. Furthermore, characterization of this gain-of-function version of Dmc1 reveals that it forms longer than normal filaments and displays higher than normal levels of IS, ectopic, and multi-chromatid recombination. We interpret these observations in the context of recent studies showing that a single strand exchange filament can simultaneously engage more than one dsDNA molecule.

## 3.3 Results

In order to better understand the function of Mei5-Sae3 and Rad51 in Dmc1-mediated HR, we sought to identify a *DMC1* allele that would bypass the requirement for one of these accessory factors. Analysis of Dmc1-mediated recombination in the absence of an accessory factor would then allow us to identify regulatory features that depend on the accessory protein by comparison to the wild-type process. To this end, we constructed two *dmc1* mutants based on previously characterized gain-of-function mutations in Dmc1 homologs, RecA-E96D and Rad51-I345T [42,80,81]. Sequence alignments indicated that the amino acid residues altered in RecA-E96 and Rad54-

I145T mutants are conserved allowing us to construct corresponding mutant forms of Dmc1; for RecA-E96D the corresponding mutant is Dmc1-E157D and for Rad51-I134T the corresponding mutant is Dmc1-I282T. The RecA-E96D mutation shortens the length of a critical amino acid side chain in the ATPase active site, increasing the distance between the water molecule that acts as the nucleophile for hydrolysis and the activating carboxylate [80]. The mutation dramatically reduces the rate of ATP hydrolysis thereby maintaining RecA in the ATP-bound form, which is active for DNA binding, homology search, and strand exchange. Due to the high sequence conservation of this site, Dmc1-E157D is very likely to be defective in ATPase activity, like RecA-E96D. The Rad51-I345T mutation suppresses defects conferred by the heterodimeric accessory protein Rad55-Rad57, which stabilizes Rad51 filaments [81]; we reasoned that the corresponding mutation in Dmc1 might suppress the requirement for Mei5-Sae3 as biochemical studies on Swi5-Sfr1, which is homologous to Mei5-Sae3, indicated Swi5-Sfr1 also acts by stabilizing strand exchange filaments [67,74].

To assess whether either of these Dmc1 mutants would bypass Mei5-Sae3 and/or Rad51, we constructed diploid yeast lacking either Mei5 or Rad51 with the corresponding Dmc1 mutation, and assessed sporulation efficiency and spore viability alongside *DMC1*$^{+}$ *mei5* and *DMC1*$^{+}$ *rad51* controls. In a *mei5* strain, tetrads are formed very inefficiently, whereas in a *rad51* mutant, tetrads are formed, but almost all spores within them are dead [4,62,63]. We found that *dmc1-E157D* bypasses Mei5-Sae3 with respect to sporulation and spore viability (Table 3.1). The spore viabilities of *dmc1-E157D*, *dmc1-E157D mei5*, and *dmc1-E157D sae3* are nearly identical to one another (57.6%, 50.3%, and 57.0% respectively), suggesting that Dmc1-E157D function is

largely independent of Mei5-Sae3. In contrast, *dmc1-E157D* does not bypass the requirement for *rad51* with respect to spore viability (<0.6% in *rad51* versus 0.7% in *dmc1-E157D rad51*).

| **Strain** | **n (tetrads)** | **Spore viability (%)** | **p-value (two-proportion z-score)** |
|---|---|---|---|
| wild-type | 153 | 98.4 | N.A. |
| *dmc1-E157D* | 215 | 57.6 | $p < 0.01$ |
| *mei5* | no tetrads formed | N.A. | N.A. |
| *rad51* | 40 | <0.6 | N.A. |
| *rad51-II3A* | 19 | 82.9 | $p < 0.01$ |
| *rdh54* | 40 | 91.9 | $p < 0.01$ |
| *dmc1-E157D mei5* | 267 | 50.3 | $p < 0.01$ |
| *dmc1-E157D rad51* | 34 | 0.7 | N.A. |
| *dmc1-E157D rad51-II3A* | 22 | 17.0 | $p < 0.01$ |
| *dmc1-E157D rdh54* | no tetrads formed | N.A. | N.A. |
| *dmc1-E157D sae3* | 39 | 57.0 | $p = 0.4$ (not significant) |
| *dmc1-E157D mei5 rad51* | no tetrads formed | N.A. | N.A. |
| *DMC1$^+$/dmc1-E157D* | 47 | 91.2 | $p < 0.01$ |
| *DMC1$^+$/dmc1-E157D mei5/"* | 69 | 58.8 | $p < 0.01$ |

**Table 3.1** Spore viabilities for strains in study. p-values are reported for z-scores using a two-proportion z-score test [82]. Comparison for single mutants is to wild-type. Comparison for double mutants is to each of the single mutants (for example, *dmc1-E157D sae3* is compared to *dmc1-E157D*). Comparison for heterozygotes is to homozygotes. N.A. = not applicable; for samples that do not meet the success/failure condition for z-scores and wild-type to itself. Strains used in experiments in the order in which they appear in table, top to bottom: DKB3698, DKB6320, DKB3710, DKB3689, DKB2526, DKB6342, DKB6299, DKB6300, DKB6539, DKB6540, DKB6393, DKB6400, DKB6583, DKB6412, DKB6413, DKB6525, DKB6619, DKB6406, DKB6407.

Spore viability data from a *dmc1-E157D/DMC1$^+$ mei5/mei5* heterozygote indicates that Dmc1-E157D is dominant to wild-type Dmc1 (Dmc1-WT) with respect to formation of viable spores in a *mei5* mutant background (58.8% in *dmc1-E157D/DMC1$^+$ mei5/mei5*, vs. 50.3% in *dmc1-E157D/dmc1-E157D mei5/mei5)*. In contrast, Dmc1-E157D causes only a minor reduction in spore viability when both

Dmc1-WT and Mei5 proteins are present (91.2% in *dmc1-E157D/DMC1+ MEI5+/MEI5+* vs. 98.4% in WT). In contrast to *dmc1-E157D*, we did not detect phenotypic suppression in *dmc1-I282T* mutants, either with respect to prophase arrest in a *mei5* mutant background, or with respect to spore viability in a *rad51* background. Importantly, the Dmc1-E157D mutation does not result in increased expression or stability of the protein as assayed by Western blotting of meiotic yeast whole cell extracts, thus ruling out a trivial explanation for Dmc1-E157D's bypass of the *mei5* and *sae3* mutations (Supplemental Figure 3.1).

### 3.3.1 Dmc1-E157D forms meiotic immunostaining foci in the absence of Mei5 and Rad51

We next performed immunofluorescence staining of spread meiotic nuclei to examine Dmc1 focus formation in the *dmc1-E157D* and *dmc1-E157D mei5* strains. As shown previously, meiotic Dmc1-WT focus formation is severely defective in *mei5* mutant cells, but Dmc1-E157D forms bright foci in the *mei5* mutant background (Figure 3.1a) [62,63]. Notably, Dmc1 foci accumulate to higher levels and persist for longer in *dmc1-E157D* and *dmc1-E157D mei5* when compared to wild-type (Figure 3.1b).
One model suggests that Mei5-Sae3 and Rad51 cooperate to promote Dmc1 filament formation [14]. Because *dmc1-E157D* bypasses *mei5*, we reasoned that if this model is correct, *dmc1-E157D* might also bypass the defect seen for formation of brightly-staining Dmc1 foci in *rad51* cells, even though it does not suppress the spore viability defect observed in these cells. To test this, we constructed *dmc1-E157D rad51* and *dmc1-E157D mei5 rad51* strains, and looked for Dmc1 focus formation in spread meiotic nuclei. In contrast to a *rad51* single mutant, in which Dmc1-WT staining intensity

is reduced, the Dmc1 foci observed in *dmc1-E157D rad51* and *dmc1-E157D mei5 rad51* nuclei were brighter and more numerous than those in wild-type (Figures 3.1c,d) [61,78]. We conclude that *dmc1-E157D* appears to bypass the role of Rad51 with respect to Dmc1 focus formation.

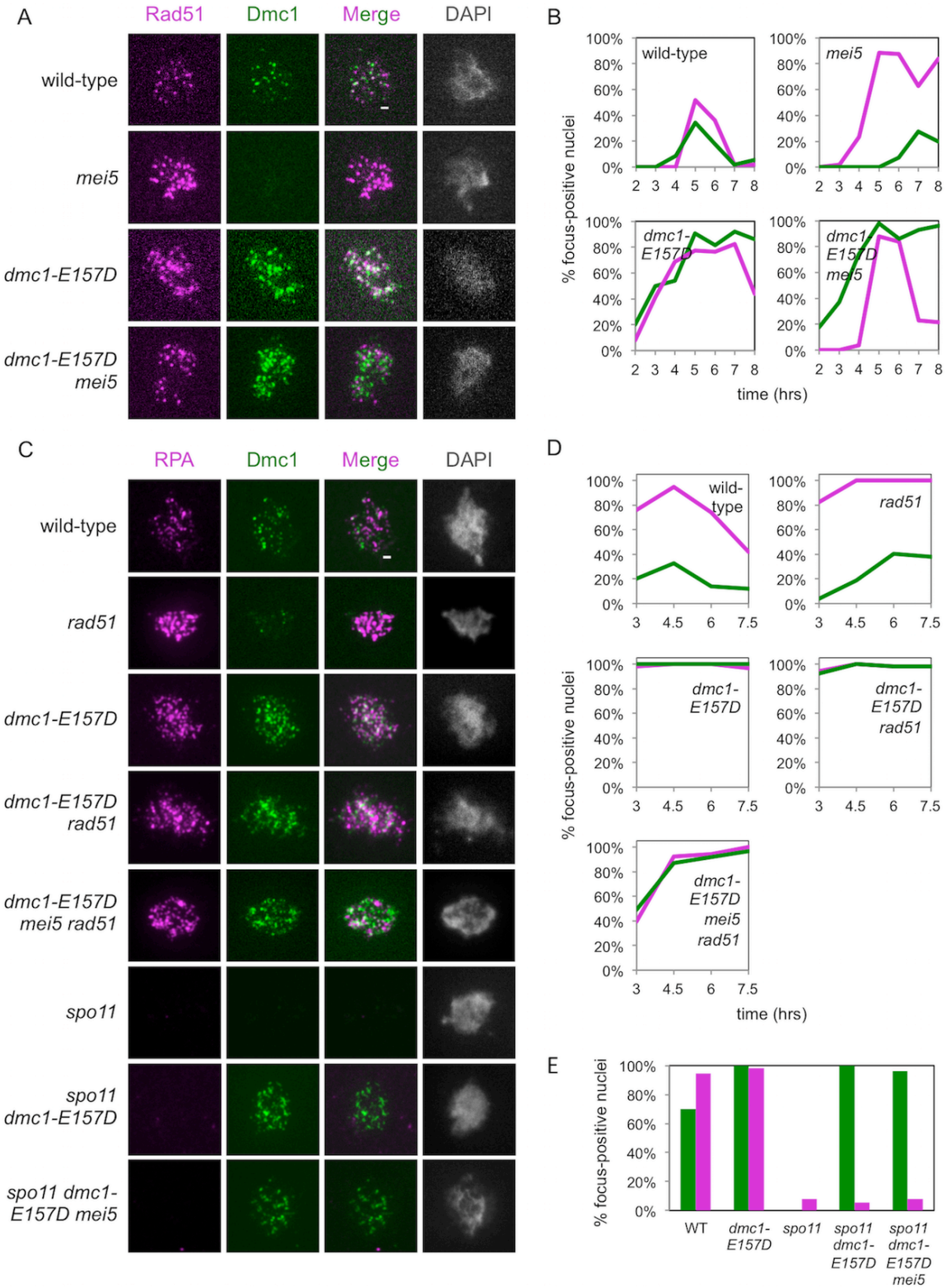


**Figure 3.1** *dmc1-E157D* bypasses *mei5*, *rad51* with respect to focus formation. (a, c)

**Figure 3.1 (continued)** Representative widefield microscopy imaging of spread meiotic nuclei are shown for each strain. Scale bars represent 1 μm. (b, d) Quantitation. Nuclei were scored as focus positive if they contained three or more foci of a given type. Dmc1 (green), Rad51 or RPA (red). (e) Quantitation of *spo11* strains and controls at 4 hours. Strains used in experiments in the order in which they appear in figure, top to bottom: DKB3698, DKB6320, DKB6342, DKB6300, DKB3710, DKB6393, DKB6412.

### 3.3.2 *dmc1-E157D* forms immunostaining foci in the absence of DSBs

Because the Dmc1-E157D mutant is modeled after RecA-E96D, which has been shown to form foci on undamaged DNA, we wanted to ask whether the same was true of the corresponding Dmc1 mutant [35]. To determine whether any of the foci that we observed in the *dmc1-E157D* background resulted from binding to chromosomes independent of DSBs, we introduced the *spo11* mutation into our *dmc1-E157D* strains to block DSB formation. Spo11 is the catalytic subunit of a meiosis-specific complex that induces DSBs at the outset of meiosis [6]. Immunostaining of spread meiotic nuclei for Dmc1 and RPA revealed that in contrast to the *spo11* single mutant, which typically forms few if any Dmc1 foci, nearly all *spo11 dmc1-E157D* nuclei contained numerous Dmc1 foci (Figures 3.1c,e) [51]. RPA serves as a marker for DSB-associated tracts of ssDNA in mid-to-late prophase I. RPA foci are detected early in prophase in *spo11* mutants owing to the role of RPA in pre-meiotic DNA replication, but then disappear 4 hours after induction of meiosis [83]. We found that at 4 hours, the majority of nuclei lacking RPA foci contained Dmc1 foci in *spo11 dmc1-E157D* and *spo11 dmc1-E157D mei5* (100% and 96% of nuclei lacking RPA had Dmc1 foci, respectively) (Figure 3.1e) indicating that Dmc1-E157D forms DSB-independent foci. It is thus likely that a substantial fraction of the foci observed in *SPO11*$^{+}$ *dmc1-E157D* cells represent off-pathway structures formed by binding unbroken chromosomal loci. However, an

increase in the total number of DSBs formed or an increase in DSB lifespan could also partially account for the increased number of Dmc1 foci and their persistence in the *dmc1-E157D* background relative to wild-type.

### 3.3.3 *dmc1-E157D* bypasses Mei5, but not Rad51, with respect to meiotic CO formation

To examine whether Dmc1-E157D is competent to carry out recombination in the absence of Mei5, we performed one-dimensional (1D) gel electrophoresis, followed by Southern blotting, to examine DSBs and CO products at the well-characterized recombination hotspot *HIS4::LEU2* [84]. XhoI digestion of genomic DNA from meiotic time course experiments followed by 1D gel electrophoresis and Southern blotting to detect the *HIS4::LEU2* hotspot can be used to detect DSB intermediates and IH CO products, as well as products that result from ectopic recombination between the *HIS4::LEU2* locus and the native *LEU2* locus, which are separated by ~23 kilobases on chromosome III [12,84]. As shown previously, DSBs accumulate and CO formation is very limited in *DMC1*$^{+}$ *mei5* (Figures 3.2a,b) [62,63]. In contrast, although *dmc1-E157D* and *dmc1-E157D mei5* cells initially accumulate DSBs (Figure 3.2a,b, Supplemental Figure 3.2b), those breaks are resolved by 24 hours, at which point CO formation is equivalent to wild-type. Further examination of DSB formation in wild-type and *dmc1-E157D* cells using PstI digestion of genomic DNA from meiotic samples to look at DSB resection status revealed that although DSBs accumulate to somewhat higher levels in *dmc1-E157D* relative to wild-type, there are little or no differences in resection status between the two strains (Supplemental Figure 3.2a,b). Interestingly, ectopic recombination is elevated ~3.5-fold in *dmc1-E157D* and *dmc1-E157D mei5* relative to

wild-type. In addition, whereas only 8.7% of *DMC1*$^{+}$ *mei5* cells progress through a meiotic division, 50.0% of *dmc1-E157D mei5* cells progress, a level nearly equivalent to *dmc1-E157D* (58.4%) (Figure 3.2b). These results show that Dmc1-E157D bypasses the normal requirement for Mei5 during meiotic recombination.

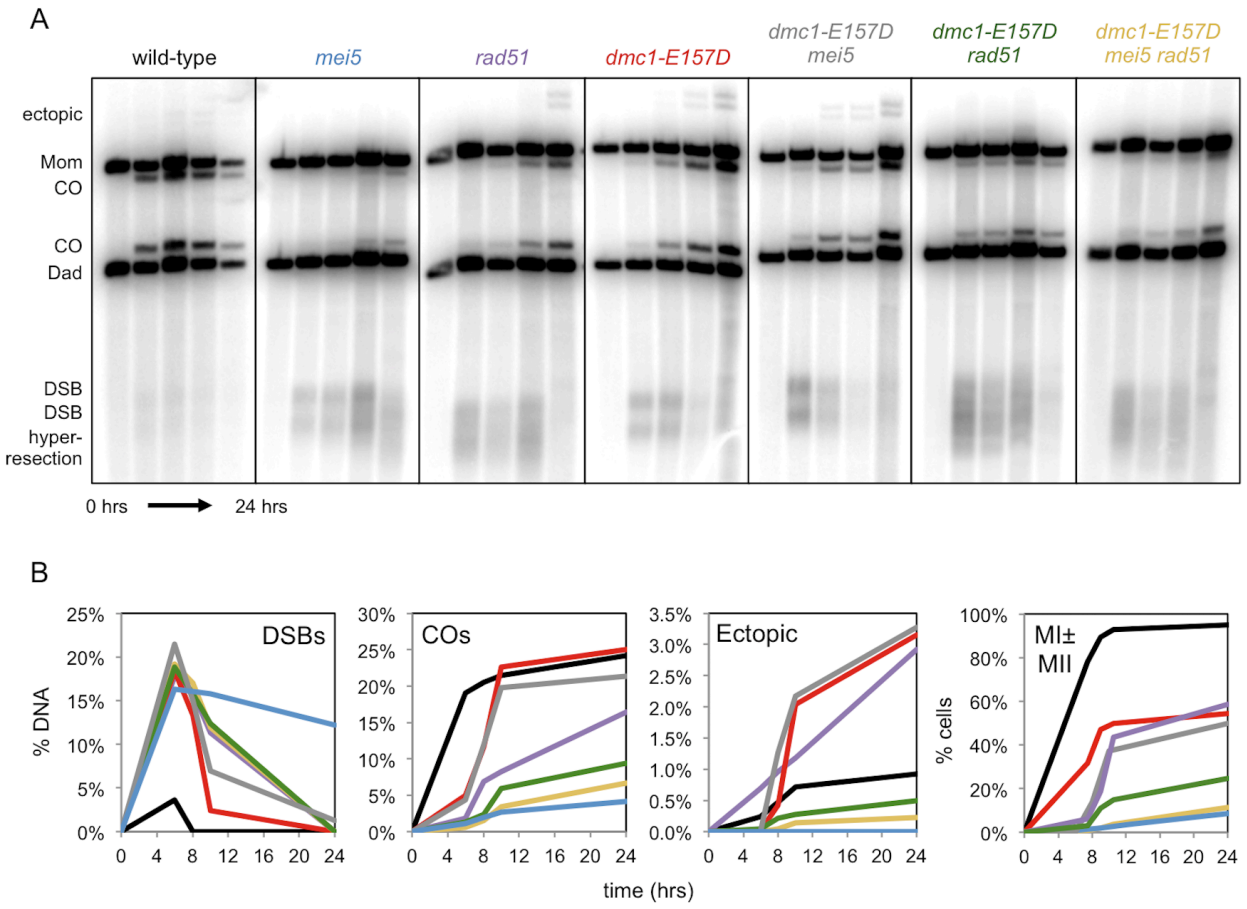


**Figure 3.2** *dmc1-E157D* bypasses *mei5* but not *rad51* with respect to CO formation. (a) Southern blot analysis at the *HIS4::LEU2* hotspot following digestion of genomic DNA from meiotic time course experiments with XhoI. Time points shown from left to right are: 0h, 6h, 8h, 10h, 24h. (b) Quantitation of 1D gels shown in (a) and meiotic progression data; black – wild-type, light blue – *mei5*, purple – *rad51*, red – *dmc1-E157D*, gray – *dmc1-E157D mei5*, green – *dmc1-E157D rad51*, yellow – *dmc1-E157D mei5 rad51.* To score meiotic progression, ≥50 cells were scored per time point. Strains used in experiments in the order in which they appear in figure, right to left: DKB3698, DKB6320, DKB3710, DKB6342, DKB6300, DKB6393, DKB6412.

Because Dmc1-E157D also bypasses Rad51 with respect to forming brightly staining Dmc1 foci, we wanted to ask whether it similarly bypasses Rad51 for CO formation and DSB resolution at *HIS4::LEU2*. Previous studies of *rad51* mutants showed that DSBs accumulate and undergo more extensive resection than wild-type [4]. In addition, the final level of COs that form in *rad51* was reported to be 5-fold lower than wild-type, and ectopic recombination is ~1.6-fold higher at 10 hours in sporulation medium [4,85]. We confirmed these phenotypes for the *rad51* single mutant (Figures 3.2a,b). Consistent with the failure of *dmc1-E157D* to rescue the low spore viability phenotype of *rad51* (Table 3.1), we found that *dmc1-E157D rad51* accumulates hyper-resected DSBs (Figure 3.2a). Surprisingly, *dmc1-E157D rad51* makes fewer COs than *rad51*, implying that the *dmc1-E157D rad51* double mutant is more defective than either the *dmc1-E157D* or the *rad51* single mutants. Meiotic progression data similarly indicate that *dmc1-E157D rad51* is more defective than both *dmc1-E157D* and *rad51*; only 24.8% of *dmc1-E157D rad51* cells execute at least one meiotic division, compared to 58.4% and 54.5% of *dmc1-E157D* and *rad51* cells, respectively (Figure 3.2b). Additionally, very little ectopic recombination is detected in *dmc1-E157D rad51*, possibly reflecting the fact that there is less recombination overall, or indicating that there is a change in the pattern of JM formation or their resolution. Overall our results indicate that *dmc1-E157D* does not bypass *rad51* with respect to resolution of meiotic DSBs.

The *dmc1-E157D mei5 rad51* triple mutant was similar to the *dmc1-E157D rad51* double mutant, with the triple mutant displaying slightly more pronounced defects in final CO levels (Figure 3.2a,b). We also found that the efficiency of the first meiotic division is somewhat reduced in the *dmc1-E157D mei5 rad51* mutant (11.3%) compared to the

*dmc1-E157D rad51* (24.8%) mutant (Figure 3.2b). These results indicate that recombination in *dmc1-E157D* displays a strong dependence on Rad51, but very limited dependence on Mei5 unless Rad51 is absent.

### 3.3.4 *spo11* rescues the meiotic progression and segregation defects associated with *dmc1-E157D*

In contrast to the typical MI segregation that is observed in wild-type cells, in which there are two well-defined and equally-sized DAPI staining bodies, MI segregation in *dmc1-E157D* often appears to be abnormal, and can include defects such as a single elongated DAPI staining body rather than two separated bodies, as well as separated DAPI staining bodies of dramatically different sizes (Supplemental Figure 3.3a,b). Introduction of the *spo11* mutation into the *dmc1-E157D* background largely rescued these deficiencies. In addition, the *spo11* mutation suppressed the MI division delay that occurs in *dmc1-E157D* cells (Supplemental Figure 3.3c). Thus the meiotic segregation and progression defects observed in the *dmc1-E157D* background are DSB-dependent. This finding suggests that although there are likely numerous DSB-independent Dmc1 foci in these strains, these Dmc1-dsDNA complexes do not dramatically interfere with chromosome segregation.

### 3.3.5 Dmc1-mediated meiotic recombination is independent of Mei5-Sae3 in *dmc1-E157D*

We next sought to further characterize Dmc1-E157D-mediated recombination in the absence of Mei5 by 2D gel electrophoresis and Southern blotting. Using this method, an array of JM recombination intermediates can be detected at the *HIS4::LEU2* locus, including SEIs, intersister-dHJs (IS-dHJs), IH-dHJs, and multi-chromatid JMs

(mcJMs) (Figure 3.3a) [86]. As expected, JM formation is severely compromised in *mei5* (Figures 3.3b,c). In contrast, in *dmc1-E157D mei5*, JM formation is efficient, with IH-dHJ levels equivalent to those in wild-type. IS-dHJs, however, are increased ~3-fold, reducing the IH-dHJ/IS-dHJ ratio from 5.0 in wild-type to ~1.5 in *dmc1-E157D* (Figure 3.3c). *dmc1-E157D mei5* phenocopies *dmc1-E157D*, also having increased IS-dHJs and a reduced IH/IS ratio of ~1.6. SEIs form at the similar levels in the *dmc1-E157D* and *dmc1-E157D mei5* mutants as in wild-type (Figure 3.3c). Like IS-dHJs, mcJMs are increased relative to wild-type in both *dmc1-E157D* and *dmc1-E157D mei5* (3.0-fold and 2.7-fold respectively). The similar array of JMs observed in *dmc1-E157D* and *dmc1-E157D mei5* cells further indicates that Dmc1-E157D-mediated recombination occurs independent of Mei5-Sae3. Although a decrease in the IH/IS ratio can be interpreted as a defect in the mechanism of IH bias, this case is unusual in that the decreased ratio results from increased IS-dHJs, with no reciprocal decrease in IH-dHJs. The fact that the level of IH-dHJs in *dmc1-E157D mei5* cells is equivalent to that in wild-type suggests that the mechanism of homolog bias is intact in this mutant, and reveals that Mei5-Sae3 is not required for IH bias. The data also suggest that the *dmc1-E157D* mutant is hyper-recombinant, displaying higher than normal levels of IS-dHJs and mcJMs (Figure 3.3c), as well as increased ectopic COs (Figure 3.2b).

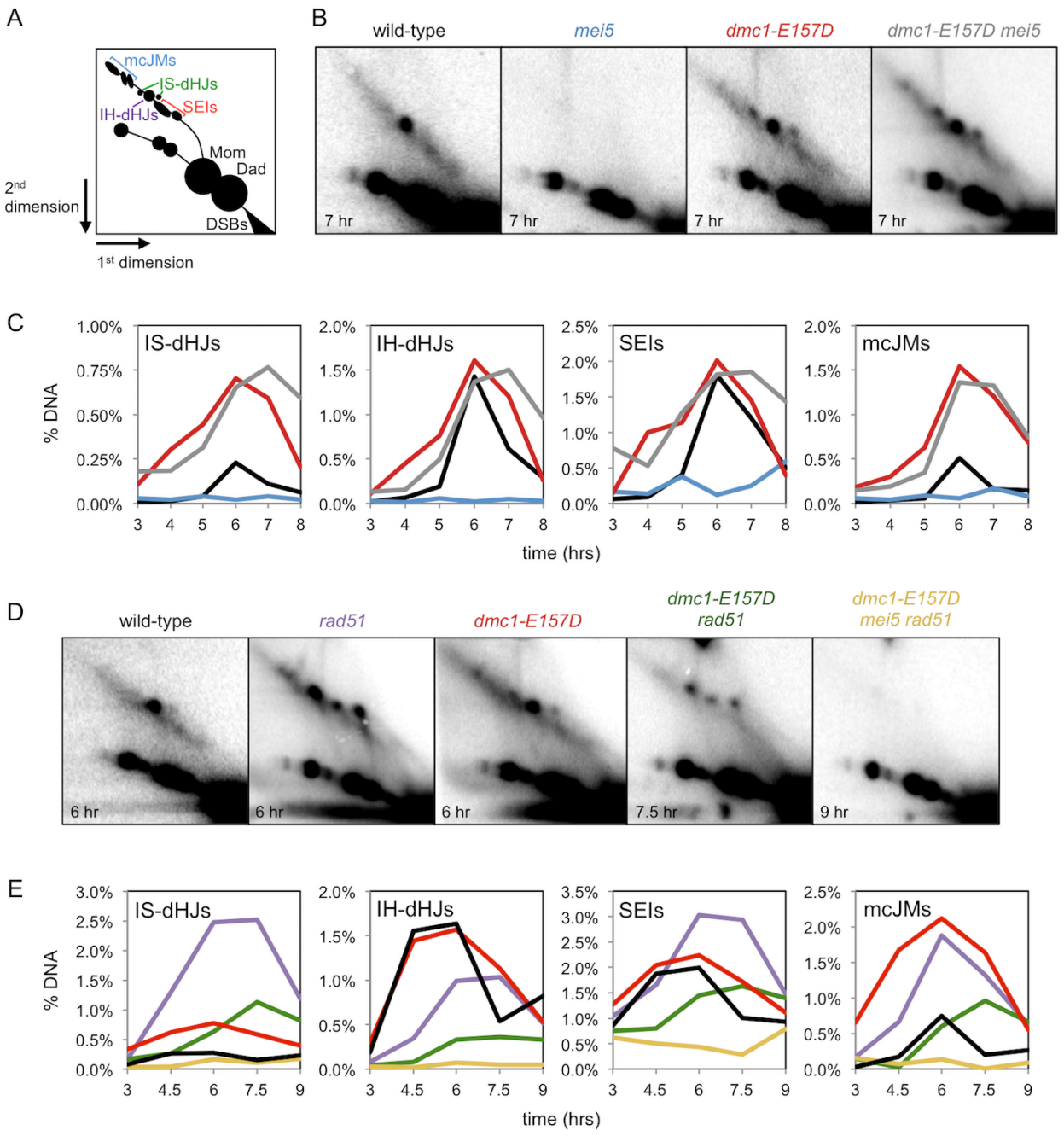


**Figure 3.3** Recombination in *dmc1-E157D* is abnormal and dependent on Rad51, with little effect of Mei5-Sae3. (a) JMs that can be detected at the *HIS4::LEU2* meiotic recombination hotspot. (b) Southern analysis at the *HIS4::LEU2* hotspot from meiotic time course experiments following 2D gel electrophoresis. Time point for representative image is shown in the bottom left corner. (c) 2D gel quantitation; black – wild-type, light blue – *mei5*, red – *dmc1-E157D*, gray – *dmc1-E157D mei5*. (d) 2D gels as in (b). (e) 2D gel quantitation; black – wild-type, light purple – *rad51*, red – *dmc1-E157D*, green – *dmc1-E157D rad51*, yellow – *dmc1-E157D mei5 rad51*. Strains used in experiments in

**Figure 3.3 (continued)** the order in which they appear in figure, right to left and top to bottom: DKB3698, DKB6320, DKB6342, DKB6300, DKB3710, DKB6393, DKB6412.

### 3.3.6 The *ndt80* mutation increases total JMs, but does not change their distribution

To rule out the possibility that certain JM species have longer lifespans in the *dmc1-E157D* background, we introduced the *ndt80* mutation. Deletion of *NDT80*$^{+}$ prevents recombination intermediate processing, and JMs accumulate to high levels in this background (Supplemental Figure 3.4b) [19]. Importantly, we found that IS-dHJs and mcJMs are also elevated in *ndt80 dmc1-E157D* relative to *ndt80*, with no appreciable differences in SEIs and IH-dHJs (Supplemental Figure 3.4a,b). These findings support a model in which the elevated levels of IS-dHJs and mcJMs are a result of increased formation of these species by Dmc1-E157D, as opposed these species being less efficiently resolved in *dmc1-E157D* and *dmc1-E157D mei5* cells.

### 3.3.7 *dmc1-E157D rad51* exhibits a profound IH bias defect and a reduction in JM formation

We next examined Dmc1-E157D-mediated recombination in the absence of Rad51 using 2D gel electrophoresis. In a *rad51* mutant, Dmc1 carries out recombination, but there is a profound IH bias defect, and most recombination occurs between sisters [79]. The IH-dHJ/IS-dHJ ratio in *rad51* is 0.4 and the same ratio is observed for *dmc1-E157D rad51* (Figures 3.3d,e, Supplemental Figure 3.5a,b). This defect in the IH/IS ratio is the result of increased IS-dHJs and at the expense of IH-dHJs. The profound defect in IH bias in *dmc1-E157D rad51* contrasts with the *dmc1-E157D* single mutant, in which the IH-dHJ/IS-dHJ ratio is ~1.6. We conclude that *rad51*

is epistatic to *dmc1-E157D* with respect to its impact on partner choice. The impact of a *rad51* mutation on the IH/IS ratio in *dmc1-E157D* cells further supports the view that the mechanism of IH bias is intact in *dmc1-E157D mei5* cells and therefore the conclusion that Mei5-Sae3 is not required for IH bias. The levels of IS-dHJs, IH-dHJs, SEIs, and mcJMs are all reduced approximately 2-fold in *dmc1-E157D rad51* relative to *rad51* (Figure 3.3e); thus, the hyper-recombinant phenotype of *dmc1-E157D* cells is Rad51-dependent. These findings are also consistent with the observation that CO levels in *dmc1-E157D* are reduced about 2-fold by the *rad51* mutation (Figure 3.2b).

### 3.3.8 JM formation is absent in triple mutant *dmc1-E157D mei5 rad51*

We also analyzed the *dmc1-E157D mei5 rad51* triple mutant by 2D gel electrophoresis. Surprisingly, while both *dmc1-E157D mei5* and *dmc1-E157D rad51* formed readily-detectable levels of JMs (Figures 3.3b,d), and Dmc1 foci were detected in *dmc1-E157D mei5 rad51* spread meiotic nuclei (Figure 3.1c,d), no JMs were detected in the triple mutant (Figure 3.3d,e). Because *rad51* strains are genetically unstable, we constructed an independent *dmc1-E157D mei5 rad51* diploid and repeated this experiment to ensure that our original strain had not picked up an additional mutation that suppressed the formation of JMs. Meiotic JMs were also undetectable in the duplicate *dmc1-E157D mei5 rad51* strain (Supplemental Figure 3.5a,b). Given that resected and unrepaired DSBs trigger delays in meiotic progression, the 2D gel analyses are consistent with our finding that only ~10% of cells progress through a meiotic division in *dmc1-E157D mei5 rad51*, and that there is hyper-resection and limited CO formation in this strain (Figures 3.2a,b). We conclude that recombination is further compromised in the triple mutant *dmc1-E157D mei5 rad51* when compared to

either double mutant. These results provide additional evidence that although Dmc1-E157D's activity is essentially Mei5-Sae3 independent in *RAD51*$^{+}$ cells, Mei5-Sae3 can promote limited Dmc1-E157D activity when Rad51 is absent.

### 3.3.9 The defects associated with *dmc1-E157D* and *dmc1-E157D mei5* are independent of Rad51's catalytic activity

One possible explanation for the results we obtained from our JM analysis in Figure 3.3 is that the *dmc1-E157D* mutation changes the behavior of Dmc1 in a manner that activates the strand exchange activity of Rad51. This possibility is emphasized by previous results suggesting that Dmc1 itself inhibits Rad51's strand exchange activity [87,88]. Normally, Rad51's strand exchange activity is repressed by Dmc1 and by the meiosis-specific Rad51 inhibitor Hed1 [3,76]. However, it was important to determine if Rad51's strand exchange activity plays a greater role in promoting recombination in *dmc1-E157D* cells than in wild-type [88]. To test this, we crossed the *rad51-II3A* mutation into our *dmc1-E157D* strains. The three alanine substitutions coded by *rad51-II3A* eliminate DNA binding site II, the secondary, low affinity DNA binding site required for homology searching. Rad51-II3A forms filaments, but lacks the ability to catalyze D-loop formation [3].

Our results indicate that the *rad51-II3A* mutation does not alter the efficiency and pattern of JM formation in the *dmc1-E157D* mutant (Supplemental Figure 3.6a,b). This observation indicates that Dmc1, not Rad51, promotes the majority of homology search and strand exchange in *dmc1-E157D* cells, as is the case in wild-type cells. Thus, the hyper-recombinant phenotype observed in *dmc1-E157D* results from increased Dmc1 activity rather than activation of Rad51's activity. On the other hand, *rad51-II3A* causes

a greater reduction in spore viability in *a dmc1-E157D* background than in a wild-type background (Table 3.1; from 57.6% to 17.0% for *dmc1-E157D* compared to 98.6% to 82.9% for *DMC1*$^{+}$, $p < 0.01$). The modest reduction in viability seen in *rad51-II3A* single mutants was previously interpreted to suggest that Rad51's strand exchange activity is only required at a small subset of the roughly 200 DSB sites where Dmc1-dependent DSB repair fails [3]. In the context of this interpretation, the data presented here can be explained if the fraction of attempted recombination events that require Rad51's strand exchange activity, although still small, is higher in *dmc1-E157D* than in wild-type.

### 3.3.10 Meiotic two-hybrid analysis indicates that direct Rad51-Dmc1 interaction is independent of Mei5

The results presented in Figure 3.3 show that Rad51 can impact Dmc1's activity in the absence of Mei5-Sae3. To determine if Rad51's influence on Dmc1 can be explained by direct interaction of the two proteins, we carried out meiotic two-hybrid analysis. A previous two-hybrid study in budding yeast using the conventional mitotic method detected a low level of direct interaction between Rad51 and Dmc1, although the authors of that study did not ascribe significance to the interaction because it was much weaker than that observed for homotypic Rad51-Rad51 and Dmc1-Dmc1 interactions [89]. We wished to determine if Mei5-Sae3 enhanced the interaction between the two proteins and therefore used the meiotic two-hybrid method to test the interaction in a cell type that expresses the accessory protein. As in the previous study, the level of interaction observed for Rad51-Dmc1 was much lower than that in the Rad51-Rad51 and Dmc1-Dmc1 homotypic controls, but nonetheless reproducibly higher than the background level observed in empty vector controls (Supplemental

Figure 3.7a,b). Importantly, an equivalent two-hybrid signal was detected in a *mei5* background as in a wild-type background ($p = 0.5$ using a Wilcoxon signed-rank test) indicating that, in this system, Rad51-Dmc1 interaction is independent of Mei5-Sae3.

### 3.3.11 Super-resolution imaging of *dmc1-E157D* mutants reveals abnormalities in Dmc1 and RPA foci

Because Dmc1-E157D forms foci at high density, we expected that the wide-field microscopy method was not resolving closely spaced foci. Therefore, in order to obtain more accurate focus measurements, we re-examined chromosome spreads using stimulated emission depletion (STED) microscopy, which improves the resolution limit from around 200 nanometers (nm) to under 50 nm (see Chapter 2, Supplemental Figure 3.8a). For each strain, we imaged at least 13 randomly selected RPA-positive nuclei (Figure 3.4a). The average number of RPA foci detected was lowest in wild-type (70.0 ± 22.2 foci) (Figure 3.4b). All other strains displayed higher average RPA focus counts including *rad51* (140.5 ± 44.9 foci), *dmc1-E157D* (111.5 ± 28.8 foci), *dmc1-E157D mei5* (130.8 ± 21.2 foci), *dmc1-E157D rad51* (132.0 ± 21.7 foci), and *dmc1-E157D mei5 rad51* (131.3 ± 38.6 foci). We also measured focus lengths, and found that wild-type RPA foci are the shortest (76.8 ± 27.0 nm), while *rad51*, *dmc1-E157D rad51*, and *dmc1-E157D mei5 rad51* foci are all significantly longer (134.0 ± 70.4 nm, 136.0 ± 77.8 nm, 130.8 ± 63.8 nm respectively; $p < 0.01$, Wilcoxon test), but not significantly different from one another (pairwise $p = 0.53$, 0.60, and 0.94, respectively) (Figure 3.4c). The fact that RPA foci are longer in these strains is unsurprising given that we observed hyper-resection in these strains by 1D gel electrophoresis (Figure 3.2a). *dmc1-E157D* and *dmc1-E157D mei5* mutant RPA foci are significantly different from both wild-type

and *rad51* mutants (107.4 ± 49.5 nm, 97.7 ± 39.6 nm respectively; $p < 0.01$), being an intermediate average length between the two. This finding contrasts with our Southern blotting analysis of DSBs (Figure 3.2a and Supplemental Figure 3.2a), in which little to no difference between these two mutants and wild-type was detected with respect to resection tract lengths (see section 3.4).

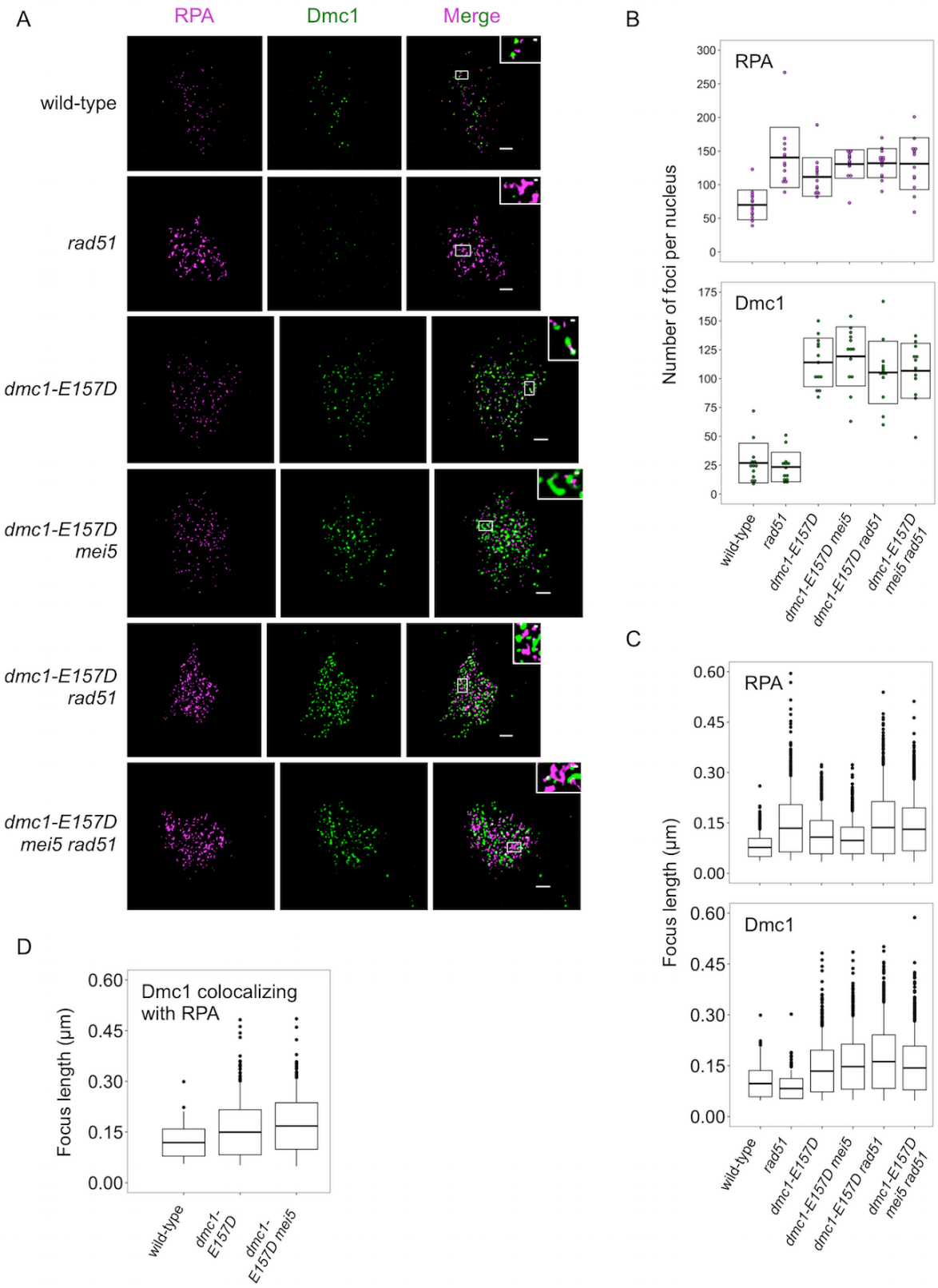


**Figure 3.4** Super-resolution imaging shows abnormalities in RPA, Dmc1 foci in mutants. (a) Representative STED microscopy imaging of spread meiotic nuclei are

**Figure 3.4 (continued)** shown for each strain. Scale bars represent 1 μm; scale bars in inset represent 0.1 μm. For *dmc1-E157D mei5*, time point was taken at 5 hours in sporulation media; for all other strains, time point was taken at 4.5 hours. (b) Quantitation of foci counts for Dmc1, RPA, is shown for each strain. For each strain, 13 randomly selected nuclei were quantitated. (c) Quantitation of RPA and Dmc1 foci lengths is shown for each strain. (d) Quantitation of Dmc1 foci lengths colocalizing with RPA is shown for the strains indicated. Strains used in this experiment in the order in which they appear in figure, top to bottom: DKB3698, DKB3710, DKB6342, DKB6300, DKB6393, DKB6412.

The average number of Dmc1 foci per nucleus was similar in wild-type and *rad51* single mutants (26.9 ± 17.7 foci and 23.3 ± 12.8 foci, respectively, Figure 3.4a,b). All *dmc1-E157D* strains displayed higher than normal focus counts including *dmc1-E157D* (114.0 ± 21.0 foci), *dmc1-E157D mei5* (119.2 ± 25.6 foci), *dmc1-E157D rad51* (105.3 ± 27.0 foci), and *dmc1-E157D mei5 rad51* (106.8 ± 23.8 foci) (Figure 3.4b). This result can be explained by the mutant's ability to form DSB-independent foci, by a longer lifespan of DSB-dependent foci, and/or by an increase in the total number of DSBs formed (Figure 3.1e, Supplemental Figure 3.2b). We also measured the lengths of these Dmc1 foci, and found that Dmc1 foci are significantly shorter in *rad51* (82.5 ± 30.0 nm, $p < 0.01$, Wilcoxon test) than wild-type (97.1 ± 38.8 nm) (Figure 3.4c), consistent with previous wide-field microscopy analyses [78]. Dmc1 foci are longer in all *dmc1-E157D* strains, including *dmc1-E157D* (134.1 ± 61.5 nm, $p < 0.01$), *dmc1-E157D mei5* (147.1 ± 66.4 nm, $p < 0.01$), *dmc1-E157D rad51* (161.9 ± 78.9, $p < 0.01$), and *dmc1-E157D mei5 rad51* (143.3 ± 64.7 nm, $p < 0.01$) relative to wild-type (Figure 3.4c).

Although measurements of Dmc1 focus lengths shows that Dmc1-E157D makes longer than normal filaments overall, the fact that the protein likely forms high levels of off-pathway foci in addition to forming foci at sites of recombination raises the possibility that the long filaments observed might only be off-pathway forms, with no appreciable

change in the average length of recombinogenic filaments. Furthermore, the fraction of recombinogenic foci could differ in different strains. For example, off-pathway Dmc1 foci may make up a larger fraction of the total Dmc1 foci in *dmc1-E157D* strains than in wild-type and *rad51*. To provide evidence that recombinogenic foci are longer on average, we examined the lengths of Dmc1 foci that colocalized with RPA. Given that all of the mutants have more RPA foci and some have more Dmc1 foci (Figure 3.4b), the level of fortuitous colocalization is expected to be higher in the mutants than in wild-type. We therefore estimated the frequency of fortuitous colocalization in all strains by a previously described method [83]. This method may yield an overestimate of fortuitous colocalization because the most focus dense region of each nucleus was used in the analysis. Only nuclei in which the level of observed colocalization exceeded the estimated fortuitous colocalization in the same image by more than 5% were considered informative for analysis. A total of 10/13 wild-type nuclei (35.5% experimental and 18.8% fortuitous), 10/13 *dmc1-E157D* nuclei (70.1% experimental and 58.6% fortuitous colocalization), and 6/13 *dmc1-E157D mei5* nuclei (69.1% experimental and 57.1% fortuitous colocalization) met our criterion for analysis, indicating that RPA-colocalization provides a meaningful criterion to identify a subset of Dmc1 foci enriched for recombinogenic as opposed to off-pathway structures in these cells. Because of higher focus density and average focus size, none of the *dmc1-E157D rad51* and *dmc1-E157D mei5 rad51* nuclei met our criterion for detection of true co-localization. The average contour length of Dmc1 filaments that colocalized with RPA was 118.9 ± 40.0 nm in wild-type, or ~100 nucleotides, similar to the corresponding value obtained using direct stochastic optical reconstruction microscopy (dSTORM), a different super-resolution

light microscopy method (Figure 3.4d) [36]. The average focus length for RPA colocalizing Dmc1 foci in *dmc1-E157D* was significantly longer than wild-type (149.5 ± 66.8 nm, or ~ 160 nucleotides, $p<0.01$, Wilcoxon test), and also different from the total population of unselected Dmc1 foci in *dmc1-E157D* cells (134.1 ± 61.5 nm). The average focus length for RPA colocalizing Dmc1 foci in *dmc1-E157D mei5* was also significantly longer than in wild-type (168.0 ± 66.4 nm, or ~190 nucleotides, $p <0.01$), and different from the total Dmc1 foci lengths in that background (147.1 ± 66.4 nm). Thus, Dmc1-E157D not only makes longer foci overall, but Dmc1-E157D foci associated with RPA-marked recombination sites are also distinctly longer under conditions of hyper-recombination (i.e. in *dmc1-E157D* and *dmc1-E157D mei5*) compared to wild-type.

### 3.3.12 Rhd54 promotes meiotic progression in *dmc1-E157D* cells

The cytological results presented above suggest that Dmc1-E157D is more likely than Dmc1-WT to form off-pathway filaments on dsDNA. DSB-independent foci are only easily detected for Dmc1-WT when Rdh54, the key translocase involved in disassembling them, is absent [51]. This observation suggested that Dmc1-E157D might be more resistant to dsDNA dissociation by Rdh54. To determine whether Rdh54 was active in *dmc1-E157D* mutants, we constructed the *dmc1-E157D rdh54* double mutant. If Rdh54 is inefficient at promoting Dmc1-E157D dissociation from dsDNA, loss of Rdh54 in the *dmc1-E157D* background should be inconsequential. Instead, we find that although both *dmc1-E157D* and *rdh54* single mutants progress through meiosis to form tetrads in which roughly 50% or more of spores are viable, the *dmc1-E157D rdh54*

double mutant arrested in prophase and failed to form spores (Table 3.1; Supplemental Figure 3.9). Thus, Rdh54 is active in *dmc1-E157D* cells.

### 3.3.13 Mei5-Sae3 is not required for the DSB-independent foci formed by Dmc1-WT protein in the absence of Rdh54

Dmc1-E157D differs from Dmc1-WT in that it forms high levels of off-pathway foci and does so independently of Mei5-Sae3. This suggests that although the mutant bypasses the requirement for Mei5-Sae3 with respect to forming recombinogenic foci, it might not fully recapitulate Mei5-Sae3 function because Mei5-Sae3's activity has only been shown to display DSB-dependent foci. It was not known if Mei5-Sae3 is also required for the off-pathway Dmc1 foci that accumulate when disassembly of dsDNA bound structures is blocked by *RDH54*$^{+}$ deletion. Therefore, to determine if Mei5-Sae3 is normally required for Dmc1 to form off-pathway complexes on dsDNA *in vivo*, we compared Dmc1 focus formation in *spo11 rdh54 mei5* to that in the *spo11 rdh54* double mutant; a *spo11* single mutant served as the negative control. The controls generated the expected results with *spo11 rdh54* nuclei displaying an average of 37 ± 14 Dmc1 foci per nucleus and *spo11* nuclei an average of only 3 ± 4 foci per nucleus (Supplemental Figure 3.10). The *spo11 rdh54 mei5* triple mutant displayed an average of 37 ± 13 foci, like the positive control, indicating that off-pathway focus formation by Dmc1-WT protein occurs independently of Mei5. Thus, Mei5-Sae3's function is dispensable for nucleation of Dmc1 complexes on dsDNA that are substrates for Rdh54-mediated disassembly. The implications of this finding are discussed below.

## 3.4 Discussion

### 3.4.1 Mechanism of Mei5-Sae3-mediated Dmc1 filament formation

Dmc1-E157D was designed to mimic the activity of the previously characterized bacterial protein RecA-E96D. Assuming this prediction is correct and Dmc1-E157D has reduced ATPase activity, our results provide *in vivo* support for the conclusion of Chi and colleagues that Swi5-Sfr1 acts to stabilize Rad51 filaments by promoting ADP release, thereby maintaining the filament in the active, ATP-bound form [69], given that a mutation designed to favor the ATP bound form of Dmc1 bypasses the normal requirement for Mei5-Sae3. On the other hand, the regulatory defects observed in Dmc1-E157D suggest that the function of Mei5-Sae3-mediated regulation may involve more than overall enhancement of Dmc1 filament stability, because the Dmc1-E157D mutant displays abnormally high levels of *spo11*-independent Dmc1-E157D binding to chromosomes (Figure 3.1e). We also find that although Mei5-Sae3 is required for cytologically detectable Dmc1 focus formation at sites of DSBs in wild-type cells, it is not required to observe the off-pathway dsDNA-bound foci formed by Dmc1-WT in *rdh54* cells (Supplemental Figure 3.10). These findings raise the possibility that stabilizing the ATP-bound form of Dmc1 alone may not fully explain Mei5-Sae3 function; it is possible that Mei5-Sae3 also confers ssDNA specificity to Dmc1-DNA interaction *in vivo.* The proposal that Mei5-Sae3 recruits Dmc1 to ssDNA is consistent with prior observations that Mei5-Sae3 preferentially binds ssDNA, and that it directly interacts with the ssDNA-specific protein RPA [60,67,70]. Thus, Mei5-Sae3 may combine the ability to enhance Dmc1 filament stability with the ability to specifically promote filament formation on ssDNA rather than dsDNA. An alternative explanation, which we cannot rule out at present, is that Mei5-Sae3 enhances the affinity of Dmc1 for both ssDNA and dsDNA

equally, but that the concentration of available dsDNA exceeds the $K_D$ for Dmc1 binding in the absence of Mei5-Sae3, while the concentration of ssDNA does not. Further studies are required to determine if either the ssDNA or the RPA binding activities of Mei5-Sae3 recruit Dmc1 to ssDNA tracts.

The ability of Dmc1-E157D to form functional filaments on ssDNA *in vivo* in the absence of Mei5-Sae3, and to do so by a mechanism involving filament stabilization, raises the possibility that Dmc1 recruitment to and nucleation on RPA coated ssDNA in wild-type cells is not reliant on Mei5-Sae3. Given that Mei5-Sae3 binds directly to both Dmc1 and RPA [62,63,70], we continue to favor models in which Mei5-Sae3 plays a role in recruitment/nucleation of Dmc1 filaments. We note, however, that Dmc1 could be recruited to sites of DSBs through its interactions with RPA [60], and that nucleation, but not filament elongation, could be Mei5-Sae3 independent. Dmc1 nucleation events might be undetected in the absence of Mei5-Sae3 because the resulting filaments never elongate to lengths sufficient to reach the threshold of cytological detection. It is also possible that Rad51 is normally partially responsible for Dmc1 recruitment/nucleation, in addition to its roles in filament stabilization and IH bias. These considerations highlight the need for further studies on the mechanism of Dmc1 recruitment/nucleation on RPA coated ssDNA tracts *in vivo*.

### 3.4.2 Role of Rad51 in Dmc1 filament dynamics

The absence of foci observed in *mei5*, *sae3*, and *mei5 sae3* mutants, and the dimmer foci observed in *rad51* mutants, indicate that normal Dmc1 focus formation involves both proteins [61,62,78]. The fact that recombination and DSB-dependent focus formation in *rad51* yeast depends on Mei5-Sae3 suggests that Mei5-Sae3 is

epistatic to Rad51. Furthermore, the formation of brightly staining Mei5-Sae3 foci depends on Rad51, as does the formation of brightly staining Dmc1 foci [62,78]. These dependency relationships raised the possibility that Rad51's ability to influence Dmc1 filaments might require a direct interaction between Rad51 and Mei5-Sae3 [90]. However, the data presented here indicate that Rad51 promotes formation of functional Dmc1 filaments on ssDNA independently of Mei5-Sae3, thus Rad51's normal influence on Dmc1 filament dynamics does not require, and may not involve, Mei5-Sae3 binding to Rad51.

Our data provide critical evidence that Mei5-Sae3 and Rad51 function independently with respect to enhancing the formation of functional Dmc1 filaments. Whereas *dmc1-E157D mei5* forms COs at a level nearly equivalent to wild-type, *dmc1-E157D rad51* suffers a dramatic reduction in CO formation, and experiences hyper-resection (Figure 3.2a,b). In addition, 2D gel electrophoresis shows that JM formation in *dmc1-E157D mei5* is equivalent to *dmc1-E157D*, while the JMs formed in the *dmc1-E157D rad51* background are significantly reduced relative to *dmc1-E157D,* and show an IH bias defect like the *rad51* single mutant (Figure 3.3d,e). Thus, a mutation that alleviates Dmc1's need for Mei5-Sae3, retains full dependency on Rad51. If the functions of Mei5-Sae3 and Rad51 were interdependent, a mutation that bypasses the requirement for Mei5-Sae3 would also bypass the requirement for Rad51. Under this model for independent function of the two accessory proteins, the partial dependency of Mei5-Sae3 foci on Rad51 can be explained if Mei5-Sae3 binds Dmc1 filaments along their entire contour, because Dmc1 forms shorter filaments in the absence of Rad51.

Rad51 is likely to impact Dmc1 filament dynamics by direct interaction. Although a previous study did not ascribe significance to the low level of interaction detected between budding yeast Rad51 and Dmc1 [89], two-hybrid studies in other organisms detected significant levels of Rad51-Dmc1 interaction, albeit at low levels compared to the homotypic interactions [91-93]. Budding yeast Rad51 binds Dmc1 directly when pure proteins are mixed [60], consistent with similar observations in other organisms [91-93]. Using the meiotic two-hybrid method, we were able to detect Rad51-Dmc1 interaction during meiotic prophase of budding yeast, and to show that this interaction does not require Mei5-Sae3 (Supplemental Figure 3.7). These findings provide additional evidence that Rad51 and Mei5-Sae3 influence Dmc1 DNA binding dynamics independently. The finding that Rad51-Dmc1 interaction occurs, but is weaker than homotypic interactions, is consistent with a single molecule study that showed mixtures of Rad51 and Dmc1 form predominantly homo-filaments on DNA [31], and with prior cytological studies that showed the foci formed by Rad51 and Dmc1 lie adjacent to one another rather than being perfectly colocalized [61,89,94]. Finally, we note that direct interaction between the two proteins can account for the observation that Rad51 can stimulate Dmc1-mediated D-loop formation in the absence of other proteins [3].

How might Mei5-Sae3 and Rad51 promote Dmc1 filament stability by independent mechanisms? There are at least two basic mechanisms that could contribute to filament stability. First, an accessory protein could promote the high-affinity ssDNA binding form. Second, if a strand exchange protein is normally subject to enzymatically-driven disassembly, an accessory protein might act by specifically blocking the activity of that enzyme. Mei5-Sae3's role in filament stabilization *in vivo*

almost certainly involves direct enhancement of DNA binding activity during nucleation and/or elongation, as is the case for Mei5-Sae3 homolog Sfr1-Swi5 [72]. Rad51 might also enhance binding directly, by reducing the off-rate of protomers from filaments. For example, a Rad51 monomer bound to the end of a Dmc1 filament might drastically reduce the off-rate of the adjacent Dmc1 protomer with a strong overall effect on filament stability, given that disassembly of filaments is expected to occur from filament ends [95].

Alternatively, or in addition, Rad51 may block a mechanism that actively dissociates Dmc1 filaments. Although no active disassembly mechanism has been identified for Dmc1 filaments, active disassembly could involve a helicase mechanism, similar to that mediated by UvrD and Srs2 [26-29]. One observation that appears to be at odds with the idea that Rad51 functions to promote Dmc1 filament formation by blocking an Srs2-like mechanism is that Rad51 stimulates Dmc1's D-loop activity in a purified system that does not include an ssDNA-specific helicase. However, it is possible that the *in vitro* activity of Rad51 in stimulating Dmc1 does not fully recapitulate the *in vivo* function of the protein. This possibility is emphasized by previous work on the Rad51 accessory protein Rad55-Rad57. Both subunits of the Rad55-Rad57 heterodimer are structurally similar to Rad51. Rad55-Rad57 stimulates Rad51 activity *in vitro*, but *in vivo* it additionally functions to limit the Rad51 strippase activity of Srs2 [96,97]. Thus, Rad51's impact on Dmc1 activity *in vitro* might similarly not fully represent its *in vivo* role in promoting stable Dmc1 filaments.

A model invoking inhibition of Dmc1-ssDNA filament disassembly can account for the fact that *dmc1-E157D rad51* forms fewer JMs relative to *DMC1*$^{+}$ *rad51* (Figure

3.3e). Like Dmc1-E157D, the Rad51 ATPase mutant Rad51-K191R is defective in recruitment to DSB-associated tracts of ssDNA *in vivo*. The DNA binding defect of Rad51-K191R is partially suppressed by deletion of *SRS2* or by overexpression of *RAD54* [55,56]. These findings suggest that the recruitment defect displayed by Rad51-K191R results from a combination of the protein's DNA binding defect, increased off-pathway dsDNA binding, and active disassembly of Rad51-K191R filaments that do form at DSB-associated tracts of ssDNA [57]. If Dmc1-E157D filaments form more slowly than wild-type filaments as a result of increased off-pathway binding, which would result in a decreased pool of free Dmc1 protomers, Dmc1-E157D filaments may be acutely sensitive to disassembly and/or end dissociation, thus explaining Dmc1-E157D's dependency on Rad51. In addition, these models can account for the more severe phenotype of the *dmc1-E157D mei5 rad51* triple mutant compared to the *dmc1-E157D rad51* double mutant as a consequence of Mei5-Sae3 having a limited ability to block dissociation, or being able to promote fast reassembly. Such an activity of Mei5-Sae3 might be inconsequential for Dmc1-E157D DNA binding dynamics *in vivo* when Rad51 is present, explaining why the phenotypes of *dmc1-E157D* and *dmc1-E157D mei5* are nearly identical.

### 3.4.3 Mei5-Sae3 is not required for IH bias

The results presented here also reveal for the first time that although both Rad51 and Mei5-Sae3 promote the formation of stable Dmc1 filaments, Mei5-Sae3 differs from Rad51 in that Mei5-Sae3 is not required for IH bias while Rad51 is. This conclusion could not have been arrived at based on earlier observations because recombination is blocked prior to formation of JMs in *DMC1*$^{+}$ *mei5* and *DMC1*$^{+}$ *sae3* cells; bypass of the

requirement for Mei5-Sae3 for formation of functional filaments allowed us to assess the role of Mei5-Sae3 in recombination partner choice at the strand invasion stage. Previous work showed that Rad51 and Dmc1 are both required for IH bias [79,88]. The results here show that the cooperation between Rad51 and Dmc1 required for IH bias involves a Rad51-dependent mechanism that is independent of Mei5-Sae3. This interpretation is consistent with the fact that, in other species, homologs of Mei5-Sae3 regulate Rad51 activity, suggesting that the Mei5-Sae3 family of accessory proteins solves a problem common to both Rad51 and Dmc1 that is not unique to meiotic recombination.

Chromatin immunoprecipitation experiments have shown that cells lacking both Rdh54 and Rad54 fail to recruit Dmc1 to DSB hotspots as a consequence of sequestration caused by off pathway DNA binding. The failure to recruit Dmc1 to tracts of ssDNA accounts for the hyper-resection seen in *rad54 rdh54* double mutants [51,98]. Given that Dmc1-E157D forms foci in the absence of DSBs, and that it is modeled on RecA-E96D, which displays a lower than normal off-rate for dsDNA binding, one might expect that Dmc1-E157D is less efficiently removed from dsDNA by Rdh54 (and Rad54). Surprisingly, we find no evidence for a decrease in CO formation or for hyper-resection in *dmc1-E157D* (Figure 3.2a,b, Supplemental Figure 3.2a,b). Moreover, dHJ formation is increased, suggesting that Dmc1-E157D is efficiently removed from the 3' end of the heteroduplex DNA to allow for recombination-associated DNA synthesis (Figure 3.3c,e). This function is likely carried out by Rdh54 given the corresponding activity of Rad54 on Rad51 and on the evidence that Rdh54 acts to remove off-pathway Dmc1 complexes from dsDNA [49,51]. We also find that the meiotic progression and

spore formation observed in *dmc1-E157D* mutants is strongly dependent on Rdh54, indicating that Rdh54 is active in *dmc1-E157D* mutants (Table 3.1, Supplemental Figure 3.9). Thus, although Dmc1-E157D likely forms more off-pathway foci than Dmc1-WT, Rdh54 is apparently able to have some effect on Dmc1-E157D, which we presume involves dissociating the mutant Dmc1 protein from tracts of dsDNA.

### 3.4.4 Dmc1-E157D forms abnormally long filaments and is hyper-recombinant for certain JMs and recombination products

Although levels of IH CO intermediates and products are similar to those in wild-type, *dmc1-E157D* and *dmc1-E157D mei5* display higher than normal levels of certain types of recombination intermediates and products including IS-dHJs, mcJMs, and ectopic COs. For simplicity, we will refer to these unusual types of recombination events collectively as “aberrant,” but we emphasize that all three types are observed at low levels in wild-type cells. IS-dHJs, mcJMs, and ectopic COs are all elevated about 3-fold in *dmc1-E157D* and *dmc1-E157D mei5* cells (Figures 3.2b, 3.3c,e, Supplemental Figure 3.4b). The combination of aberrant recombination phenotypes observed in *dmc1-E157D* cells is reminiscent of that reported for *sgs1*, *top3*, and *rmi1* mutants during meiosis [99-101]. Sgs1, Top3, and Rmi1 have been shown to form a complex, STR, that disassembles D-loops [102-104]. In addition, during mitotic recombination, STR was shown to have a role in disassembling aberrant invasion events in which a single Rad51 filament invades two or more donor molecules (“multi-invasions”) [105]. This role of STR in multi-invasion disassembly was proposed to account for at least some of the phenotypes observed in the absence of Sgs1, Top3, or Rmi1 during meiosis [101]. In this context, maturation of a multi-invasion into a mcJM, followed by resolution of the

multi-invasion, can account for the increase in mcJMs, IS-dHJs, and ectopic recombination observed in these mutants [106]. Further evidence that multi-invasions account for the meiotic STR mutant phenotypes is the fact that both multi-invasions and JMs in the *sgs1*, *top3*, or *rmi1* mutant backgrounds are highly dependent on structure-selective nucleases Mus81-Mms4, Slx1-Slx4, and Yen1 [100,101,105,107-109].

Several possibilities account for why *dmc1-E157D* and *dmc1-E157D mei5* are phenotypically similar to the *sgs1*, *top3*, and *rmi1* mutants. Dmc1-E157D may form the same number of aberrant intermediates as wild-type, but STR-mediated disassembly could be rendered less efficient as a consequence of enhanced binding activity of Dmc1-E157D compared to Dmc1-WT. Alternatively, as a consequence of the fact that Dmc1-E157D forms longer filaments, it may also form longer D-loops. Piazza et al. have recently shown that two D-loop disassembly pathways function in somatic cells, one that relies on the activities of STR and Mph1, and another that relies on Srs2 [104]. Interestingly, Srs2-dependent D-loops may be longer than those processed by the STR and Mph1 pathway [104,110]. Thus, if Dmc1-E157D forms longer D-loops, it may perturb the balance between these two D-loop editing pathways, resulting in the phenotypes observed. Arguing against the notion that D-loop disassembly is impaired by the *dmc1-E157D* mutation is the fact that there is no appreciable increase in SEIs in *dmc1-E157D* and *dmc1-E157D mei5* cells as compared to wild-type (Figures 3.3b,d), which might be expected if the mutant protein prevented D-loop disruption.

Our preferred model to account for the defects associated with *dmc1-E157D* and *dmc1-E157D mei5* is that Dmc1-E157D makes more aberrant D-loops than Dmc1-WT. In this model, STR, and possibly other helicases, disassemble aberrant D-loops

normally, but the mutant protein generates more multi-invasions than Dmc1-WT. The two regions of homology engaged in such multi-invasion events could be on one sister and one homolog, or on both of the homologs, likely engaging one template at the allelic site, and one at the ectopic site. The formation of the multi-invasions can account for the increased mcJMs, while processing of multi-invasions to yield fully repaired chromatids can explain the increases in IS-dHJs and ectopic COs [106]. Drawing on the "intersegmental contact sampling" model of homology search [111], we propose Dmc1-E157D makes more multi-invasions as a consequence of making longer filaments (Figure 3.5). The intersegmental contact sampling model maintains that a filament has a polyvalent interaction surface capable of simultaneously searching multiple, non-contiguous dsDNA regions for homology [111]. Longer filaments are able to search duplex DNA more efficiently, as a consequence of being able to engage in a greater number of simultaneous interactions. We have demonstrated that Dmc1-E157D forms longer filaments *in vivo* (Figure 3.4c,d). We posit that because filaments are longer, Dmc1-E157D engages in a higher number of simultaneous searching interactions that results in more frequent homology-dependent engagement of two different regions of homology by a single filament. Given that multi-invasion recombination is thought to generate secondary DSBs [105,106], this interpretation explains not only the defects that we see by 2D gel electrophoresis (Figure 3.3b-e) but also why DSBs accumulate to higher levels in *dmc1-E157D* relative to wild-type (Supplemental Figure 3.2a,b) and persist longer (Figure 3.2a,b).

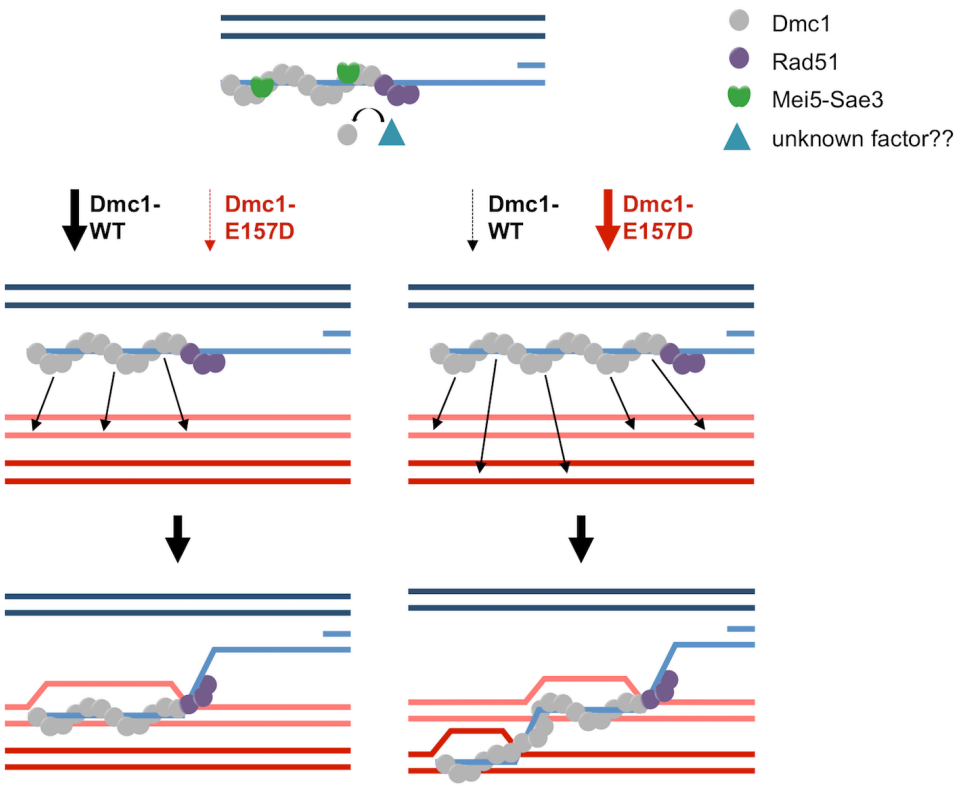


**Figure 3.5** Model for regulation of filament length *in vivo*.

Though these aberrant recombination events are increased in *dmc1-E157D*, they also make up a substantial fraction of the recombination events observed in wild-type cells [99,105]. Consistent with this finding, 14% of wild-type Dmc1 foci that colocalized with RPA were longer than 149 nm in length, the average length of Dmc1-E157D foci that colocalize with RPA in *dmc1-E157D* (Figure 3.4d). This finding suggests that although most foci are much shorter than 149 nm in wild-type cells, long filaments do occasionally form. The proposal that longer than normal filaments are responsible for higher than normal levels of multi-invasions is supported by previous work showed that (1) if longer ssDNA substrates are used, there is a higher incidence of multi-invasions [112]; (2) Rad55-Rad57 promotes both longer Rad51 filaments and the formation of multi-invasions [97,106] ; and (3) multi-invasions increased more than linearly as a

consequence of increasing homology between the broken molecule and one of the two donors sequences [105].

The aberrant event hyper-recombinant phenotype displayed by Dmc1-E157D is Rad51-dependent. The mechanism responsible for Rad51's role in promoting the aberrant hyper-recombinant activity of Dmc1-E157D remains to be determined. Analysis of RPA co-localized foci provided evidence that Dmc1-E157D forms longer filaments on ssDNA in otherwise wild-type cells and in *mei5* single mutants. The mutant protein also forms long filaments on dsDNA, given that long filaments are also observed in *spo11* mutants (Supplemental Figure 3.8b). Because both RPA and Dmc1 focus counts are increased in *dmc1-E157D rad51* and *dmc1-E157D mei5 rad51* mutants (Figure 3.4b), and because both RPA and Dmc1 foci are also longer in these mutants (Figure 3.4c), it was not possible to identify a sub-population that we could be confident was enriched for ssDNA bound structures in these mutants. As a result, it is unclear if the dependency of Dmc1-E157D's hyper-recombinant phenotype on Rad51 reflects a requirement for Rad51 in forming long Dmc1 filaments on ssDNA, or if Rad51 plays some other role in promoting the high level of aberrant recombination events observed in *dmc1-E157D* and *dmc1-E157D mei5*. It is clear, however, that Rad51's homology search and strand exchange activities are not required for the aberrant hyper-recombinant phenotype observed in *dmc1-E157D* cells because IS-dHJs and mcJMs are increased in *dmc1-E157D rad51-II3A* cells, in a manner that is nearly indistinguishable from the *dmc1-E157D* single mutant (Supplemental Figure 3.6b).

We speculate that the lengths of RecA-family strand exchange filaments are limited by regulatory mechanisms that evolved to prevent homology-dependent

translocations and other genome rearrangements. Limiting filament lengths may limit the ability of filaments to simultaneously engage more than one homologous target sequence. In this regard, it is relevant that the single molecule study that provided evidence for intersegmental transfer did not detect any homology-dependent target engagement with the shortest ssDNA substrate examined, which was 162 nucleotides in length [111]. However, *in vivo*, Dmc1 filaments are typically ~100 nucleotides in wild-type cells (Figure 3.4c) [36]. Thus, it is possible that the cost of multi-invasions to genome stability has constrained the length of strand exchange filaments such that intersegmental searching is restricted or prevented *in vivo.*

References


1. Hunter N. Meiotic Recombination: The Essence of Heredity. Cold Spring Harb Perspect Biol. Cold Spring Harbor Lab; 2015;7: a016618–35. doi:10.1101/cshperspect.a016618

2. Bishop DK, Park D, Xu L, Kleckner N. DMC1: a meiosis-specific yeast homolog of E. coli recA required for recombination, synaptonemal complex formation, and cell cycle progression. Cell. 1992;69: 439–456.

3. Cloud V, Chan Y-L, Grubb J, Budke B, Bishop DK. Rad51 is an accessory factor for Dmc1-mediated joint molecule formation during meiosis. Science. 2012;337: 1222–1225. doi:10.1126/science.1219379

4. Shinohara A, Ogawa H, Ogawa T. Rad51 protein involved in repair and recombination in S. cerevisiae is a RecA-like protein. Cell. 1992;69: 457–470.

5. Sung P, Robberson DL. DNA strand exchange mediated by a RAD51-ssDNA nucleoprotein filament with polarity opposite to that of RecA. Cell. 1995;82: 453–461. doi:10.1016/0092-8674(95)90434-4

6. Keeney S, Giroux CN, Kleckner N. Meiosis-specific DNA double-strand breaks are catalyzed by Spo11, a member of a widely conserved protein family. Cell. 1997;88: 375–384.

7. Symington LS. Mechanism and regulation of DNA end resection in eukaryotes. Critical Reviews in Biochemistry and Molecular Biology. 2016;51: 195–212. doi:10.3109/10409238.2016.1172552

8. Bell JC, Kowalczykowski SC. RecA: Regulation and Mechanism of a Molecular Search Engine. Trends Biochem Sci. 2016;41: 491–507. doi:10.1016/j.tibs.2016.04.002

9. Jinks-Robertson S, Petes TD. High-frequency meiotic gene conversion between repeated genes on nonhomologous chromosomes in yeast. Proc Natl Acad Sci USA. National Academy of Sciences; 1985;82: 3350–3354. doi:10.1073/pnas.82.10.3350

10. Lichten M, Borts RH, Haber JE. Meiotic gene conversion and crossing over between dispersed homologous sequences occurs frequently in Saccharomyces cerevisiae. Genetics. Genetics Society of America; 1987;115: 233–246.

11. Goldman AS, Lichten M. The efficiency of meiotic recombination between dispersed sequences in Saccharomyces cerevisiae depends upon their chromosomal location. Genetics. Genetics Society of America; 1996;144:

43–55.

12. Grushcow JM, Holzen TM, Park KJ, Weinert T, Lichten M, Bishop DK. Saccharomyces cerevisiae checkpoint genes MEC1, RAD17 and RAD24 are required for normal meiotic recombination partner choice. Genetics. Genetics Society of America; 1999;153: 607–620.

13. Schwacha A, Kleckner N. Identification of joint molecules that form frequently between homologs but rarely between sister chromatids during yeast meiosis. Cell. 1994;76: 51–63.

14. Brown MS, Bishop DK. DNA Strand Exchange and RecA Homologs in Meiosis. Cold Spring Harb Perspect Biol. 2015;7: a016659–31. doi:10.1101/cshperspect.a016659

15. Wright WD, Shah SS, Heyer W-D. Homologous recombination and the repair of DNA double-strand breaks. J Biol Chem. 2018;293: 10524–10535. doi:10.1074/jbc.TM118.000372

16. McVey M, Khodaverdian VY, Meyer D, Cerqueira PG, Heyer W-D. Eukaryotic DNA Polymerases in Homologous Recombination. Annu Rev Genet. 2016;50: 393–421. doi:10.1146/annurev-genet-120215-035243

17. McMahill MS, Sham CW, Bishop DK. Synthesis-dependent strand annealing in meiosis. Lichten M, editor. PLoS Biol. Public Library of Science; 2007;5: e299. doi:10.1371/journal.pbio.0050299

18. Merker JD, Dominska M, Petes TD. Patterns of heteroduplex formation associated with the initiation of meiotic recombination in the yeast. Genetics. Genetics Society of America; 2003;165: 47–63.

19. Allers T, Lichten M. Differential timing and control of noncrossover and crossover recombination during meiosis. Cell. 2001;106: 47–57. doi:10.1016/s0092-8674(01)00416-0

20. Hunter N, Kleckner N. The single-end invasion: an asymmetric intermediate at the double-strand break to double-holliday junction transition of meiotic recombination. Cell. 2001;106: 59–70.

21. Schwacha A, Kleckner N. Identification of double Holliday junctions as intermediates in meiotic recombination. Cell. 1995;83: 783–791. doi:10.1016/0092-8674(95)90191-4

22. Zakharyevich K, Tang S, Ma Y, Hunter N. Delineation of joint molecule resolution pathways in meiosis identifies a crossover-specific resolvase. Cell. 2012;149: 334–347. doi:10.1016/j.cell.2012.03.023

23. Heyer W-D. Regulation of recombination and genomic maintenance. Cold Spring Harb Perspect Biol. 2015;7: a016501. doi:10.1101/cshperspect.a016501

24. Krejci L, Altmannova V, Spirek M, Zhao X. Homologous recombination and its regulation. Nucleic Acids Res. 2012;40: 5795–5818. doi:10.1093/nar/gks270

25. Kowalczykowski SC. An Overview of the Molecular Mechanisms of Recombinational DNA Repair. Cold Spring Harb Perspect Biol. 2015;7. doi:10.1101/cshperspect.a016410

26. Krejci L, Van Komen S, Li Y, Villemain J, Reddy MS, Klein H, et al. DNA helicase Srs2 disrupts the Rad51 presynaptic filament. Nature. Nature Publishing Group; 2003;423: 305–309. doi:10.1038/nature01577

27. Veaute X, Jeusset J, Soustelle C, Kowalczykowski SC, Le Cam E, Fabre F. The Srs2 helicase prevents recombination by disrupting Rad51 nucleoprotein filaments. Nature. 2003;423: 309–312. doi:10.1038/nature01585

28. Veaute X, Delmas S, Selva M, Jeusset J, Le Cam E, Matic I, et al. UvrD helicase, unlike Rep helicase, dismantles RecA nucleoprotein filaments in Escherichia coli. EMBO J. EMBO Press; 2005;24: 180–189. doi:10.1038/sj.emboj.7600485

29. Petrova V, Chen SH, Molzberger ET, Tomko E, Chitteni-Pattu S, Jia H, et al. Active displacement of RecA filaments by UvrD translocase activity. Nucleic Acids Res. 2015;43: 4133–4149. doi:10.1093/nar/gkv186

30. Sasanuma H, Furihata Y, Shinohara M, Shinohara A. Remodeling of the Rad51 DNA strand-exchange protein by the Srs2 helicase. Genetics. Genetics; 2013;194: 859–872. doi:10.1534/genetics.113.150615

31. Crickard JB, Kaniecki K, Kwon Y, Sung P, Greene EC. Meiosis-specific recombinase Dmc1 is a potent inhibitor of the Srs2 antirecombinase. Proc Natl Acad Sci USA. 2018;115: E10041–E10048. doi:10.1073/pnas.1810457115

32. Bishop DK, Ear U, Bhattacharyya A, Calderone C, Beckett M, Weichselbaum RR, et al. Xrcc3 is required for assembly of Rad51 complexes in vivo. Journal of Biological Chemistry. American Society for Biochemistry and Molecular Biology; 1998;273: 21482–21488. doi:10.1074/jbc.273.34.21482

33. Gasior SL, Olivares H, Ear U, Hari DM, Weichselbaum R, Bishop DK. Assembly of RecA-like recombinases: distinct roles for mediator proteins in

mitosis and meiosis. Proc Natl Acad Sci USA. National Academy of Sciences; 2001;98: 8411–8418. doi:10.1073/pnas.121046198

34. Haaf T, Golub EI, Reddy G, Radding CM, Ward DC. Nuclear foci of mammalian Rad51 recombination protein in somatic cells after DNA damage and its localization in synaptonemal complexes. Proc Natl Acad Sci USA. National Academy of Sciences; 1995;92: 2298–2302. doi:10.1073/pnas.92.6.2298

35. Gataulin DV, Carey JN, Li J, Shah P, Grubb JT, Bishop DK. The ATPase activity of E. coli RecA prevents accumulation of toxic complexes formed by erroneous binding to undamaged double stranded DNA. Nucleic Acids Res. 2018;46: 9510–9523. doi:10.1093/nar/gky748

36. Brown MS, Grubb J, Zhang A, Rust MJ, Bishop DK. Small Rad51 and Dmc1 Complexes Often Co-occupy Both Ends of a Meiotic DNA Double Strand Break. Lichten M, editor. PLoS Genet. Public Library of Science; 2015;11: e1005653. doi:10.1371/journal.pgen.1005653

37. Egelman EH, Stasiak A. Structure of helical RecA-DNA complexes. Complexes formed in the presence of ATP-gamma-S or ATP. J Mol Biol. 1986;191: 677–697.

38. Zakharyevich K, Ma Y, Tang S, Hwang PY-H, Boiteux S, Hunter N. Temporally and biochemically distinct activities of Exo1 during meiosis: double-strand break resection and resolution of double Holliday junctions. Molecular Cell. 2010;40: 1001–1015. doi:10.1016/j.molcel.2010.11.032

39. Menetski JP, Bear DG, Kowalczykowski SC. Stable DNA heteroduplex formation catalyzed by the Escherichia coli RecA protein in the absence of ATP hydrolysis. Proc Natl Acad Sci USA. National Academy of Sciences; 1990;87: 21–25. doi:10.1073/pnas.87.1.21

40. Rosselli W, Stasiak A. Energetics of RecA-mediated recombination reactions. Without ATP hydrolysis RecA can mediate polar strand exchange but is unable to recycle. J Mol Biol. 1990;216: 335–352. doi:10.1016/S0022-2836(05)80325-0

41. Sung P, Stratton SA. Yeast Rad51 recombinase mediates polar DNA strand exchange in the absence of ATP hydrolysis. Journal of Biological Chemistry. American Society for Biochemistry and Molecular Biology; 1996;271: 27983–27986. doi:10.1074/jbc.271.45.27983

42. Campbell MJ, Davis RW. Toxic mutations in the recA gene of E. coli prevent proper chromosome segregation. J Mol Biol. 1999;286: 417–435. doi:10.1006/jmbi.1998.2456

43. Stasiak A, Egelman EH. Visualization of recombination intermediates. Kucherlapati R, Smith GR, editors. 1988:265–307.

44. Sung P. Catalysis of ATP-dependent homologous DNA pairing and strand exchange by yeast RAD51 protein. Science. 1994;265: 1241–1243.

45. Zaitseva EM, Zaitsev EN, Kowalczykowski SC. The DNA binding properties of Saccharomyces cerevisiae Rad51 protein. Journal of Biological Chemistry. American Society for Biochemistry and Molecular Biology; 1999;274: 2907–2915. doi:10.1074/jbc.274.5.2907

46. Hong EL, Shinohara A, Bishop DK. Saccharomyces cerevisiae Dmc1 protein promotes renaturation of single-strand DNA (ssDNA) and assimilation of ssDNA into homologous super-coiled duplex DNA. Journal of Biological Chemistry. 2001;276: 41906–41912. doi:10.1074/jbc.M105563200

47. Solinger JA, Kiianitsa K, Heyer W-D. Rad54, a Swi2/Snf2-like recombinational repair protein, disassembles Rad51:dsDNA filaments. Molecular Cell. 2002;10: 1175–1188.

48. Sheridan SD, Yu X, Roth R, Heuser JE, Sehorn MG, Sung P, et al. A comparative analysis of Dmc1 and Rad51 nucleoprotein filaments. Nucleic Acids Res. 2008;36: 4057–4066. doi:10.1093/nar/gkn352

49. Li X, Heyer W-D. RAD54 controls access to the invading 3'-OH end after RAD51-mediated DNA strand invasion in homologous recombination in Saccharomyces cerevisiae. Nucleic Acids Res. 2009;37: 638–646. doi:10.1093/nar/gkn980

50. Chi P, Kwon Y, Seong C, Epshtein A, Lam I, Sung P, et al. Yeast recombination factor Rdh54 functionally interacts with the Rad51 recombinase and catalyzes Rad51 removal from DNA. Journal of Biological Chemistry. 2006;281: 26268–26279. doi:10.1074/jbc.M602983200

51. Holzen TM, Shah PP, Olivares HA, Bishop DK. Tid1/Rdh54 promotes dissociation of Dmc1 from nonrecombinogenic sites on meiotic chromatin. Genes Dev. 2006;20: 2593–2604. doi:10.1101/gad.1447106

52. Shah PP, Zheng X, Epshtein A, Carey JN, Bishop DK, Klein HL. Swi2/Snf2-related translocases prevent accumulation of toxic Rad51 complexes during mitotic growth. Molecular Cell. 2010;39: 862–872. doi:10.1016/j.molcel.2010.08.028

53. Mason JM, Dusad K, Wright WD, Grubb J, Budke B, Heyer W-D, et al. RAD54 family translocases counter genotoxic effects of RAD51 in human tumor cells. Nucleic Acids Res. 2015;43: 3180–3196. doi:10.1093/nar/gkv175

54. Hilario J, Amitani I, Baskin RJ, Kowalczykowski SC. Direct imaging of human Rad51 nucleoprotein dynamics on individual DNA molecules. Proc Natl Acad Sci USA. 2009;106: 361–368. doi:10.1073/pnas.0811965106

55. Morgan EA, Shah N, Symington LS. The requirement for ATP hydrolysis by Saccharomyces cerevisiae Rad51 is bypassed by mating-type heterozygosity or RAD54 in high copy. Mol Cell Biol. 2002;22: 6336–6343. doi:10.1128/mcb.22.18.6336-6343.2002

56. Fung CW, Fortin GS, Peterson SE, Symington LS. The rad51-K191R ATPase-defective mutant is impaired for presynaptic filament formation. Mol Cell Biol. 2006;26: 9544–9554. doi:10.1128/MCB.00599-06

57. Li X, Zhang X-P, Solinger JA, Kiianitsa K, Yu X, Egelman EH, et al. Rad51 and Rad54 ATPase activities are both required to modulate Rad51-dsDNA filament dynamics. Nucleic Acids Res. 2007;35: 4124–4140. doi:10.1093/nar/gkm412

58. Conway AB, Lynch TW, Zhang Y, Fortin GS, Fung CW, Symington LS, et al. Crystal structure of a Rad51 filament. Nat Struct Mol Biol. 2004;11: 791–796. doi:10.1038/nsmb795

59. Galkin VE, Wu Y, Zhang X-P, Qian X, He Y, Yu X, et al. The Rad51/RadA N-terminal domain activates nucleoprotein filament ATPase activity. Structure. 2006;14: 983–992. doi:10.1016/j.str.2006.04.001

60. Chan Y-L, Zhang A, Weissman BP, Bishop DK. RPA resolves conflicting activities of accessory proteins during reconstitution of Dmc1-mediated meiotic recombination. Nucleic Acids Res. 2019;47: 747–761. doi:10.1093/nar/gky1160

61. Bishop DK. RecA homologs Dmc1 and Rad51 interact to form multiple nuclear complexes prior to meiotic chromosome synapsis. Cell. 1994;79: 1081–1092.

62. Hayase A, Takagi M, Miyazaki T, Oshiumi H, Shinohara M, Shinohara A. A Protein Complex Containing Mei5 and Sae3 Promotes the Assembly of the Meiosis-Specific RecA Homolog Dmc1. Cell. 2004;119: 927–940. doi:10.1016/j.cell.2004.10.031

63. Tsubouchi H, Roeder GS. The budding yeast mei5 and sae3 proteins act together with dmc1 during meiotic recombination. Genetics. 2004;168: 1219–1230. doi:10.1534/genetics.103.025700

64. Zierhut C, Berlinger M, Rupp C, Shinohara A, Klein F. Mnd1 Is Required for Meiotic Interhomolog Repair. Current Biology. 2004;14: 752–762. doi:10.1016/j.cub.2004.04.030

65. Henry JM, Camahort R, Rice DA, Florens L, Swanson SK, Washburn MP, et al. Mnd1/Hop2 facilitates Dmc1-dependent interhomolog crossover formation in meiosis of budding yeast. Mol Cell Biol. 2006;26: 2913–2923. doi:10.1128/MCB.26.8.2913-2923.2006

66. Argunhan B, Murayama Y, Iwasaki H. The differentiated and conserved roles of Swi5-Sfr1 in homologous recombination. FEBS Lett. 2017;591: 2035–2047. doi:10.1002/1873-3468.12656

67. Haruta N, Kurokawa Y, Murayama Y, Akamatsu Y, Unzai S, Tsutsui Y, et al. The Swi5-Sfr1 complex stimulates Rhp51/Rad51- and Dmc1-mediated DNA strand exchange in vitro. Nat Struct Mol Biol. 2006;13: 823–830. doi:10.1038/nsmb1136

68. Yuan J, Chen J. The role of the human SWI5-MEI5 complex in homologous recombination repair. J Biol Chem. 2011;286: 9888–9893. doi:10.1074/jbc.M110.207290

69. Su G-C, Chung C-I, Liao C-Y, Lin S-W, Tsai C-T, Huang T, et al. Enhancement of ADP release from the RAD51 presynaptic filament by the SWI5-SFR1 complex. Nucleic Acids Res. 2014;42: 349–358. doi:10.1093/nar/gkt879

70. Ferrari SR, Grubb J, Bishop DK. The Mei5-Sae3 Protein Complex Mediates Dmc1 Activity in Saccharomyces cerevisiae. Journal of Biological Chemistry. 2009;284: 11766–11770. doi:10.1074/jbc.C900023200

71. Bugreev DV, Mazin AV. Ca2+ activates human homologous recombination protein Rad51 by modulating its ATPase activity. Proc Natl Acad Sci USA. National Academy of Sciences; 2004;101: 9988–9993. doi:10.1073/pnas.0402105101

72. Lu C-H, Yeh H-Y, Su G-C, Ito K, Kurokawa Y, Iwasaki H, et al. Swi5-Sfr1 stimulates Rad51 recombinase filament assembly by modulating Rad51 dissociation. Proc Natl Acad Sci USA. National Academy of Sciences; 2018;115: E10059–E10068. doi:10.1073/pnas.1812753115

73. McKee AH, Kleckner N. Mutations in Saccharomyces cerevisiae that block meiotic prophase chromosome metabolism and confer cell cycle arrest at pachytene identify two new meiosis-specific genes SAE1 and SAE3. Genetics. Genetics Society of America; 1997;146: 817–834.

74. Akamatsu Y, Tsutsui Y, Morishita T, Siddique MSP, Kurokawa Y, Ikeguchi M, et al. Fission yeast Swi5/Sfr1 and Rhp55/Rhp57 differentially regulate Rhp51-dependent recombination outcomes. EMBO J. EMBO Press; 2007;26: 1352–1362. doi:10.1038/sj.emboj.7601582

75. Akamatsu Y, Jasin M. Role for the mammalian Swi5-Sfr1 complex in DNA strand break repair through homologous recombination. PLoS Genet. 2010;6: e1001160. doi:10.1371/journal.pgen.1001160

76. Tsubouchi H, Roeder GS. Budding yeast Hed1 down-regulates the mitotic recombination machinery when meiotic recombination is impaired. Genes Dev. Cold Spring Harbor Lab; 2006;20: 1766–1775. doi:10.1101/gad.1422506

77. Busygina V, Sehorn MG, Shi IY, Tsubouchi H, Roeder GS, Sung P. Hed1 regulates Rad51-mediated recombination via a novel mechanism. Genes Dev. 2008;22: 786–795. doi:10.1101/gad.1638708

78. Shinohara A, Gasior S, Ogawa T, Kleckner N, Bishop DK. Saccharomyces cerevisiae recA homologues RAD51 and DMC1 have both distinct and overlapping roles in meiotic recombination. Genes Cells. 1997;2: 615–629.

79. Schwacha A, Kleckner N. Interhomolog bias during meiotic recombination: meiotic functions promote a highly differentiated interhomolog-only pathway. Cell. 1997;90: 1123–1135.

80. Campbell MJ, Davis RW. On the in vivo function of the RecA ATPase. J Mol Biol. 1999;286: 437–445. doi:10.1006/jmbi.1998.2457

81. Fortin GS, Symington LS. Mutations in yeast Rad51 that partially bypass the requirement for Rad55 and Rad57 in DNA repair by increasing the stability of Rad51-DNA complexes. EMBO J. EMBO Press; 2002;21: 3160–3170. doi:10.1093/emboj/cdf293

82. Peck R, Olsen C. Statistics: Learning from Data (AP Edition). 1st ed. Boston: Cengage Learning.

83. Gasior SL, Wong AK, Kora Y, Shinohara A, Bishop DK. Rad52 associates with RPA and functions with rad55 and rad57 to assemble meiotic recombination complexes. Genes Dev. Cold Spring Harbor Lab; 1998;12: 2208–2221. doi:10.1101/gad.12.14.2208

84. Cao L, Alani E, Kleckner N. A pathway for generation and processing of double-strand breaks during meiotic recombination in S. cerevisiae. Cell. 1990;61: 1089–1101.

85. Shinohara M, Shinohara A. Multiple pathways suppress non-allelic homologous recombination during meiosis in Saccharomyces cerevisiae. PLoS ONE. 2013;8: e63144. doi:10.1371/journal.pone.0063144

86. Oh SD, Jessop L, Lao JP, Allers T, Lichten M, Hunter N. Stabilization and electrophoretic analysis of meiotic recombination intermediates in

Saccharomyces cerevisiae. Methods Mol Biol. Totowa, NJ: Humana Press; 2009;557: 209–234. doi:10.1007/978-1-59745-527-5_14

87. Hong S, Sung Y, Yu M, Lee M, Kleckner N, Kim KP. The Logic and Mechanism of Homologous Recombination Partner Choice. Molecular Cell. Elsevier Inc; 2013;51: 440–453. doi:10.1016/j.molcel.2013.08.008

88. Lao JP, Cloud V, Huang C-C, Grubb J, Thacker D, Lee C-Y, et al. Meiotic Crossover Control by Concerted Action of Rad51-Dmc1 in Homolog Template Bias and Robust Homeostatic Regulation. Lichten M, editor. PLoS Genet. 2013;9: e1003978–22. doi:10.1371/journal.pgen.1003978

89. Dresser ME, Ewing DJ, Conrad MN, Dominguez AM, Barstead R, Jiang H, et al. DMC1 functions in a Saccharomyces cerevisiae meiotic pathway that is largely independent of the RAD51 pathway. Genetics. Genetics Society of America; 1997;147: 533–544.

90. Bishop DK. Rad51, the lead in mitotic recombinational DNA repair, plays a supporting role in budding yeast meiosis. Cell Cycle. 2012;11: 4105–4106. doi:10.4161/cc.22396

91. Masson JY, Davies AA, Hajibagheri N, Van Dyck E, Benson FE, Stasiak AZ, et al. The meiosis-specific recombinase hDmc1 forms ring structures and interacts with hRad51. EMBO J. EMBO Press; 1999;18: 6552–6560. doi:10.1093/emboj/18.22.6552

92. Tarsounas M, Morita T, Pearlman RE, Moens PB. RAD51 and DMC1 form mixed complexes associated with mouse meiotic chromosome cores and synaptonemal complexes. J Cell Biol. Rockefeller University Press; 1999;147: 207–220. doi:10.1083/jcb.147.2.207

93. Siaud N, Dray E, Gy I, Gérard E, Takvorian N, Doutriaux M-P. Brca2 is involved in meiosis in Arabidopsis thaliana as suggested by its interaction with Dmc1. EMBO J. EMBO Press; 2004;23: 1392–1401. doi:10.1038/sj.emboj.7600146

94. Shinohara M, Gasior SL, Bishop DK, Shinohara A. Tid1/Rdh54 promotes colocalization of rad51 and dmc1 during meiotic recombination. Proc Natl Acad Sci USA. National Academy of Sciences; 2000;97: 10814–10819. doi:10.1073/pnas.97.20.10814

95. Shan Q, Bork JM, Webb BL, Inman RB, Cox MM. RecA protein filaments: end-dependent dissociation from ssDNA and stabilization by RecO and RecR proteins. J Mol Biol. 1997;265: 519–540. doi:10.1006/jmbi.1996.0748

96. Sung P. Yeast Rad55 and Rad57 proteins form a heterodimer that functions with replication protein A to promote DNA strand exchange by Rad51

recombinase. Genes Dev. Cold Spring Harbor Lab; 1997;11: 1111–1121. doi:10.1101/gad.11.9.1111

97. Liu J, Renault L, Veaute X, Fabre F, Stahlberg H, Heyer W-D. Rad51 paralogues Rad55-Rad57 balance the antirecombinase Srs2 in Rad51 filament formation. Nature. 2011;479: 245–248. doi:10.1038/nature10522

98. Shinohara M, Shita-Yamaguchi E, Buerstedde JM, Shinagawa H, Ogawa H, Shinohara A. Characterization of the roles of the Saccharomyces cerevisiae RAD54 gene and a homologue of RAD54, RDH54/TID1, in mitosis and meiosis. Genetics. 1997;147: 1545–1556.

99. Oh SD, Lao JP, Hwang PY-H, Taylor AF, Smith GR, Hunter N. BLM ortholog, Sgs1, prevents aberrant crossing-over by suppressing formation of multichromatid joint molecules. Cell. 2007;130: 259–272. doi:10.1016/j.cell.2007.05.035

100. Kaur H, De Muyt A, Lichten M. Top3-Rmi1 DNA single-strand decatenase is integral to the formation and resolution of meiotic recombination intermediates. Molecular Cell. 2015;57: 583–594. doi:10.1016/j.molcel.2015.01.020

101. Tang S, Wu MKY, Zhang R, Hunter N. Pervasive and essential roles of the Top3-Rmi1 decatenase orchestrate recombination and facilitate chromosome segregation in meiosis. Molecular Cell. 2015;57: 607–621. doi:10.1016/j.molcel.2015.01.021

102. Cejka P, Plank JL, Bachrati CZ, Hickson ID, Kowalczykowski SC. Rmi1 stimulates decatenation of double Holliday junctions during dissolution by Sgs1-Top3. Nat Struct Mol Biol. 2010;17: 1377–1382. doi:10.1038/nsmb.1919

103. Fasching CL, Cejka P, Kowalczykowski SC, Heyer W-D. Top3-Rmi1 dissolve Rad51-mediated D loops by a topoisomerase-based mechanism. Molecular Cell. 2015;57: 595–606. doi:10.1016/j.molcel.2015.01.022

104. Piazza A, Shah SS, Wright WD, Gore SK, Koszul R, Heyer W-D. Dynamic Processing of Displacement Loops during Recombinational DNA Repair. Molecular Cell. 2019;73: 1255–1266.e4. doi:10.1016/j.molcel.2019.01.005

105. Piazza A, Wright WD, Heyer W-D. Multi-invasions Are Recombination Byproducts that Induce Chromosomal Rearrangements. Cell. 2017;170: 760–773.e15. doi:10.1016/j.cell.2017.06.052

106. Piazza A, Heyer W-D. Multi-Invasion-Induced Rearrangements as a Pathway for Physiological and Pathological Recombination. Bioessays. 2018;40: e1700249. doi:10.1002/bies.201700249

107. Oh SD, Lao JP, Taylor AF, Smith GR, Hunter N. RecQ helicase, Sgs1, and XPF family endonuclease, Mus81-Mms4, resolve aberrant joint molecules during meiotic recombination. Molecular Cell. 2008;31: 324–336. doi:10.1016/j.molcel.2008.07.006

108. Jessop L, Lichten M. Mus81/Mms4 endonuclease and Sgs1 helicase collaborate to ensure proper recombination intermediate metabolism during meiosis. Molecular Cell. 2008;31: 313–323. doi:10.1016/j.molcel.2008.05.021

109. De Muyt A, Jessop L, Kolar E, Sourirajan A, Chen J, Dayani Y, et al. BLM helicase ortholog Sgs1 is a central regulator of meiotic recombination intermediate metabolism. Molecular Cell. 2012;46: 43–53. doi:10.1016/j.molcel.2012.02.020

110. Piazza A, Heyer W-D. Moving forward one step back at a time: reversibility during homologous recombination. Current Genetics. Springer Berlin Heidelberg; 2019;: 1–8. doi:10.1007/s00294-019-00995-7

111. Forget AL, Kowalczykowski SC. Single-molecule imaging of DNA pairing by RecA reveals a three-dimensional homology search. Nature. Nature Publishing Group; 2012;482: 423–427. doi:10.1038/nature10782

112. Wright WD, Heyer W-D. Rad54 functions as a heteroduplex DNA pump modulated by its DNA substrates and Rad51 during D loop formation. Molecular Cell. 2014;53: 420–432. doi:10.1016/j.molcel.2013.12.027

Supplemental figures

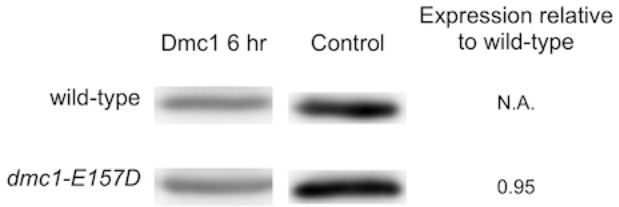


**Supplemental Figure 3.1** *DMC1* expression for wild-type, *dmc1-E157D*. Left column, W. blot against Dmc1 for 5μL sample prepared from meiotic yeast cultures at 6 hours as described in Methods Section for each strain. Control column is 20 ng purified Dmc1 protein that was run in parallel with sample and used to quantitate blots. Sample concentration is estimated concentration in comparison to 20 ng purified Dmc1 protein. Similar results were obtained from an independent meiotic time course. Strains used in this experiment in the order in which they appear in figure, top to bottom: DKB3698, DKB6342.

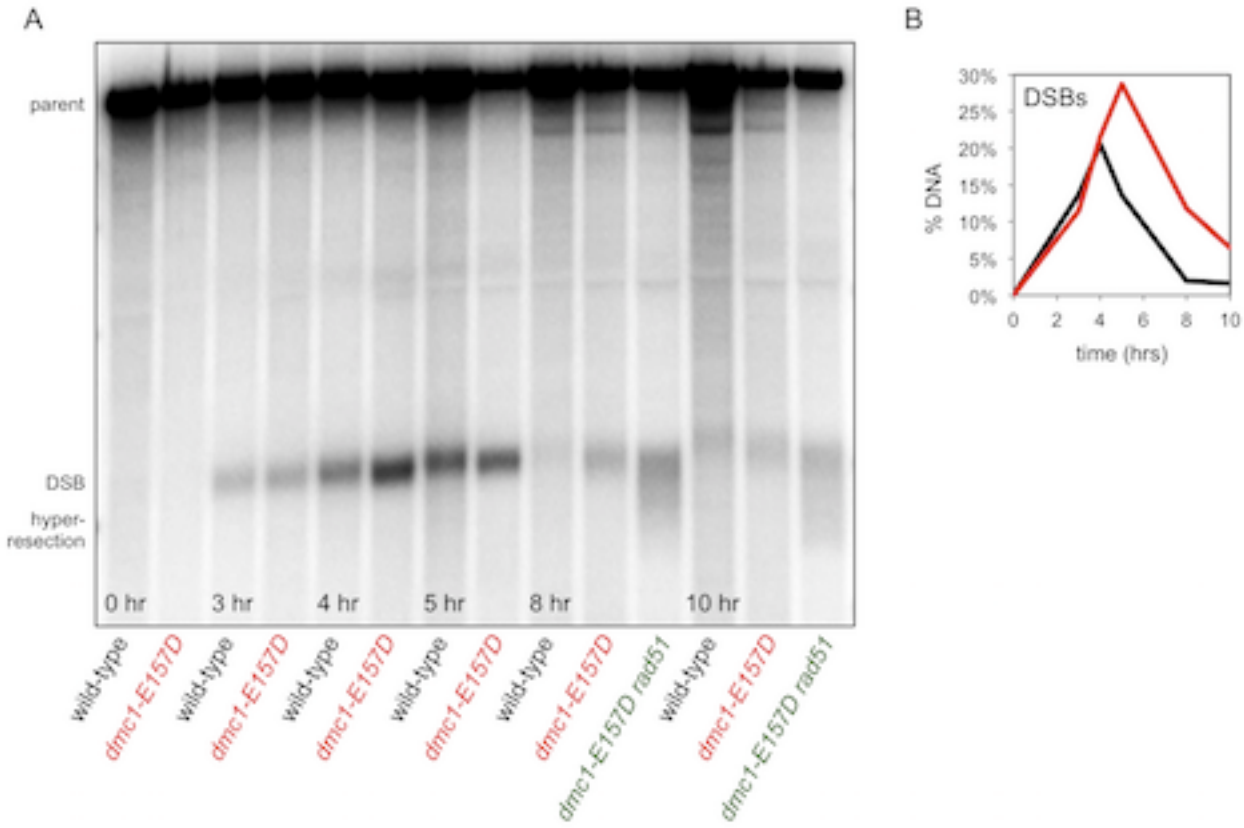


**Supplemental Figure 3.2** Additional Southern blot analysis at the *HIS4::LEU2* hotspot. (a) Southern blot analysis at the *HIS4::LEU2* hotspot following digestion of genomic DNA from meiotic time course experiments with PstI. Time points and strains are indicated beneath each lane. Note that *dmc1-E157D rad51* is shown at late time points as a reference for hyper-resection. (b) Quantitation of 1D gels shown in (a); black –

**Supplemental Figure 3.2 (continued)** wild-type, red – *dmc1-E157D.* Strains used in experiments in the order in which they appear in figure, right to left: DKB3698, DKB6342, DKB6393.

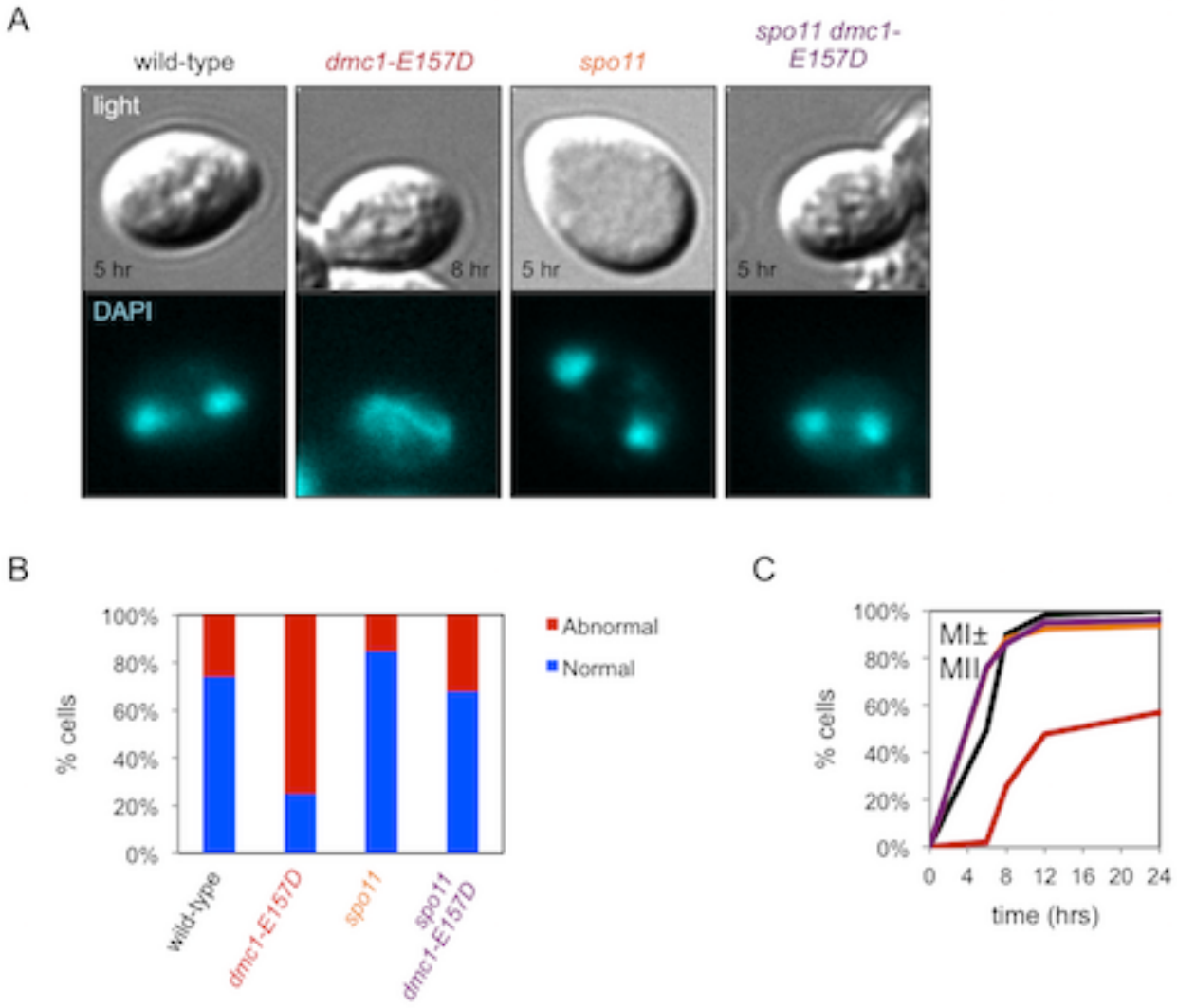


**Supplemental Figure 3.3** *spo11* suppresses the meiotic progression defect associated with *dmc1-E157D*. (a) Representative images showing MI segregation in the strains indicated. (b) Quantitation of MI division defects observed in the strains indicated. A "normal" division is defined as having two equally-sized and well-defined DAPI staining bodies, whereas an "abnormal" division is defined as having unequal DAPI bodies or DNA connecting the two DAPI bodies. (c) Meiotic progression data for strains indicated. For each time point, ≥50 cells were scored. Strains used in this experiment in the order in which they appear in figure, top to bottom: DKB3698, DKB2123, DKB6342, DKB6419.

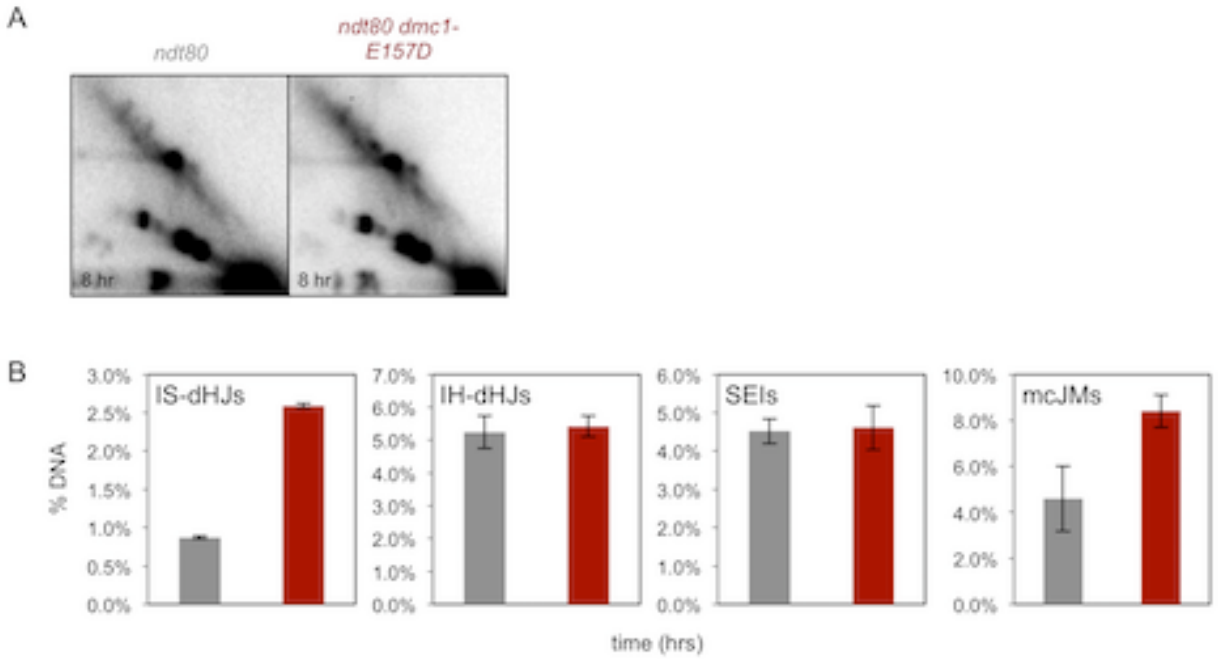


**Supplemental Figure 3.4** JMs accumulate at the *HIS4::LEU2* recombination hotspot in the absence of *ndt80*. (a) Southern analysis at the *HIS4::LEU2* hotspot at 8 hours following 2D gel electrophoresis. (b) 2D gel quantitation; dark gray – *ndt80*, dark red – *ndt80 dmc1-E157D*. Quantitation for each strain represents an average of two independently cultured diploids. Strains used in this experiment in the order in which they appear in figure, right to left: DKB3689, DKB3428, DKB6676, DKB6682.

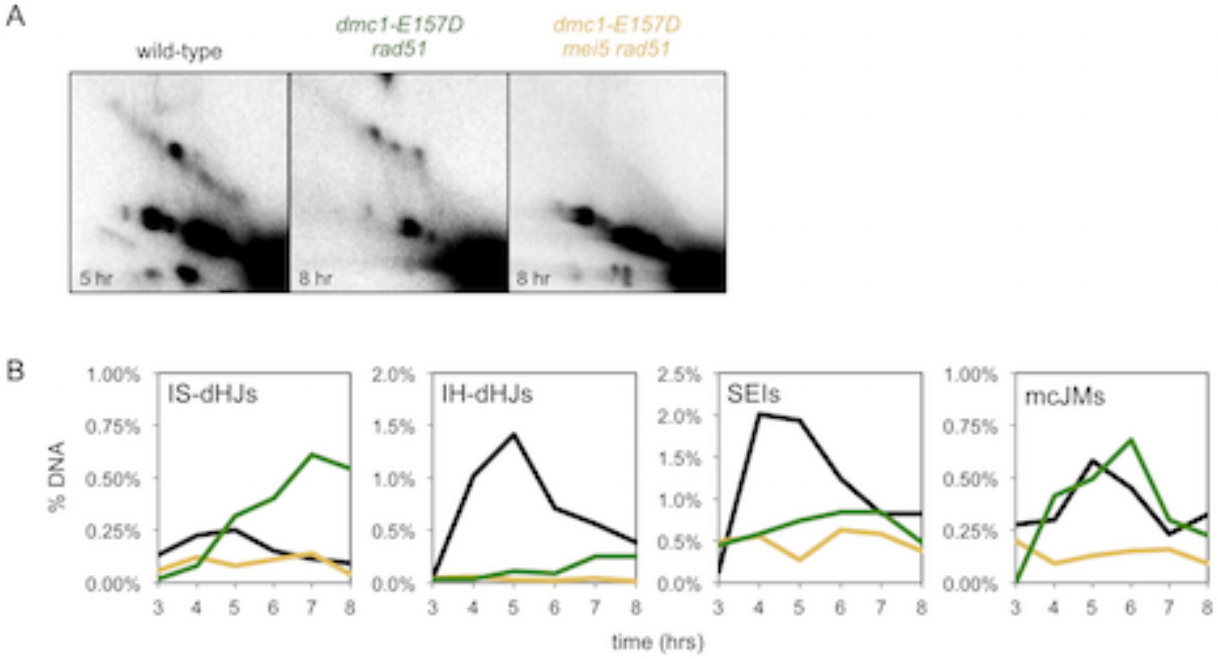


**Supplemental Figure 3.5** Duplicate meiotic time course experiments for *dmc1-E157D rad51* and *dmc1-E157D mei5 rad51*. For *dmc1-E157D mei5 rad51*, two independently

**Supplemental Figure 3.5 (continued)** derived diploids were used. (a) Southern analysis at the *HIS4::LEU2* hotspot from meiotic time course experiments following 2D gel electrophoresis. Time point for representative image is shown in the bottom left corner. (b) 2D gel quantitation; black – wild-type, dark green – *dmc1-E157D rad51*, yellow – *dmc1-E157D mei5 rad51.* Strains used in this experiment in the order in which they appear in figure, right to left: DKB3698, DKB6393, DKB6413.

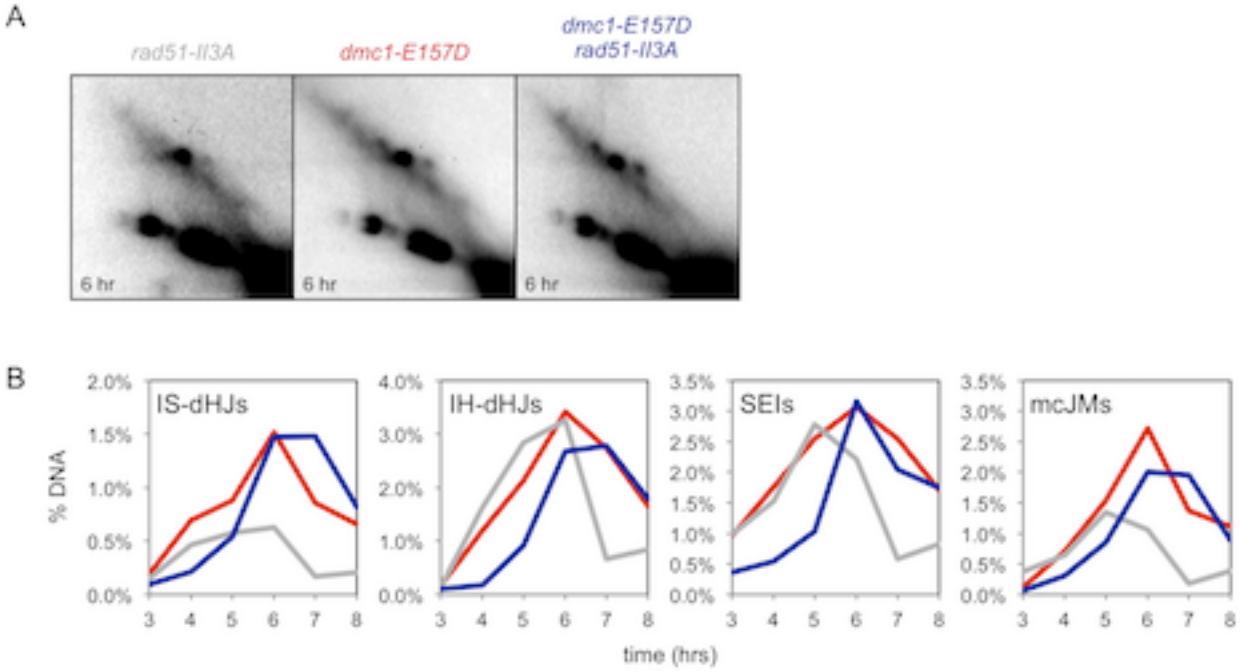


**Supplemental Figure 3.6** The defects associated with *dmc1-E157D rad51* are independent of Rad51's catalytic activity. (a) Southern analysis at the *HIS4::LEU2* hotspot from meiotic time course experiments following 2D gel electrophoresis. Time point for representative image is shown in the bottom left corner. (b) 2D gel quantitation; gray – *rad51-II3A*, red – *dmc1-E157D*, dark blue – *dmc1-E157D rad51-II3A*. Strains used in this experiment in the order in which they appear in figure, right to left: DKB3689, DKB6342, DKB6400.

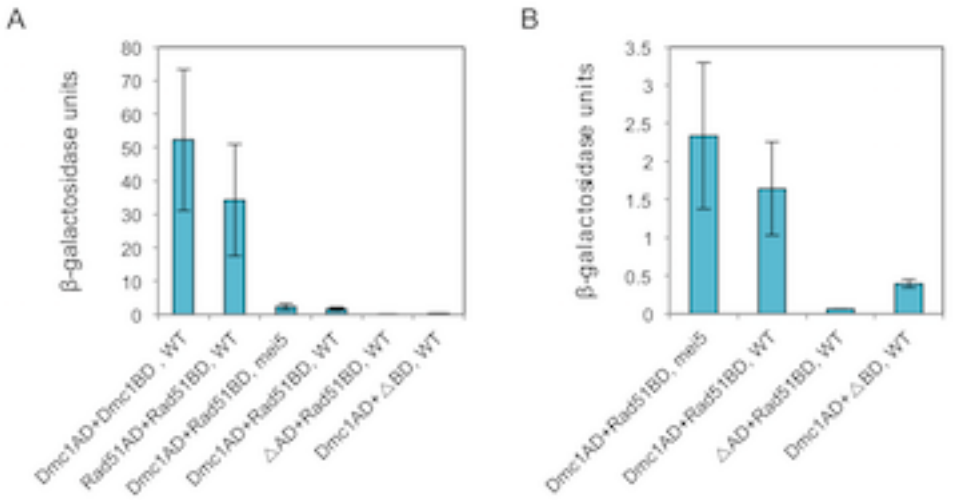


**Supplemental Figure 3.7** Meiotic two-hybrid analysis detects a weak interaction between Rad51 and Dmc1 that is independent of Mei5. (a) All interactions examined are plotted. (b) Subset of the same data shown in (a) to facilitate comparison of measurements of the Rad51-Dmc1 interaction with empty vector controls. The difference between Dmc1AD+Rad51BD *mei5* and Dmc1AD+Rad51BD WT (wild-type) is not statistically significant (p = 0.5 using a Wilcoxon signed-rank test). ΔBD and ΔAD represent the empty vectors. Strains used in this experiment: DKB6501, DKB6503, DKB6508, DKB6509, DKB6513, DKB6515.

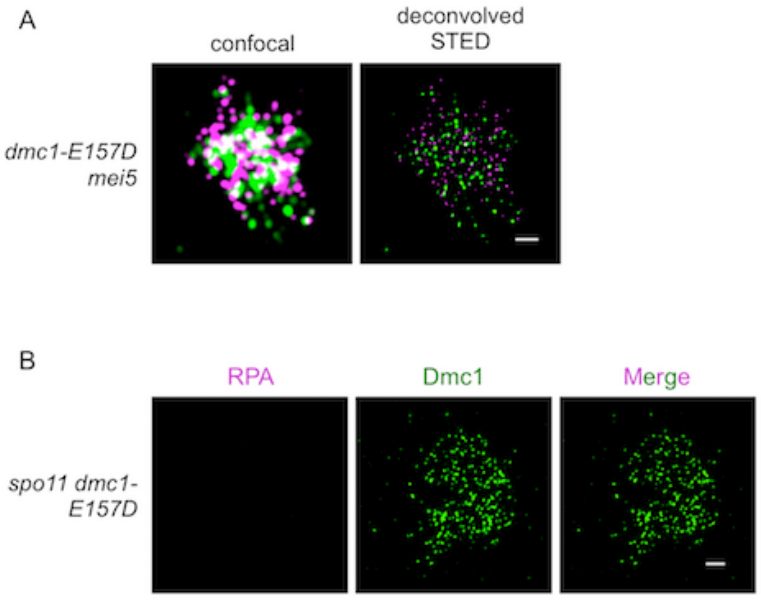


**Supplemental Figure 3.8** Super-resolution imaging resolves closely spaced foci, but elongated Dmc1 foci still form in *spo11 dmc1-E157D*. (a) Spread meiotic nuclei prepared from a *dmc1-E157D mei5* 5 hour sample imaged using confocal and STED microscopy methods. (b) STED imaging of a *spo11 dmc1-E157D* spread meiotic nuclei at 5 hours. For both, scale bar represents 1 micrometer. Red, RPA, green, Dmc1.

**Supplemental Figure 3.8 (continued)** Strains used in this experiment: DKB6300, DKB6419.

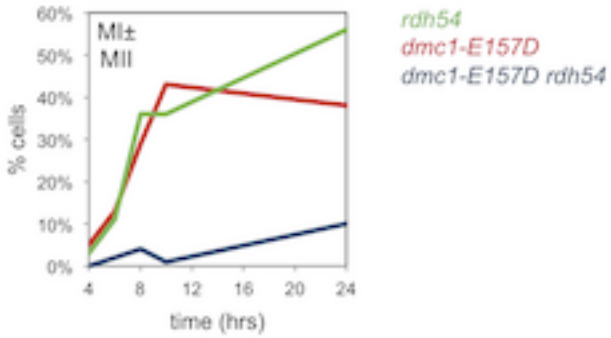


**Supplemental Figure 3.9** *dmc1-E157D rdh54* is more defective in meiotic progression than either of the single mutants, *dmc1-E157D* and *rdh54*. Meiotic progression data for strains indicated. For each time point, ≥100 cells were scored. Strains used in this experiment in the order in which they appear in figure, top to bottom: DKB2526, DKB6342, DKB6583.

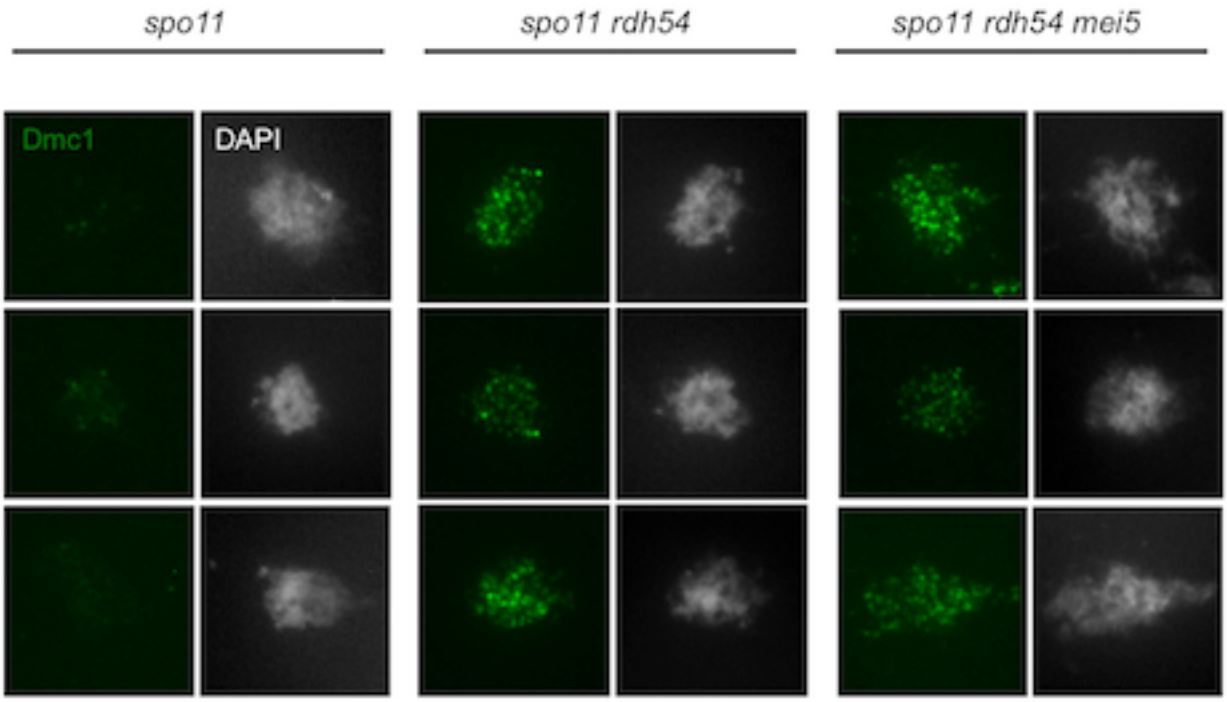


**Supplemental Figure 3.10** DSB-independent Dmc1-WT focus formation does not require Mei5. Samples were collected 4 hours after induction of meiosis in liquid medium and immunostained for Dmc1 and Hop2. Because Hop2 staining is Spo11 independent and specific for meiotic prophase, random prophase nuclei were selected on the basis of being Hop2 positive and then imaged for Dmc1 staining. 50 nuclei were examined for each sample with 3 representative nuclei shown for each of the three strains examined. Images were generated by wide-field microscopy using the same

**Supplemental Figure 3.10 (continued)** camera settings for all strains. Strains used in this experiment in the order in which they appear in figure, top to bottom: DKB2524, DKB2523, and DKB6571.

# Chapter 4: Biochemical attributes of Dmc1-E157D, a hyper-recombinant Dmc1 mutant that bypasses Mei5-Sae3

*Yuen-Ling Chan provided instruction and supervision to me as I purified Dmc1-E157D and ran D-loop assays. Additionally, she purified many of the proteins that were used in the D-loop assay.

## 4.1 Chapter overview

In the previous chapter, a *dmc1* mutant that bypasses Mei5-Sae3 was characterized through genetic and cytological analysis *in vivo*. In this chapter, the expression and purification of this Dmc1 mutant from *Escherichia coli* is described. Using D-loop assays to reconstitute strand invasion *in vitro*, we show that this Dmc1 mutant is hyper-recombinant and that it preferentially forms abnormal structures known as multi-invasions. Though this data is preliminary, this biochemical analysis provides evidence that a Dmc1 mutant that generates increased IS-dHJs, mcJMs, and ectopic COs also forms more multi-invasions *in vitro*, correlating these two distinct genetic and biochemical observations for the first time.

## 4.2 Introduction

RecA and RecA homologs Rad51 and Dmc1 are DNA-dependent ATPases, however ATP hydrolysis is not required to catalyze the strand invasion reaction [1-3]. Instead, ATP binding induces a conformational change in the protein, converting it to an active, high affinity form [4,5].

We demonstrated that the *dmc1-E157D* allele would bypass Dmc1 accessory factor Mei5-Sae3. *dmc1-E157D* is modeled on the *recA* mutant *recA-E96D* [6-8]. The *recA-E96D* mutation is located in the protein's ATPase domain, where it shortens a critical amino acid side chain, thereby increasing the distance between the water molecule that will act as the nucleophile in the hydrolysis reaction and the activating carboxylate, leading to a significantly diminished rate of ATP hydrolysis [6,7]. Because ATP hydrolysis is diminished in this mutant, RecA-E96D displays a higher affinity for both ss- and dsDNA [7,8], and, as a consequence, forms off-pathway foci on undamaged DNA [8]. However, in spite of these deficiencies, RecA-E96D is still competent to carry out strand exchange [7,8].

Given that RecA and Dmc1 have high sequence identity to one another [9], and that the ATPase site in particular is highly conserved, we predicted that Dmc1-E157D would also have a reduced rate of ATP hydrolysis. Like its prokaryotic counterpart, Dmc1-E157D also forms foci independent of DSB formation, but is competent carry out strand exchange. Moreover, *dmc1-E157D* bypasses the requirement for Mei5-Sae3 *in vivo*, and biochemical studies of Mei5-Sae3 homolog Swi5-Sfr1 suggests that it promotes ADP release to maintain filaments in the active, ATP-bound form [10-12]. It makes sense that a mutant with a dramatically reduced rate of ATP hydrolysis would be able to act independently of such a factor because ADP release is not required if no ATP is hydrolyzed. Lastly, using super-resolution imaging we observed that *dmc1-E157D* forms longer Dmc1 foci *in vivo*. We hypothesize that filaments may be longer because ATP promotes cooperative binding by RecA/Rad51/Dmc1 protomers, leading

to the formation of longer filaments *in vitro* [13,14]. Taken together, our results suggest that Dmc1-E157D is also defective in ATP hydrolysis.

However, our *in vivo* analysis of *dmc1-E157D* also revealed an unexpected result: by 2D gel electrophoresis, *dmc1-E157D* forms more IS-dHJs, mcJMs, and ectopic COs than wild-type, with no decrease in IH-dHJs or SEIs, making it hyper-recombinant for certain joint molecule species. Interestingly, this same phenotype has been observed in meiotic cells in the absence of Sgs1, Top3, and Rmi1 [15-17]. Sgs1, Top3, and Rmi1 together form a complex, Sgs1-Top3-Rmi1, that is involved in disassembling nascent D-loops in somatic cells [18,19]. Related to this function, it is also known to dismantle abnormal recombination events involving more than one donor, or so-called “multi-invasions” [20]. Multi-invasions form when a broken DNA end encounters and invades two distinct regions of homologous dsDNA.

It had been postulated that the abnormal meiotic phenotypes associated with the *sgs1*, *top3*, and *rmi1* mutants were related to its somatic role in disassembling multi-invasions [17,21]. In this model, the formation of a multi-invasion between a broken strand at the *HIS4::LEU2* meiotic DSB hotspot and two donors, one at the allelic site and one at the ectopic site, would lead to an increase in ectopic COs. Given that there is only one sister, this multi-invasion would likely involve at least one if not both homologous chromatids, thereby leaving the total level of IH-dHJs formed unchanged. However, resolution of aberrant multi-invasion intermediate by nucleolytic processing would lead to the formation of secondary one-ended DSBs. Repair of these one-ended DSBs would require the formation of an IS-dHJ. We thus aimed to determine whether

the aberrant recombination phenotypes associated with *dmc1-E157D* could be explained by an increased tendency of the protein to form multi-invasions.

Multi-invasions can be detected in somatic cells through use of a proximity ligation based assay (the multi-invasion capture assay), but their formation can also be observed *in vitro* in D-loop reactions if a long ssDNA oligonucleotide is used to form the Rad51/Dmc1 filament [20,22,23]. Because the multi-invasion capture assay has not yet been validated in meiotic cells, we instead sought to determine whether Dmc1-E157D forms more multi-invasion in D-loop assays. Our results show that indeed these genetic and biochemical properties are correlated, at least in the context of Dmc1-E157D-promoted recombination.

## 4.3 Results

### 4.3.1 Purification of Dmc1-E157D from *Escherichia coli*

Expression of both wild-type Dmc1 (Dmc1-WT) and RecA-E96D is toxic to *E. coli* [7,24]. Therefore, we expected that expression and purification of Dmc1-E157D from *E. coli* could be problematic. Briefly, using quick-change PCR, the E157D mutation was introduced into *DMC1* overexpression plasmid pNRB150, generating plasmid pNRB756, and this plasmid was introduced into the *E. coli* strain Rosetta(DE3)pLysS [24]. The next day, single colonies were inoculated in 3 milliliters media, *dmc1-E157D* expression was induced by addition of IPTG, samples were collected after 1.5 hours, and whole cell lysate was prepared and run on a SDS polyachrylamide gel (Figure 4.1a). As expected, a prominent 37 kDa band was observed in samples in which IPTG had been added and

was fainter in samples lacking IPTG. We conclude that under these conditions, Dmc1-E157D is sufficiently expressed in Rosetta(DE3)pLysS *E. coli.*

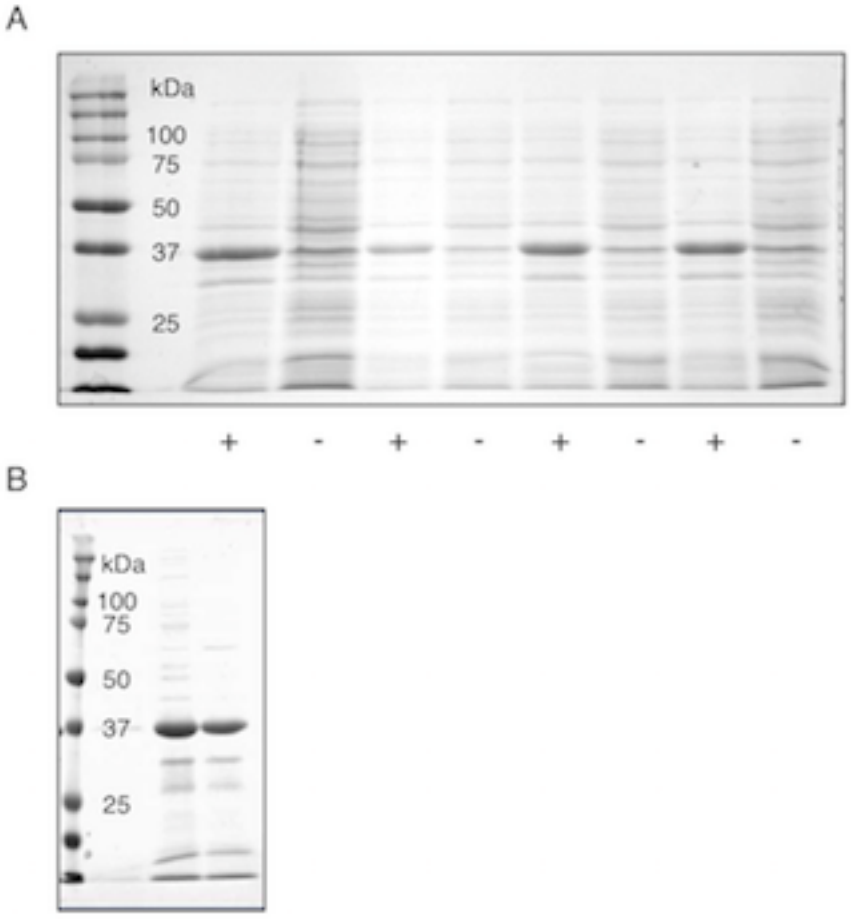


**Figure 4.1** Expression and purification of Dmc1-E157D from *Escherichia coli.* (a) Whole cell lysate prepared from Rosetta(DE3)pLysS *E. coli* was run out on a 12% SDS-PAGE and stained with Coomassie Brilliant Blue. *dmc1-E157D* is overexpressed from the plasmid pNRB576, as described previously [2]. (+) and (-) indicate with and without added IPTG to induce expression. Dmc1 is a 37 kDa protein. (b) Purified Dmc1-E157D was run out on a 12% SDS-PAGE and stained with Coomassie Brilliant Blue.

Dmc1-E157D was then purified using methods described previously (Figure 4.1b) [2,24]. Because we were initially unable to purify full-length protein, we modified the method to decrease the growing time and prevent degradation of the protein (see Chapter 2).

### 4.3.2 Dmc1-E157D is hyper-recombinant in *in vitro* D-loop assays and forms more multi-invasions than Dmc1-WT

Next, we tested Dmc1-E157D for its capacity to perform strand invasion in a D-loop assay stimulated by Hop2-Mnd1 and Rdh54 (Figure 4.2a). Addition of Hop2-Mnd1 to Dmc1-WT-mediated D-loop reactions greatly increases yield [25], and Rdh54 was previously observed to promote the formation of multi-invasions by Dmc1-WT *in vitro* [23]. Consistent with our *in vivo* results, total D-loop formation by Dmc1-E157D was markedly higher than Dmc1-WT (Figure 4.2b,c). In the experiment, the activity of Dmc1-WT was not optimal. However, in previously published D-loop assays using RPA, Dmc1-WT, Hop2-Mnd1, and Rdh54, the activity of Dmc1-WT was at least half of what was seen in this experiment for Dmc1-E157D [23]. Moreover, whereas in this experiment, Dmc1-WT forms ~18 primary D-loops to every multi-invasion, this ratio is dramatically reduced for Dmc1-E157D, which forms ~1.6 primary D-loops to every multi-invasion.

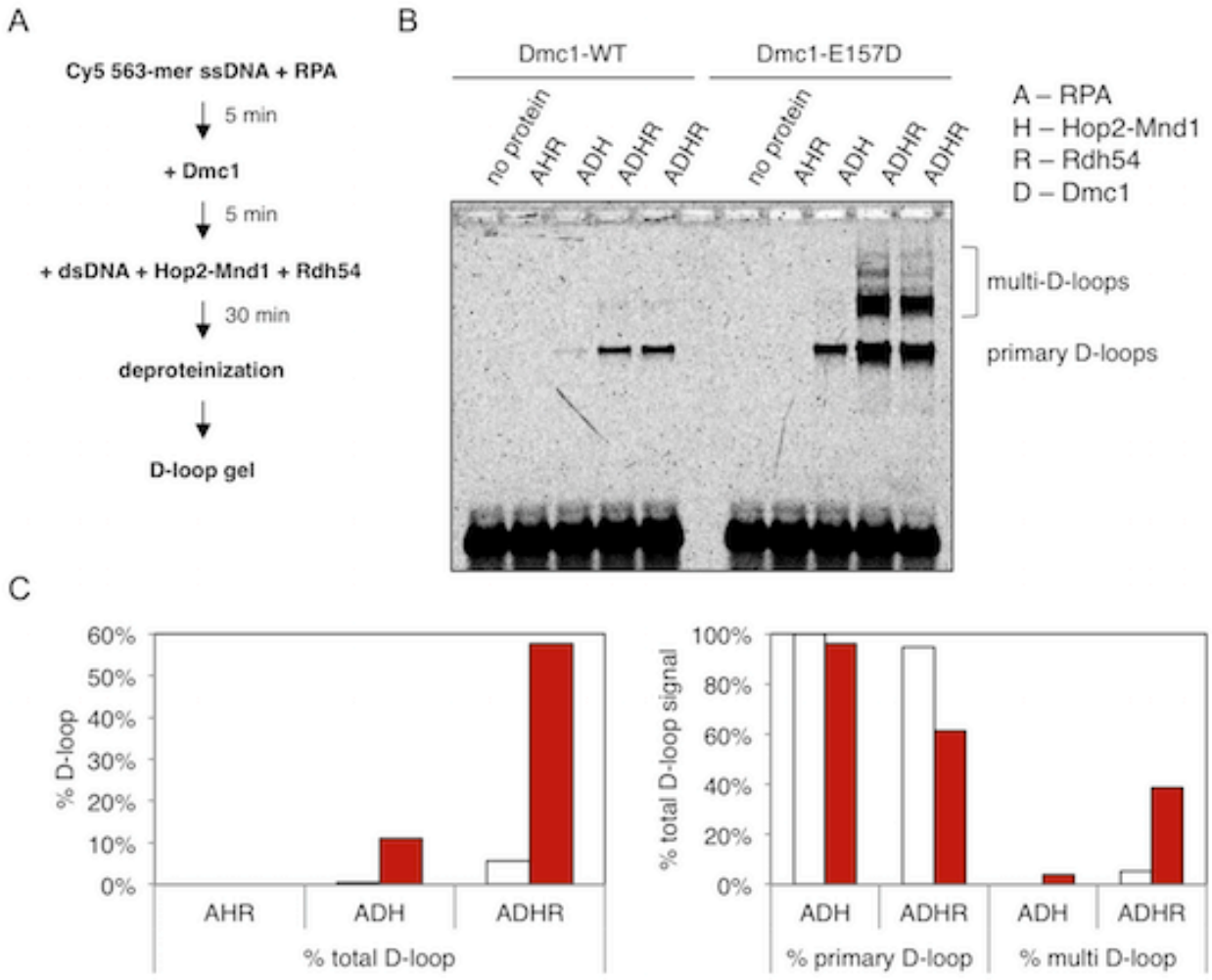


**Figure 4.2** Dmc1-E157D is hyper-recombinant and forms proportionally more multi-invasions in D-loop assays. (a) Reaction scheme as described previously [24]. (b) D-loop formation by Dmc1-WT and Dmc1-E157D, stimulated by RPA, Hop2-Mnd1, and Rdh54 (Tid1). (c) Quantitation of D-loop formation shown in (b) shown as the total number of D-loops formed (left), and as the percentage of multi-invasion D-loops out of the total signal (right). Dmc1-WT (white), Dmc1-E157D (red).

Further experiments are required to validate these preliminary results. In addition to D-loop assays, we will use ATPase assays to determine whether Dmc1-E157D's rate of ATP hydrolysis is reduced relative to Dmc1-WT, and we will directly visualize Dmc1-WT and Dmc1-E157D filaments by electron microscopy to determine whether Dmc1-E157D forms longer filaments.

## 4.4 Conclusions

We have obtained preliminary evidence that Dmc1-E157D is hyper-recombinant *in vitro*, complementing our genetic observations and supporting our model that the defects conferred by the mutant protein *in vivo* reflect the tendency to form multi-invasion D-loops (Figure 4.3b,c). Based on previous work by the Hunter, Lichten, and Heyer labs [16,17,20,21], we predicted that the aberrant formation of recombination intermediates and products observed in the *dmc1-E157D* background by 1D and 2D gel electrophoresis was caused by an increased tendency of the protein to form multi-invasions. *In vitro* reconstitution of Dmc1-E157D-mediated D-loop formation substantiates this prediction. The fact that we observed only a ~3-fold increase in IS-dHJs, mcJMs, and ectopic COs for *dmc1-E157D in vivo*, but an ~11-fold increase in multi-invasion formation in reconstitution experiments could be interpreted to mean that *in vivo*, the pathways that disassemble multi-invasions are active, but that they become overwhelmed by the large number of aberrant multi-invasions created by Dmc1-E157D. Consistent with this inference, spore formation was nearly absent in a *dmc1-E157D sgs1* double mutant (data not shown).

A critical element of our model is that Dmc1-E157D's tendency to form multi-invasions is caused by an increase in the average length of Dmc1-E157D filaments relative to Dmc1-WT. While we were able to directly observe Dmc1-E157D filaments by electron microscopy (data not shown), further analysis is required to determine whether Dmc1-E157D filaments are on average longer than those formed by Dmc1-WT.

References


1. Sung P, Stratton SA. Yeast Rad51 recombinase mediates polar DNA strand exchange in the absence of ATP hydrolysis. Journal of Biological Chemistry. American Society for Biochemistry and Molecular Biology; 1996;271: 27983–27986. doi:10.1074/jbc.271.45.27983

2. Hong EL, Shinohara A, Bishop DK. Saccharomyces cerevisiae Dmc1 protein promotes renaturation of single-strand DNA (ssDNA) and assimilation of ssDNA into homologous super-coiled duplex DNA. Journal of Biological Chemistry. 2001;276: 41906–41912. doi:10.1074/jbc.M105563200

3. Morgan EA, Shah N, Symington LS. The requirement for ATP hydrolysis by Saccharomyces cerevisiae Rad51 is bypassed by mating-type heterozygosity or RAD54 in high copy. Mol Cell Biol. 2002;22: 6336–6343. doi:10.1128/mcb.22.18.6336-6343.2002

4. Kowalczykowski SC. An Overview of the Molecular Mechanisms of Recombinational DNA Repair. Cold Spring Harb Perspect Biol. 2015;7. doi:10.1101/cshperspect.a016410

5. Robertson RB, Moses DN, Kwon Y, Chan P, Chi P, Klein H, et al. Structural transitions within human Rad51 nucleoprotein filaments. Proc Natl Acad Sci USA. National Academy of Sciences; 2009;106: 12688–12693. doi:10.1073/pnas.0811465106

6. Campbell MJ, Davis RW. On the in vivo function of the RecA ATPase. J Mol Biol. 1999;286: 437–445. doi:10.1006/jmbi.1998.2457

7. Campbell MJ, Davis RW. Toxic mutations in the recA gene of E. coli prevent proper chromosome segregation. J Mol Biol. 1999;286: 417–435. doi:10.1006/jmbi.1998.2456

8. Gataulin DV, Carey JN, Li J, Shah P, Grubb JT, Bishop DK. The ATPase activity of E. coli RecA prevents accumulation of toxic complexes formed by erroneous binding to undamaged double stranded DNA. Nucleic Acids Res. 2018;46: 9510–9523. doi:10.1093/nar/gky748

9. Masson JY, West SC. The Rad51 and Dmc1 recombinases: a non-identical twin relationship. Trends Biochem Sci. 2001;26: 131–136.

10. Haruta N, Kurokawa Y, Murayama Y, Akamatsu Y, Unzai S, Tsutsui Y, et al. The Swi5-Sfr1 complex stimulates Rhp51/Rad51- and Dmc1-mediated DNA strand exchange in vitro. Nat Struct Mol Biol. 2006;13: 823–830. doi:10.1038/nsmb1136

11. Su G-C, Chung C-I, Liao C-Y, Lin S-W, Tsai C-T, Huang T, et al. Enhancement of ADP release from the RAD51 presynaptic filament by the SWI5-SFR1 complex.

Nucleic Acids Res. 2014;42: 349–358. doi:10.1093/nar/gkt879

12. Lu C-H, Yeh H-Y, Su G-C, Ito K, Kurokawa Y, Iwasaki H, et al. Swi5-Sfr1 stimulates Rad51 recombinase filament assembly by modulating Rad51 dissociation. Proc Natl Acad Sci USA. National Academy of Sciences; 2018;115: E10059–E10068. doi:10.1073/pnas.1812753115

13. Conway AB, Lynch TW, Zhang Y, Fortin GS, Fung CW, Symington LS, et al. Crystal structure of a Rad51 filament. Nat Struct Mol Biol. 2004;11: 791–796. doi:10.1038/nsmb795

14. Galkin VE, Wu Y, Zhang X-P, Qian X, He Y, Yu X, et al. The Rad51/RadA N-terminal domain activates nucleoprotein filament ATPase activity. Structure. 2006;14: 983–992. doi:10.1016/j.str.2006.04.001

15. Oh SD, Lao JP, Hwang PY-H, Taylor AF, Smith GR, Hunter N. BLM ortholog, Sgs1, prevents aberrant crossing-over by suppressing formation of multichromatid joint molecules. Cell. 2007;130: 259–272. doi:10.1016/j.cell.2007.05.035

16. Kaur H, De Muyt A, Lichten M. Top3-Rmi1 DNA single-strand decatenase is integral to the formation and resolution of meiotic recombination intermediates. Molecular Cell. 2015;57: 583–594. doi:10.1016/j.molcel.2015.01.020

17. Tang S, Wu MKY, Zhang R, Hunter N. Pervasive and essential roles of the Top3-Rmi1 decatenase orchestrate recombination and facilitate chromosome segregation in meiosis. Molecular Cell. 2015;57: 607–621. doi:10.1016/j.molcel.2015.01.021

18. Fasching CL, Cejka P, Kowalczykowski SC, Heyer W-D. Top3-Rmi1 dissolve Rad51-mediated D loops by a topoisomerase-based mechanism. Molecular Cell. 2015;57: 595–606. doi:10.1016/j.molcel.2015.01.022

19. Piazza A, Shah SS, Wright WD, Gore SK, Koszul R, Heyer W-D. Dynamic Processing of Displacement Loops during Recombinational DNA Repair. Molecular Cell. 2019;73: 1255–1266.e4. doi:10.1016/j.molcel.2019.01.005

20. Piazza A, Wright WD, Heyer W-D. Multi-invasions Are Recombination Byproducts that Induce Chromosomal Rearrangements. Cell. 2017;170: 760–773.e15. doi:10.1016/j.cell.2017.06.052

21. Piazza A, Heyer W-D. Multi-Invasion-Induced Rearrangements as a Pathway for Physiological and Pathological Recombination. Bioessays. 2018;40: e1700249. doi:10.1002/bies.201700249

22. Wright WD, Heyer W-D. Rad54 functions as a heteroduplex DNA pump modulated by its DNA substrates and Rad51 during D loop formation. Molecular Cell. 2014;53: 420–432. doi:10.1016/j.molcel.2013.12.027

23. Chan Y-L, Zhang A, Weissman BP, Bishop DK. RPA resolves conflicting activities of accessory proteins during reconstitution of Dmc1-mediated meiotic recombination. Nucleic Acids Res. 2019;47: 747–761. doi:10.1093/nar/gky1160

24. Chan Y-L, Bishop DK. Purification of Saccharomyces cerevisiae Homologous Recombination Proteins Dmc1 and Rdh54/Tid1 and a Fluorescent D-Loop Assay. Meth Enzymol. Elsevier; 2018;600: 307–320. doi:10.1016/bs.mie.2017.12.003

25. Chan Y-L, Brown MS, Qin D, Handa N, Bishop DK. The third exon of the budding yeast meiotic recombination gene HOP2 is required for calcium-dependent and recombinase Dmc1-specific stimulation of homologous strand assimilation. J Biol Chem. American Society for Biochemistry and Molecular Biology; 2014;289: 18076–18086. doi:10.1074/jbc.M114.558601

# Chapter 5: Perspectives and future directions

## 5.1 Chapter overview

The results presented in this thesis offer new insight into the roles of Dmc1 accessory factors Mei5-Sae3 and Rad51 in Dmc1-mediated recombination. Genetic and biochemical analysis of a *DMC1* mutant that bypasses Mei5-Sae3 showed that Mei5-Sae3 is not required for interhomolog (IH) bias, and that it affects Dmc1 filament formation and stability via a mechanism that is independent of Rad51. Moreover, the mutant forms longer filaments *in vivo*, and this is correlated with hyper-recombination and the formation of abnormal recombination intermediates and products, revealing an unexpected role for regulation of filament length in preventing aberrant recombination. Purification of the Dmc1 mutant and examination of its *in vitro* strand exchange activities confirmed and extended these results. This work thus provides a mechanistic understanding of the role of an important Dmc1 accessory factor, Mei5-Sae3, and sheds light on why filament lengths may be constrained in wild-type cells. Further research is required to determine the regulatory components that drive this pressure on filament lengths *in vivo*.

## 5.2 Dmc1 accessory factors in filament formation and stability

### 5.2.1 Mei5-Sae3 and Rad51 exert independent effects on Dmc1 filaments

Mei5-Sae3's importance to Dmc1-mediated strand exchange was established previously [1-3]. Mei5-Sae3 is required for Dmc1 focus formation in spread meiotic nuclei, and it stimulates Dmc1-loading onto RPA coated ssDNA [2-4]. Consistent with

these observations, no joint molecules and very limited recombination products are detected in *mei5*, *sae3*, and *mei5 sae3* meiotic samples [2,3,5]. From these observations, it was inferred that Mei5-Sae3 acts as a Dmc1 mediator.

Missing from this understanding of Mei5-Sae3's activity was mechanistic insight into how Mei5-Sae3 is able to promote Dmc1 filament formation and stability. One model hypothesized that Mei5-Sae3 may act by bridging Rad51 and Dmc1 filaments, thereby allowing Rad51 to act on Dmc1 filaments [6]. This model was motivated by (1) certain similarities between the *mei5*, *sae3*, and *rad51* mutants, such as reduced or absent focus formation, joint molecules, and COs; (2) the observations that Mei5-Sae3 interacts directly with Dmc1 [2] and may interact with Rad51 [7]; and (3) the observation that homo-typic interactions between Rad51/Dmc1 and itself are much stronger than hetero-typic interactions [8]. This model posits that Mei5-Sae3 and Rad51 cooperate to promote the formation and stability of Dmc1 filaments. In addition, it predicts that the defects associated with the *mei5* and *sae3* mutants stem largely from an inability for Dmc1 and Rad51.

Based on the data presented in Chapter 3, we can now reject this model. We have shown that a *dmc1* mutant that bypasses Mei5-Sae3 is still dependent on Rad51, which would not be predicted if the two proteins cooperated with one another to carry out a shared activity, though it is possible that the mutant behaves differently than wild-type in this regard. In addition, we have now shown that Dmc1 and Rad51 interact directly. In conjunction with previous observations, such as the fact that Mei5-Sae3 and Rad51 can each stimulate Dmc1-mediated D-loop activity in the absence of the other [9], and that Mei5-Sae3 appears to colocalize more with Dmc1 rather than Rad51 [2],

these data strongly suggest that the similarities seen in the phenotypes of *mei5*, *sae3*, and *rad51* mutants are related to the fact that the two factors function at the same stage in the recombination pathway (i.e. pre-synapsis). Thus Mei5-Sae3 and Rad51 share a relationship that is much like Rad51 accessory proteins Rad52 and Rad55-Rad57. Rad51 focus formation and recombination is defective in *rad52*, *rad55*, and *rad57* mutants [10,11], but each factor has a separate role in Rad51 filament formation and stability [12].

### 5.2.2 Architecture of meiotic pre-synaptic filaments

A detailed understanding of the architecture of Dmc1 presynaptic filaments would allow us to better understand how Mei5-Sae3 and Rad51 exert their distinct effects on Dmc1 filament formation and stability. In particular, it is not currently well understood how Mei5-Sae3 and Rad51 interact with Dmc1 filaments, such as whether they preferentially associate with one end of the filament to prevent dissociation, or whether they bind along the length of the filament. *In vivo* imaging suggests that Mei5-Sae3 may bind along the entire Dmc1 filament, given that Mei5-Sae3 and Dmc1 closely associate with one another by wide-filed microscopy, whereas Rad51 may act to “cap” one end, as analysis of spread meiotic nuclei by direct stochastic optical reconstruction microscopy (dSTORM) showed that the two proteins form side-by-side foci and do not occupy the same space on a strand of ssDNA [2,13].

Further insight into the architecture of Dmc1 filaments could be gained via *in vitro* assembly of Dmc1 filaments in the presence of RPA, Mei5-Sae3, and Rad51 as visualized with two complementary approaches, electron microscopy and super-resolution imaging. Whereas electron microscopy is higher resolution and therefore can

offer a more detailed structural understanding of how these factors interact with one another, it is limited in that it is difficult to distinguish each of the proteins from one another. Super-resolution imaging of the same filaments would complement this analysis, because all three factors can be visualized using this approach [13].

### 5.2.3 Mei5-Sae3 and Rad51 and IH bias

*Mei5-Sae3 is not required for IH bias*

We now know that Mei5-Sae3 is not required for IH bias. This conclusion is based on 2D gel electrophoresis analysis of the recombination intermediates that are formed in the *dmc1-E157D*, *dmc1-E157D mei5* and *dmc1-E157D rad51* backgrounds. While IS-dHJs are elevated in *dmc1-E157D*, there is no decrease in IH-dHJs, implying that IH-dHJs form normally. Loss of Rad51 leads to the formations of significantly more IS-dHJs, and there is a corresponding decrease in IH-dHJs. However, joint molecule formation in the *dmc1-E157D mei5* mutant is nearly indistinguishable from *dmc1-E157D*, indicating that the absence of Mei5 does not alter the ratio of IH- to IS-dHJs. Given that a widely accepted model for IH bias is that it is achieved through interactions between Dmc1 and its accessory factors, and that Mei5-Sae3 is important Dmc1 mediator, this result is surprising. Because Dmc1-mediated recombination is impaired in the absence of Mei5 or Sae3 as a result of a failure to form filaments, it was not possible to make this determination without the use of the *dmc1-E157D* allele [2,3].

*Relationship between Rad51's activities in stabilizing Dmc1 filaments and promoting IH bias*

Though Rad51 has well characterized roles in Dmc1 focus formation and IH bias, what is not known is whether these two activities are directly related to one another [14-

17]. In other words, is IH bias a consequence of normal Dmc1 filaments, or does Rad51 play a role in IH bias that is separable from its role in promoting the formation and stabilization of Dmc1 filaments? One model suggests that the two ends of the DSB act independent of one another, and that Rad51 achieves IH bias by forming a homology-dependent association with the sister, thereby precluding invasion by Dmc1, and "forcing" it to invade one of the homologous chromatids instead [6,18]. This model is unlikely based on the fact that (1) Rad51's DNA binding site II, which is responsible for homology search, is dispensable for meiotic recombination, and (2) super-resolution imaging showed that there is no evidence for asymmetric loading of recombination proteins on the two ends of the DSB [9,13]. It is also incompatible with the observation that Dmc1 frequently invades the sister [19]. However, other models to explain Rad51's role in IH bias are scarce.

Because *dmc1-E157D* bypasses Rad51 with respect to the formation of bright immunostaining foci, this could allow one to investigate whether Rad51 has distinct functions in IH bias and Dmc1 filament formation/stability. In Chapter 3, we showed that Dmc1 filaments are longer in *dmc1-E157D rad51* relative to wild-type, but due to crowding, we were unable to assess whether those Dmc1 foci that are closely associated with RPA, and therefore on ssDNA, were also longer. To reduce focus crowding, several approaches could be undertaken, either separately or in combination with one another. First, the number of DSBs in the cell, and therefore the number of RPA foci, could be reduced using a *SPO11* hypomorph [13]. Second, since Rdh54 is likely capable of disassembling Dmc1-E157D-dsDNA complexes, *RDH54* could be overexpressed to reduce off-pathway foci. These approaches could be used separately

or in combination with one another. While it is possible that with these modifications, super-resolution microscopy could allow one to identify and analyze Dmc1 filaments that are unambiguously associated with RPA, looking at the Dmc1's spread around the *HIS4::LEU2* DSB hotspot via ChIP followed by paired-end sequencing would be a complementary approach [20].

### 5.2.4 Molecular mechanism through which Mei5-Sae3 promotes Dmc1 filament formation

*Mei5-Sae3 likely stabilizes Dmc1 filaments by stimulating ADP release*

Offering further insight into the mechanism through which Mei5-Sae3 stimulates Dmc1 filament formation and stability, we have provided evidence that *dmc1-E157D* is likely defective in ATP hydrolysis. This is inferred through (1) the high level of sequence identity between RecA and *S. cerevisiae* Dmc1, (2) the observation that off-pathway foci form on undamaged DNA in both *recA-E96D* and *dmc1-E157D*, and (3) the fact that RecA-E96D and Dmc1-E157D are both hyper-recombinant in D-loop assays [21,22]. The latter two observations are likely caused by RecA-E96D's increased affinity for DNA, which results from its defective ATPase activity [22-24]. However, ATPase assays should be performed with purified Dmc1-E157D to determine whether its rate of ATP hydrolysis is indeed reduced.

Our *in vivo* bypass of Mei5-Sae3 via a Dmc1 mutant that is likely deficient for ATP hydrolysis is significant because the homolog of Mei5-Sae3, Sfr1-Swi5, has been shown to stabilize Rad51 filaments through stimulating ADP release, thus maintaining the filament in the active, ATP-bound form [25,26]. This was demonstrated most compellingly in recent single molecule work from Lu et al. [26]. Briefly, using purified

fission yeast and mouse proteins, Lu and coworkers monitored Rad51 filaments formed in the presence or absence of Sfr1-Swi5 using single-molecule tethered particle motion experiments. They found that Sfr1-Swi5 promotes Rad51 nucleation and filament stability expressly by prohibiting Rad51 dissociation. These findings imply that Sfr1-Swi5/Mei5-Sae3 acts on Rad51/Dmc1 filaments through a unique mediator mechanism. Importantly, ADP release is believed to be the most rate-limiting step in the ATP hydrolysis cycle, at least for the human Rad51 protein [27,28]. The results presented in Chapter 3 furnish genetic support of this model for the first time. Moreover, our results extend this model by suggesting that Mei5-Sae3 acts to promote Dmc1 filaments to form principally at sites of ssDNA.

*Mei5-Sae3 may couple mediator activity with ssDNA specificity*

While single molecule experiments have offered great insight into the role of Mei5-Sae3/Sfr1-Swi5, the model that Mei5-Sae3/Sfr1-Swi5 promotes Dmc1/Rad51 filament formation and stability specifically on ssDNA can be tested using ensemble biochemistry. First, one needs to establish that like its fission yeast and mouse counterparts, Mei5-Sae3 promotes ADP release by Dmc1 to maintain the filament in the active form. Dmc1's ATPase activity is dependent on DNA binding, and should therefore directly correlate with the length of DNA substrate used in the ATPase assay [29]. If Dmc1 remains associated with the ssDNA for longer in the presence of Mei5-Sae3, or if it forms more filaments, this should be detected in ATPase assays as an increase in hydrolyzed ATP [25]. This analysis can also be extended to test the idea that Mei5-Sae3 promotes Dmc1 filament formation/stability on ssDNA but not dsDNA. By comparing Dmc1's rate of ATP hydrolysis with matched ss- and dsDNA substrates in

the presence and absence of Mei5-Sae3, one can determine whether Mei5-Sae3 functions to promote Dmc1 filament formation/stability exclusively on ssDNA.

The primary mechanisms through which Mei5-Sae3 could achieve mediator function specifically at sites of ssDNA, the biologically relevant substrate for Dmc1 filament formation *in vivo*, are (1) through its interaction with RPA, or (2) through it preferential binding of ssDNA over dsDNA [4,7,30]. *In vitro* studies of deletion mutants have established that Mei5 confers ssDNA binding to the heterodimer through its N-terminal domain [7]. To determine whether interaction with RPA or ssDNA is more relevant to its *in vivo* function, one could identify point mutations in Mei5 that prevent or reduce Mei5-Sae3 binding to ssDNA *in vitro*, but that preserve the interaction with RPA. Introduction of these mutations into budding yeast and comparison of their meiotic phenotypes to the *mei5* and *sae3* null mutants, as well as cytological observation of Mei5-Sae3 focus formation in this background, could be used to distinguish between these two possibilities for how Mei5-Sae3 specifically targets Dmc1 filaments to form on ssDNA.

It is also important to know whether Mei5-Sae3 stabilizes Dmc1 filaments in the absence of RPA. *In vitro* DNA pull-down assays showed that Mei5-Sae3 promotes Dmc1 loading onto RPA-coated ssDNA [4]. However, based on the molecular mechanism that we have proposed for Mei5-Sae3 function, it is also possible that Mei5-Sae3 may stabilize Dmc1 filaments independent of its mediator activity. This could easily be assessed by salt sensitivity assays, a method that was used previously to assess whether Rad55-Rad57 can stabilize Rad51 filaments [31]. Dmc1 filaments would be formed in the presence or absence of Mei5-Sae3, then challenged with buffer

containing a high salt concentration that is sufficient to destabilize Dmc1 filaments formed in the absence of any mediators. If Mei5-Sae3 is able to promote Dmc1 filament stability, then Dmc1 should remain associated with the ssDNA. Similar analyses could also be performed with and without Rad51 to gain insight into Rad51's activity as a Dmc1 accessory factor.

Finally, given that very little is known about the function of Sae3 within the Mei5-Sae3 heterodimer, systematic analysis of Sae3 deletion mutants could also be useful. Mei5 bestows Mei5-Sae3 with ssDNA binding and its interaction with Dmc1 [2,7]. While Mei5-Sae3 has no ATPase activity and neither of the proteins have an ATPase domain, it is possible that the residues responsible for promoting Dmc1 ADP release are contained within Sae3 [7]. By looking for Sae3 mutants that retain their ability to interact with Mei5, but that fail to stimulate Dmc1, Sae3's functional domains could be identified. This analysis would provide greater insight into how Mei5-Sae3 moderates Dmc1 filament dynamics.

## 5.3 Consequences of abnormal filament lengths *in vivo*

### 5.3.1 Filament length and its relationship to recombination proficiency

Conventional and super-resolution imaging of RecA, Rad51, and Dmc1 double-stranded break (DSB)-dependent foci has shown that the structures that these proteins form as detected by immunostaining of spread nuclei are less than ~100-400 nucleotides in length [13,14,22,32]. The super-resolution microscopy data presented in Chapter 3 is in agreement with these previously published results.

Several lines of evidence support the inference that these relatively short Rad51/Dmc1 filament lengths arise through a balance between positive and negative regulators. First, ssDNA resection tracts are significantly longer than Rad51/Dmc1 filaments, extending for as far as several kilobases in somatic cells, and an average of ~800 nucleotides in meiotic cells [33-35]. These findings indicate that the ssDNA substrate itself does not limit a filament's length. Additionally, we have shown that Dmc1 filaments are on average longer in the *dmc1-E157D* background. Whereas a previous super-resolution imaging study of Dmc1 filaments in the *mnd1* background had also provided evidence that Dmc1 filaments can elongate under certain conditions [13], this analysis was complicated by the fact that *mnd1* cells undergo hyper-resection [36,37], meaning that the lengths of the underlying ssDNA tracts are also longer in this context. In contrast, we found no evidence for hyper-resection in the *dmc1-E157D* mutant, though hyper-resection was observed in the same experiment in the *dmc1-E157D rad51* double mutant. Lastly, super-resolution imaging of Rad51 filaments assembled *in vitro* under physiologically relevant conditions shows that these filaments are significantly longer than 400 nucleotides, implying that in the absence of negative regulators, Rad51 is competent to form extensive filaments [13]. Taken together, these results indicate that Rad51/Dmc1 filament lengths are constrained *in vivo* via a mechanism that is more complex than simply being limited by the length of the ssDNA on which they are formed.

Conversely, there are deleterious consequences associated with Rad51/Dmc1 filaments that are shorter in length than wild-type. For instance, the *rad51* mutation diminishes but does eliminate Dmc1 foci [15]. Similarly, weak Rad51 foci are observed

in the *rad55* and *rad57* backgrounds, or when *SRS2* is overexpressed [10,11,38]. In all of these backgrounds, the efficiency of Rad51/Dmc1-mediated recombination is decreased, in spite of the fact that filaments are capable of forming [17,39-41]. These results are subtly different from mutants such as *mei5* and *sae3*, in that the defects in recombination associated with the *mei5* and *sae3* mutations are the result of a complete inability for Dmc1 filaments to nucleate [2,3]. From these observations, one can conclude that Rad51/Dmc1 filaments that are on average shorter than wild-type filaments are impaired for either homology search or strand exchange.

The results presented in this thesis affirm and extend these observations of Rad51/Dmc1 filament lengths by showing that longer than average Dmc1 filaments correlate with a pattern of abnormal recombination in the *dmc1-E157D* and *dmc1-E157D mei5* mutants, providing proof for the first time that longer than normal filaments are also potentially harmful to cells. Interestingly, *dmc1-E157D*, like the *srs2* mutant is also hyper-recombinant *in vivo* and *in vitro*. Though Rad51 filaments have not yet been imaged by super-resolution microscopy in the *srs2* background, Srs2 is known to disassemble Rad51 filaments, and conventional light microscopy imaging of meiotic *srs2* cells showed that they form Rad51 aggregates [42-44]. Thus Rad51 foci may also be longer in the *srs2* background where hyper-recombination is observed, suggesting that filament lengths that are on average longer than wild-type lead to hyper-recombination, whereas those that are shorter than average have decreased strand invasion activity [45].

To better understand the interplay between filament length and recombination efficiency, I suggest that this relationship be probed *in vitro* using D-loop assays. If

longer filaments lead to hyper-recombination, and shorter filaments impair strand invasion, then Rad51-WT/Dmc1-WT activity in D-loop assays should be correspondingly increased or decreased under conditions that alter filament lengths. This can be achieved through use of a range of ssDNA oligonucleotides that vary in length, in conjunction with elevated concentations of calcium, or alternatively a non-hydrolyzable ATP analog such as AMP-PNP, to ensure that the Rad51/Dmc1 filament is stable and saturates the ssDNA substrate. ATP binding promotes cooperativity between RecA/Rad51/Dmc1 protomers, and calcium has a similar effect because it inhibits ATP hydrolysis [27,46-48]. Maintaining Rad51/Dmc1 filaments in the active, ATP-bound form is necessary in this experiment to ensure that the filaments themselves are longer or shorter in relationship to the ssDNA oligo, since it is likely that under conditions where ATP hydrolysis is permitted, equivalently sized filaments would form regardless of ssDNA length. Though use of calcium and non-hydrolyzable ATP analogs are already known to stimulate Rad51/Dmc1 D-loop formation, by keeping this condition constant between samples, this experiment would allow one to determine the contribution of filament length to the efficiency of stand exchange [27,29,49].

### 5.3.2 Long filaments may increase the likelihood of multi-invasion formation

Multi-invasions are abnormal recombination events involving a single broken strand and more than one homologous dsDNA donor [50]. Rad55-Rad57 and Srs2, which have an antagonistic relationship to one another in Rad51 filament stability/disassembly, also respectively promote and prevent the formation of multi-inavsions [31,42,43,50,51]. In conjunction with the findings presented in this thesis (i.e. that *dmc1-E157D* forms longer than normal filaments and has an *in vivo* recombination

pattern that is indicative of multi-invasion formation), these findings suggest that long filaments are more prone to engaging in multi-invasion recombination. One model of homology search, the intersegmental contact sampling model, predicts that these two things are related because long filaments have a greater capacity to engage in homology search, and will thus be more likely than a short filament to simultaneously encounter two distinct regions of homology [50,52].

To better establish the relationship between filament length and multi-invasion formation, the multi-invasion assay developed by Piazza et al. should be adapted to use in meiotic cells at the *HIS4::LEU2* DSB hotspot [50]. The multi-invasion capture assay could then be combined with 1D and 2D gel electrophoresis, as well as high-resolution sequencing of recombination products, to gain insight into the frequency of multi-invasion formation and their structure in various mutant backgrounds [53]. A similar analysis could be used to assess the genetic factors that influence multi-invasion recombination in somatic cells using a modified version of the *HIS4::LEU2* locus in which an inducible break site has been introduced [54].

References


1. McKee AH, Kleckner N. Mutations in Saccharomyces cerevisiae that block meiotic prophase chromosome metabolism and confer cell cycle arrest at pachytene identify two new meiosis-specific genes SAE1 and SAE3. Genetics. Genetics Society of America; 1997;146: 817–834.

2. Hayase A, Takagi M, Miyazaki T, Oshiumi H, Shinohara M, Shinohara A. A Protein Complex Containing Mei5 and Sae3 Promotes the Assembly of the Meiosis-Specific RecA Homolog Dmc1. Cell. 2004;119: 927–940. doi:10.1016/j.cell.2004.10.031

3. Tsubouchi H, Roeder GS. The budding yeast mei5 and sae3 proteins act together with dmc1 during meiotic recombination. Genetics. 2004;168: 1219–1230. doi:10.1534/genetics.103.025700

4. Ferrari SR, Grubb J, Bishop DK. The Mei5-Sae3 Protein Complex Mediates Dmc1 Activity in Saccharomyces cerevisiae. Journal of Biological Chemistry. 2009;284: 11766–11770. doi:10.1074/jbc.C900023200

5. Cho H-R, Kong Y-J, Hong S-G, Kim KP. Hop2 and Sae3 Are Required for Dmc1-Mediated Double-Strand Break Repair via Homolog Bias during Meiosis. Molecules and Cells. 2016;39: 550–556. doi:10.14348/molcells.2016.0069

6. Brown MS, Bishop DK. DNA Strand Exchange and RecA Homologs in Meiosis. Cold Spring Harb Perspect Biol. 2015;7: a016659–31. doi:10.1101/cshperspect.a016659

7. Say AF, Ledford LL, Sharma D, Singh AK, Leung W-K, Sehorn HA, et al. The budding yeast Mei5–Sae3 complex interacts with Rad51 and preferentially binds a DNA fork structure. DNA Repair. 2011;10: 586–594. doi:10.1016/j.dnarep.2011.03.006

8. Dresser ME, Ewing DJ, Conrad MN, Dominguez AM, Barstead R, Jiang H, et al. DMC1 functions in a Saccharomyces cerevisiae meiotic pathway that is largely independent of the RAD51 pathway. Genetics. Genetics Society of America; 1997;147: 533–544.

9. Cloud V, Chan Y-L, Grubb J, Budke B, Bishop DK. Rad51 is an accessory factor for Dmc1-mediated joint molecule formation during meiosis. Science. 2012;337: 1222–1225. doi:10.1126/science.1219379

10. Gasior SL, Olivares H, Ear U, Hari DM, Weichselbaum R, Bishop DK. Assembly of RecA-like recombinases: distinct roles for mediator proteins in mitosis and meiosis. Proc Natl Acad Sci USA. National Academy of Sciences; 2001;98: 8411–8418. doi:10.1073/pnas.121046198

11. Lisby M, Barlow JH, Burgess RC, Rothstein R. Choreography of the DNA damage response: spatiotemporal relationships among checkpoint and repair proteins. Cell. 2004;118: 699–713. doi:10.1016/j.cell.2004.08.015

12. Symington LS. End resection at double-strand breaks: mechanism and regulation. Cold Spring Harb Perspect Biol. Cold Spring Harbor Lab; 2014;6: a016436–a016436. doi:10.1101/cshperspect.a016436

13. Brown MS, Grubb J, Zhang A, Rust MJ, Bishop DK. Small Rad51 and Dmc1 Complexes Often Co-occupy Both Ends of a Meiotic DNA Double Strand Break. Lichten M, editor. PLoS Genet. Public Library of Science; 2015;11: e1005653. doi:10.1371/journal.pgen.1005653

14. Bishop DK. RecA homologs Dmc1 and Rad51 interact to form multiple nuclear complexes prior to meiotic chromosome synapsis. Cell. 1994;79: 1081–1092.

15. Shinohara A, Gasior S, Ogawa T, Kleckner N, Bishop DK. Saccharomyces cerevisiae recA homologues RAD51 and DMC1 have both distinct and overlapping roles in meiotic recombination. Genes Cells. 1997;2: 615–629.

16. Shinohara M, Gasior SL, Bishop DK, Shinohara A. Tid1/Rdh54 promotes colocalization of rad51 and dmc1 during meiotic recombination. Proc Natl Acad Sci USA. National Academy of Sciences; 2000;97: 10814–10819. doi:10.1073/pnas.97.20.10814

17. Schwacha A, Kleckner N. Interhomolog bias during meiotic recombination: meiotic functions promote a highly differentiated interhomolog-only pathway. Cell. 1997;90: 1123–1135.

18. Hong S, Sung Y, Yu M, Lee M, Kleckner N, Kim KP. The Logic and Mechanism of Homologous Recombination Partner Choice. Molecular Cell. Elsevier Inc; 2013;51: 440–453. doi:10.1016/j.molcel.2013.08.008

19. Goldfarb T, Lichten M. Frequent and efficient use of the sister chromatid for DNA double-strand break repair during budding yeast meiosis. Hawley RS, editor. PLoS Biol. Public Library of Science; 2010;8: e1000520. doi:10.1371/journal.pbio.1000520

20. Holzen TM, Shah PP, Olivares HA, Bishop DK. Tid1/Rdh54 promotes dissociation of Dmc1 from nonrecombinogenic sites on meiotic chromatin. Genes Dev. 2006;20: 2593–2604. doi:10.1101/gad.1447106

21. Masson JY, West SC. The Rad51 and Dmc1 recombinases: a non-identical twin relationship. Trends Biochem Sci. 2001;26: 131–136.

22. Gataulin DV, Carey JN, Li J, Shah P, Grubb JT, Bishop DK. The ATPase activity of E. coli RecA prevents accumulation of toxic complexes formed by erroneous

binding to undamaged double stranded DNA. Nucleic Acids Res. 2018;46: 9510–9523. doi:10.1093/nar/gky748

23. Campbell MJ, Davis RW. Toxic mutations in the recA gene of E. coli prevent proper chromosome segregation. J Mol Biol. 1999;286: 417–435. doi:10.1006/jmbi.1998.2456

24. Campbell MJ, Davis RW. On the in vivo function of the RecA ATPase. J Mol Biol. 1999;286: 437–445. doi:10.1006/jmbi.1998.2457

25. Su G-C, Chung C-I, Liao C-Y, Lin S-W, Tsai C-T, Huang T, et al. Enhancement of ADP release from the RAD51 presynaptic filament by the SWI5-SFR1 complex. Nucleic Acids Res. 2014;42: 349–358. doi:10.1093/nar/gkt879

26. Lu C-H, Yeh H-Y, Su G-C, Ito K, Kurokawa Y, Iwasaki H, et al. Swi5-Sfr1 stimulates Rad51 recombinase filament assembly by modulating Rad51 dissociation. Proc Natl Acad Sci USA. National Academy of Sciences; 2018;115: E10059–E10068. doi:10.1073/pnas.1812753115

27. Bugreev DV, Mazin AV. Ca2+ activates human homologous recombination protein Rad51 by modulating its ATPase activity. Proc Natl Acad Sci USA. National Academy of Sciences; 2004;101: 9988–9993. doi:10.1073/pnas.0402105101

28. Hilario J, Amitani I, Baskin RJ, Kowalczykowski SC. Direct imaging of human Rad51 nucleoprotein dynamics on individual DNA molecules. Proc Natl Acad Sci USA. 2009;106: 361–368. doi:10.1073/pnas.0811965106

29. Hong EL, Shinohara A, Bishop DK. Saccharomyces cerevisiae Dmc1 protein promotes renaturation of single-strand DNA (ssDNA) and assimilation of ssDNA into homologous super-coiled duplex DNA. Journal of Biological Chemistry. 2001;276: 41906–41912. doi:10.1074/jbc.M105563200

30. Chan Y-L, Zhang A, Weissman BP, Bishop DK. RPA resolves conflicting activities of accessory proteins during reconstitution of Dmc1-mediated meiotic recombination. Nucleic Acids Res. 2019;47: 747–761. doi:10.1093/nar/gky1160

31. Liu J, Renault L, Veaute X, Fabre F, Stahlberg H, Heyer W-D. Rad51 paralogues Rad55-Rad57 balance the antirecombinase Srs2 in Rad51 filament formation. Nature. 2011;479: 245–248. doi:10.1038/nature10522

32. Haaf T, Golub EI, Reddy G, Radding CM, Ward DC. Nuclear foci of mammalian Rad51 recombination protein in somatic cells after DNA damage and its localization in synaptonemal complexes. Proc Natl Acad Sci USA. National Academy of Sciences; 1995;92: 2298–2302. doi:10.1073/pnas.92.6.2298

33. Chung W-H, Zhu Z, Papusha A, Malkova A, Ira G. Defective resection at DNA

double-strand breaks leads to de novo telomere formation and enhances gene targeting. Lichten M, editor. PLoS Genet. Public Library of Science; 2010;6: e1000948. doi:10.1371/journal.pgen.1000948

34. Zakharyevich K, Ma Y, Tang S, Hwang PY-H, Boiteux S, Hunter N. Temporally and biochemically distinct activities of Exo1 during meiosis: double-strand break resection and resolution of double Holliday junctions. Molecular Cell. 2010;40: 1001–1015. doi:10.1016/j.molcel.2010.11.032

35. Mimitou EP, Yamada S, Keeney S. A global view of meiotic double-strand break end resection. Science. American Association for the Advancement of Science; 2017;355: 40–45. doi:10.1126/science.aak9704

36. Gerton JL, DeRisi JL. Mnd1p: an evolutionarily conserved protein required for meiotic recombination. Proc Natl Acad Sci USA. National Academy of Sciences; 2002;99: 6895–6900. doi:10.1073/pnas.102167899

37. Tsubouchi H, Roeder GS. The Mnd1 protein forms a complex with hop2 to promote homologous chromosome pairing and meiotic double-strand break repair. Mol Cell Biol. American Society for Microbiology; 2002;22: 3078–3088. doi:10.1128/MCB.22.9.3078-3088.2002

38. Sasanuma H, Furihata Y, Shinohara M, Shinohara A. Remodeling of the Rad51 DNA strand-exchange protein by the Srs2 helicase. Genetics. Genetics; 2013;194: 859–872. doi:10.1534/genetics.113.150615

39. Hays SL, Firmenich AA, Berg P. Complex formation in yeast double-strand break repair: participation of Rad51, Rad52, Rad55, and Rad57 proteins. Proc Natl Acad Sci USA. National Academy of Sciences; 1995;92: 6925–6929. doi:10.1073/pnas.92.15.6925

40. Johnson RD, Symington LS. Functional differences and interactions among the putative RecA homologs Rad51, Rad55, and Rad57. Mol Cell Biol. American Society for Microbiology Journals; 1995;15: 4843–4850. doi:10.1128/mcb.15.9.4843

41. Sugawara N, Wang X, Haber JE. In vivo roles of Rad52, Rad54, and Rad55 proteins in Rad51-mediated recombination. Molecular Cell. 2003;12: 209–219. doi:10.1016/s1097-2765(03)00269-7

42. Krejci L, Van Komen S, Li Y, Villemain J, Reddy MS, Klein H, et al. DNA helicase Srs2 disrupts the Rad51 presynaptic filament. Nature. Nature Publishing Group; 2003;423: 305–309. doi:10.1038/nature01577

43. Veaute X, Jeusset J, Soustelle C, Kowalczykowski SC, Le Cam E, Fabre F. The Srs2 helicase prevents recombination by disrupting Rad51 nucleoprotein filaments. Nature. 2003;423: 309–312. doi:10.1038/nature01585

44. Hunt LJ, Ahmed EA, Kaur H, Ahuja JS, Hulme L, Chou T-C, et al. S. cerevisiae Srs2 helicase ensures normal recombination intermediate metabolism during meiosis and prevents accumulation of Rad51 aggregates. Chromosoma; 2019;: 1–17. doi:10.1007/s00412-019-00705-9

45. Rong L, Klein HL. Purification and characterization of the SRS2 DNA helicase of the yeast Saccharomyces cerevisiae. Journal of Biological Chemistry. 1993;268: 1252–1259.

46. Conway AB, Lynch TW, Zhang Y, Fortin GS, Fung CW, Symington LS, et al. Crystal structure of a Rad51 filament. Nat Struct Mol Biol. 2004;11: 791–796. doi:10.1038/nsmb795

47. Galkin VE, Wu Y, Zhang X-P, Qian X, He Y, Yu X, et al. The Rad51/RadA N-terminal domain activates nucleoprotein filament ATPase activity. Structure. 2006;14: 983–992. doi:10.1016/j.str.2006.04.001

48. Robertson RB, Moses DN, Kwon Y, Chan P, Chi P, Klein H, et al. Structural transitions within human Rad51 nucleoprotein filaments. Proc Natl Acad Sci USA. National Academy of Sciences; 2009;106: 12688–12693. doi:10.1073/pnas.0811465106

49. Chi P, Kwon Y, Seong C, Epshtein A, Lam I, Sung P, et al. Yeast recombination factor Rdh54 functionally interacts with the Rad51 recombinase and catalyzes Rad51 removal from DNA. Journal of Biological Chemistry. 2006;281: 26268–26279. doi:10.1074/jbc.M602983200

50. Piazza A, Wright WD, Heyer W-D. Multi-invasions Are Recombination Byproducts that Induce Chromosomal Rearrangements. Cell. 2017;170: 760–773.e15. doi:10.1016/j.cell.2017.06.052

51. Piazza A, Heyer W-D. Multi-Invasion-Induced Rearrangements as a Pathway for Physiological and Pathological Recombination. Bioessays. 2018;40: e1700249. doi:10.1002/bies.201700249

52. Forget AL, Kowalczykowski SC. Single-molecule imaging of DNA pairing by RecA reveals a three-dimensional homology search. Nature. Nature Publishing Group; 2012;482: 423–427. doi:10.1038/nature10782

53. Martini E, Borde V, Legendre M, Audic S, Regnault B, Soubigou G, et al. Genome-wide analysis of heteroduplex DNA in mismatch repair-deficient yeast cells reveals novel properties of meiotic recombination pathways. PLoS Genet. 2011;7: e1002305. doi:10.1371/journal.pgen.1002305

54. Bzymek M, Thayer NH, Oh SD, Kleckner N, Hunter N. Double Holliday junctions are intermediates of DNA break repair. Nature. 2010;464: 937–941. doi:10.1038/nature08868